5th Windsor Summer School "Quantum Phenomena in Low-Dimensional Materials and Nanostructures", Cumberland Lodge, Windsor, UK, August 9 - 21, 2010

Heterostructures of transition-metal oxides
- Experiment, mainly spectroscopy -

Atsushi Fujimori
University of Tokyo

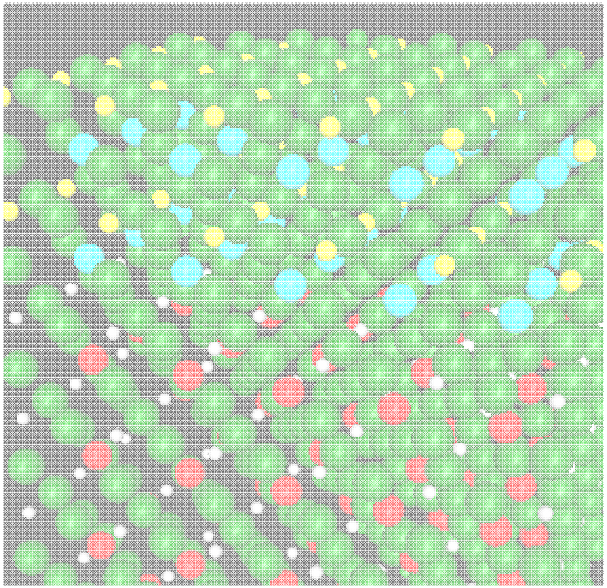

New opportunities with oxide thin films

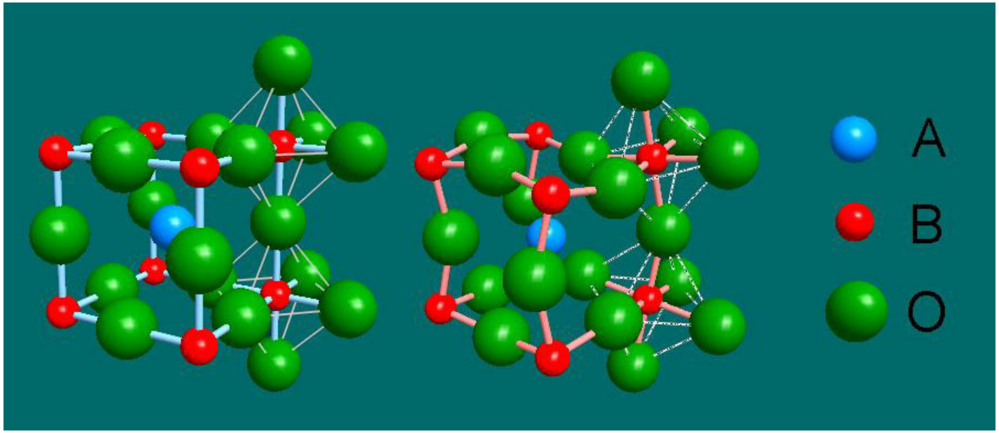

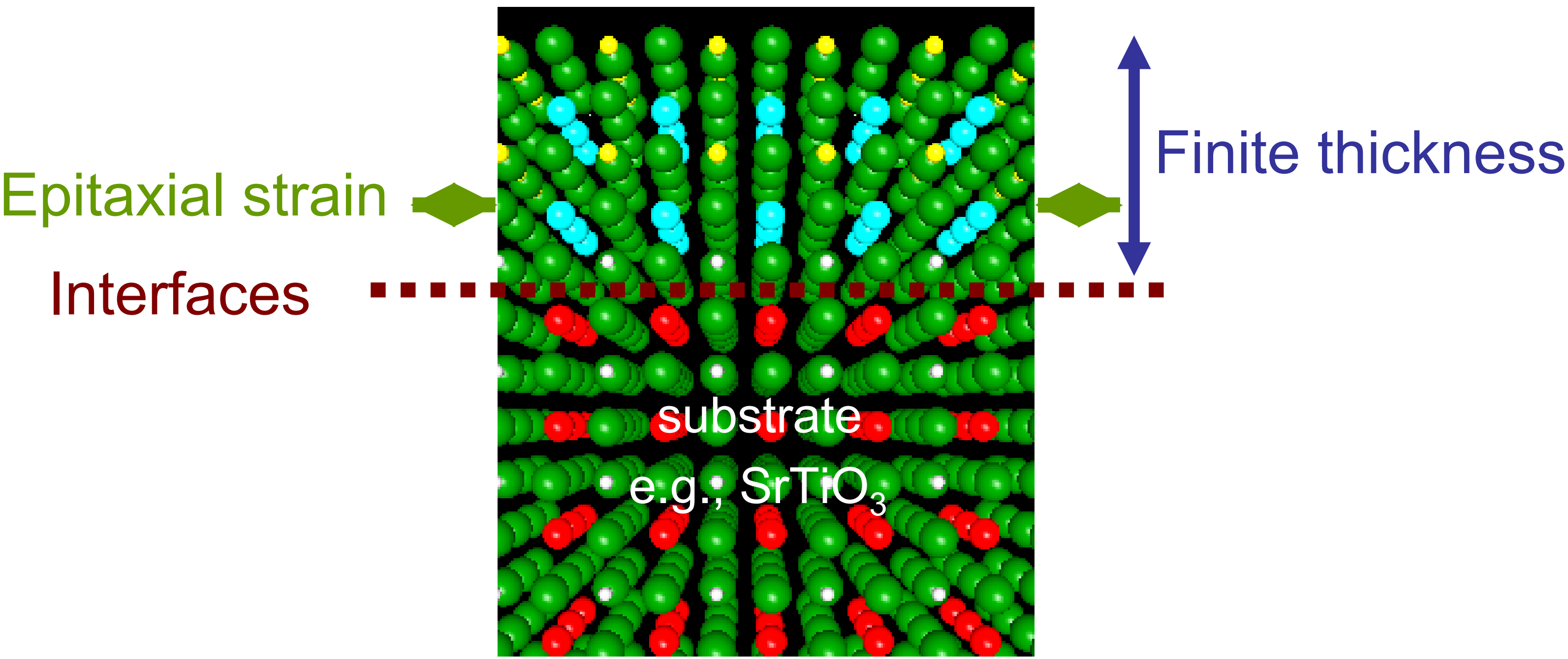

Outline

- Electronic structure of transition-metal oxides
- Fabrication and characterization

- Interfacial electronic structure
- Effects of finite thickness
- Effects of epitaxial strain

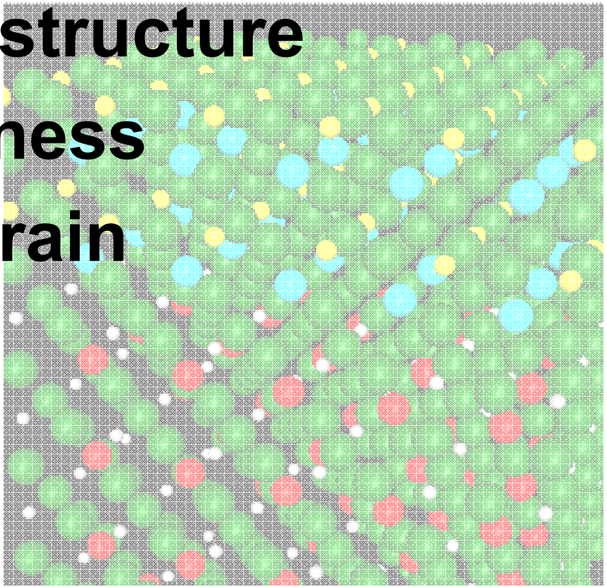

Electronic structure of transition-metal oxides

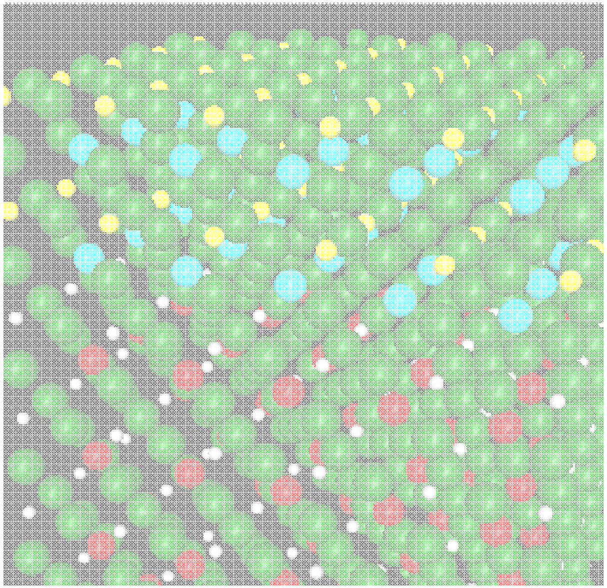

Metal-insulator transition through collapse of Mott gap – Bandwidth control

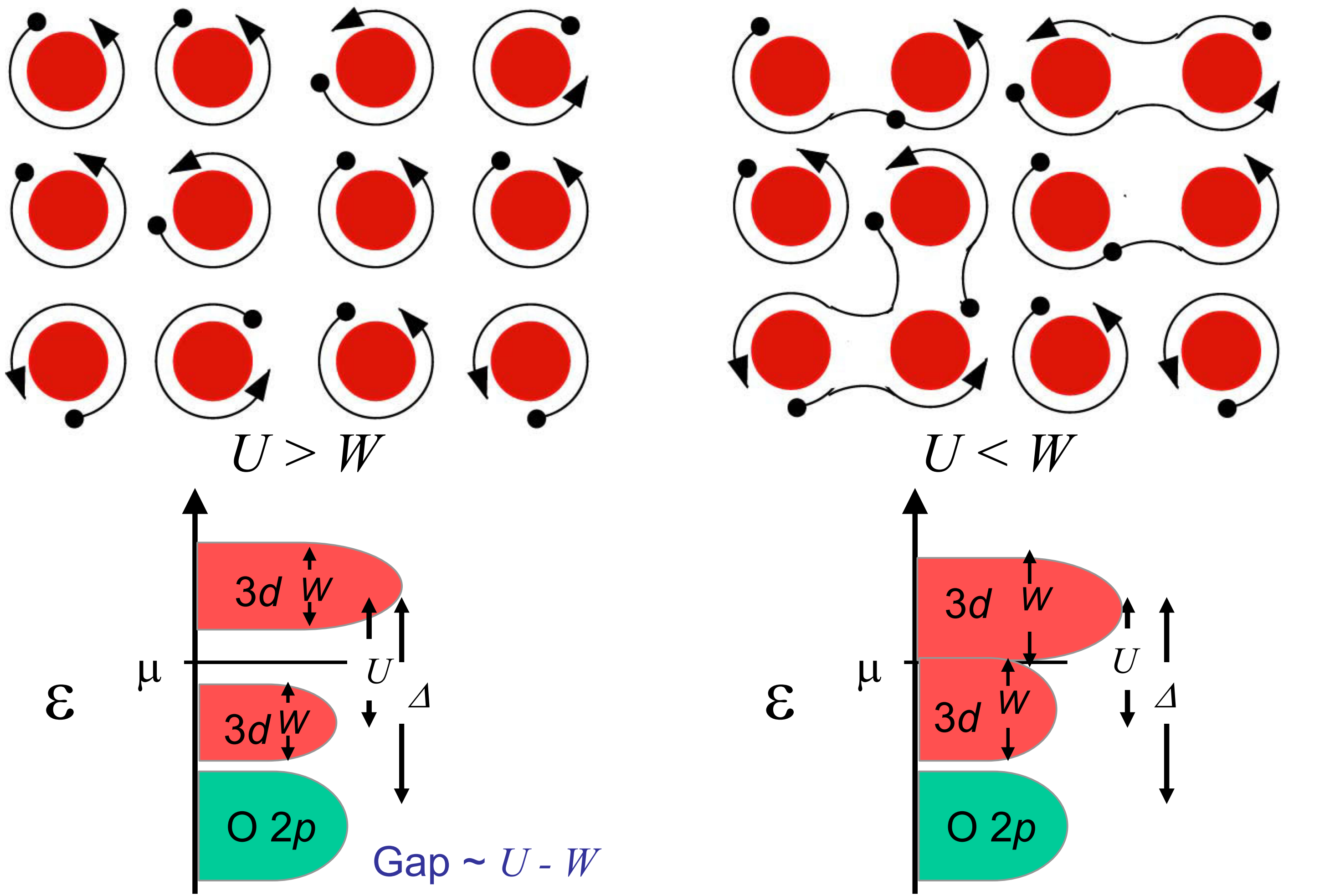

Metal-insulator transition through carrier doping into Mott insulator – Filling control

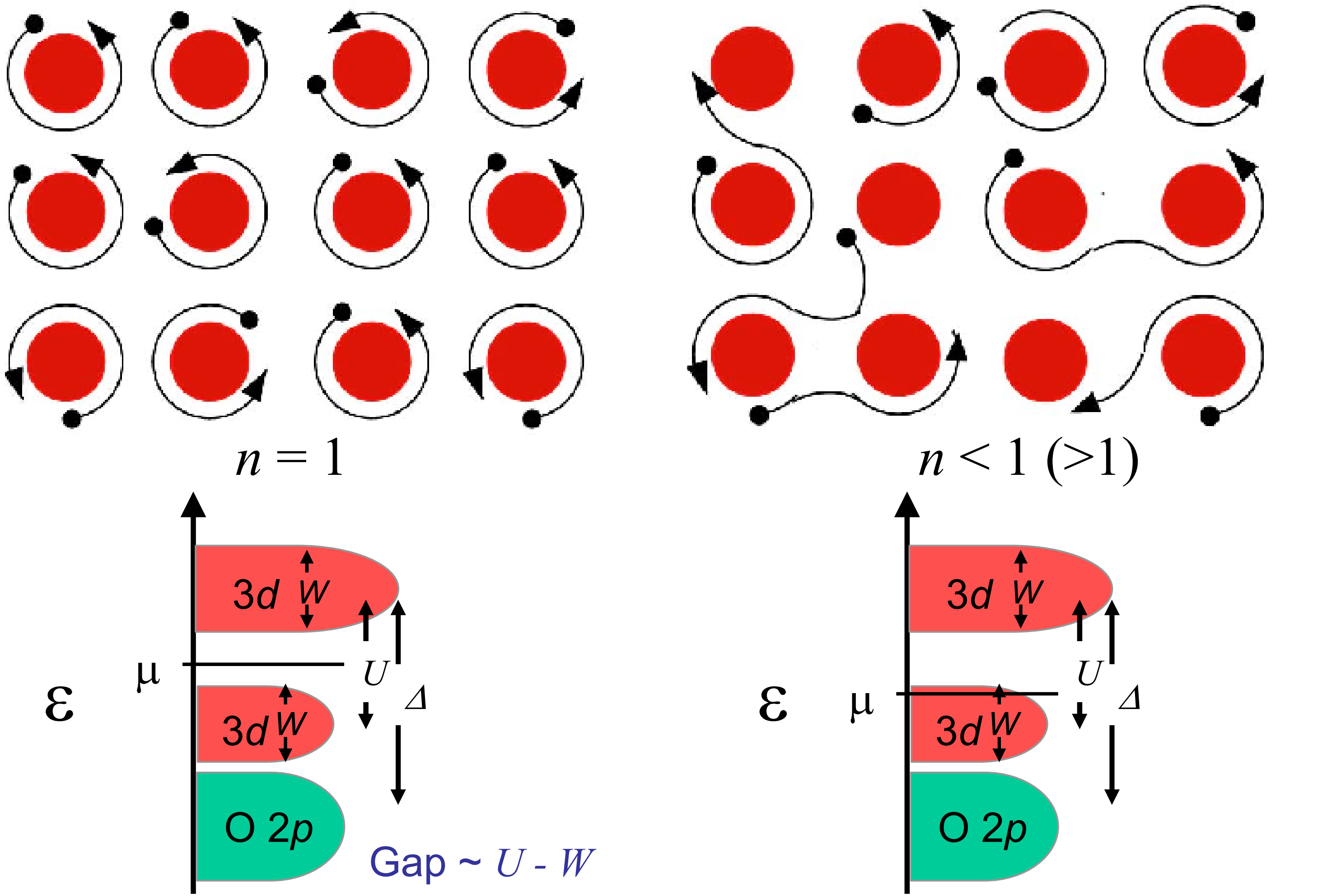

Bandwidth- *versus* filling-controlled metal-insulator transition

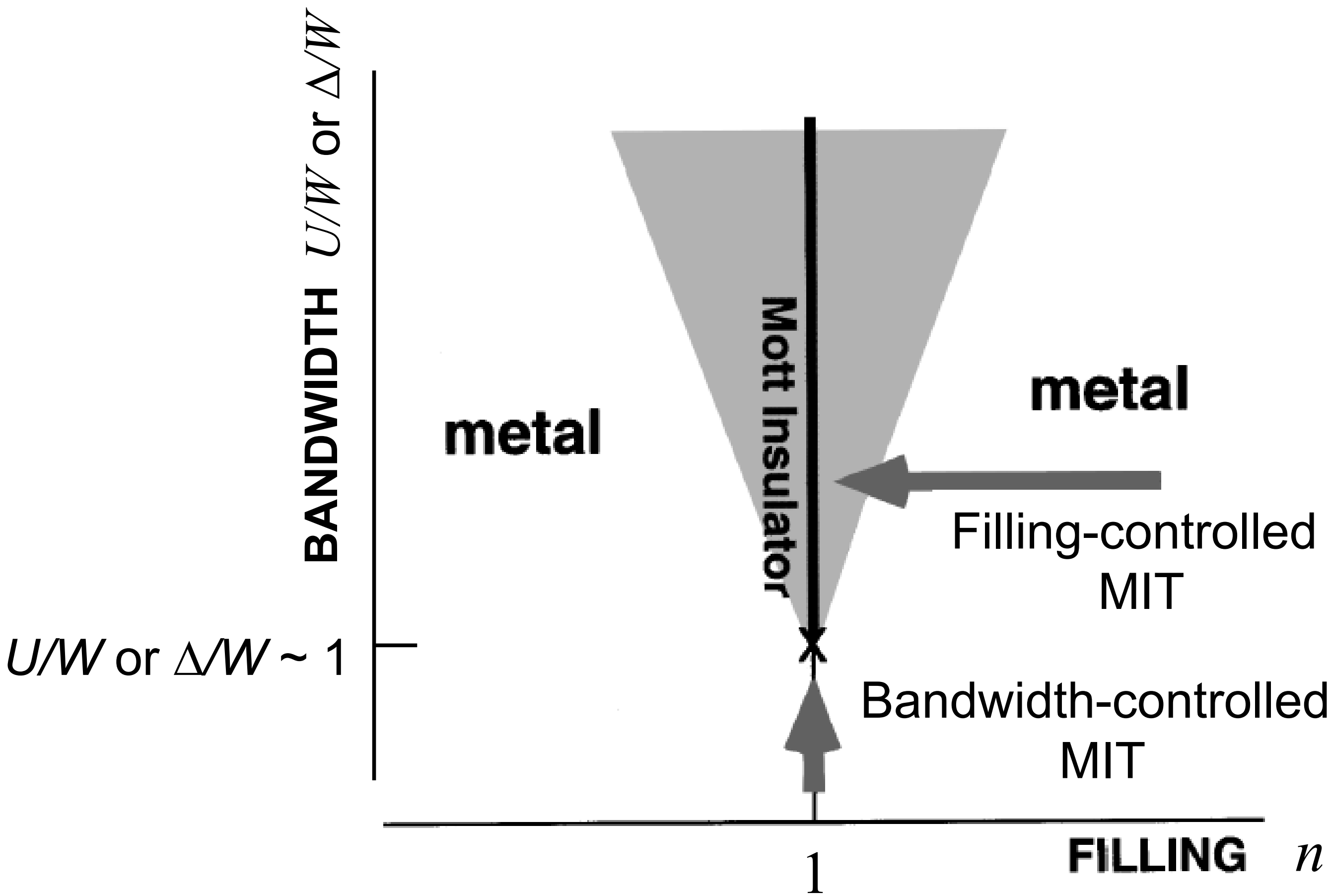

M. Imada, A. Fujimori and Y. Tokura, Rev. Mod. Phys. 1998

Electronic structure change across bandwidth-controlled metal-insulator transition

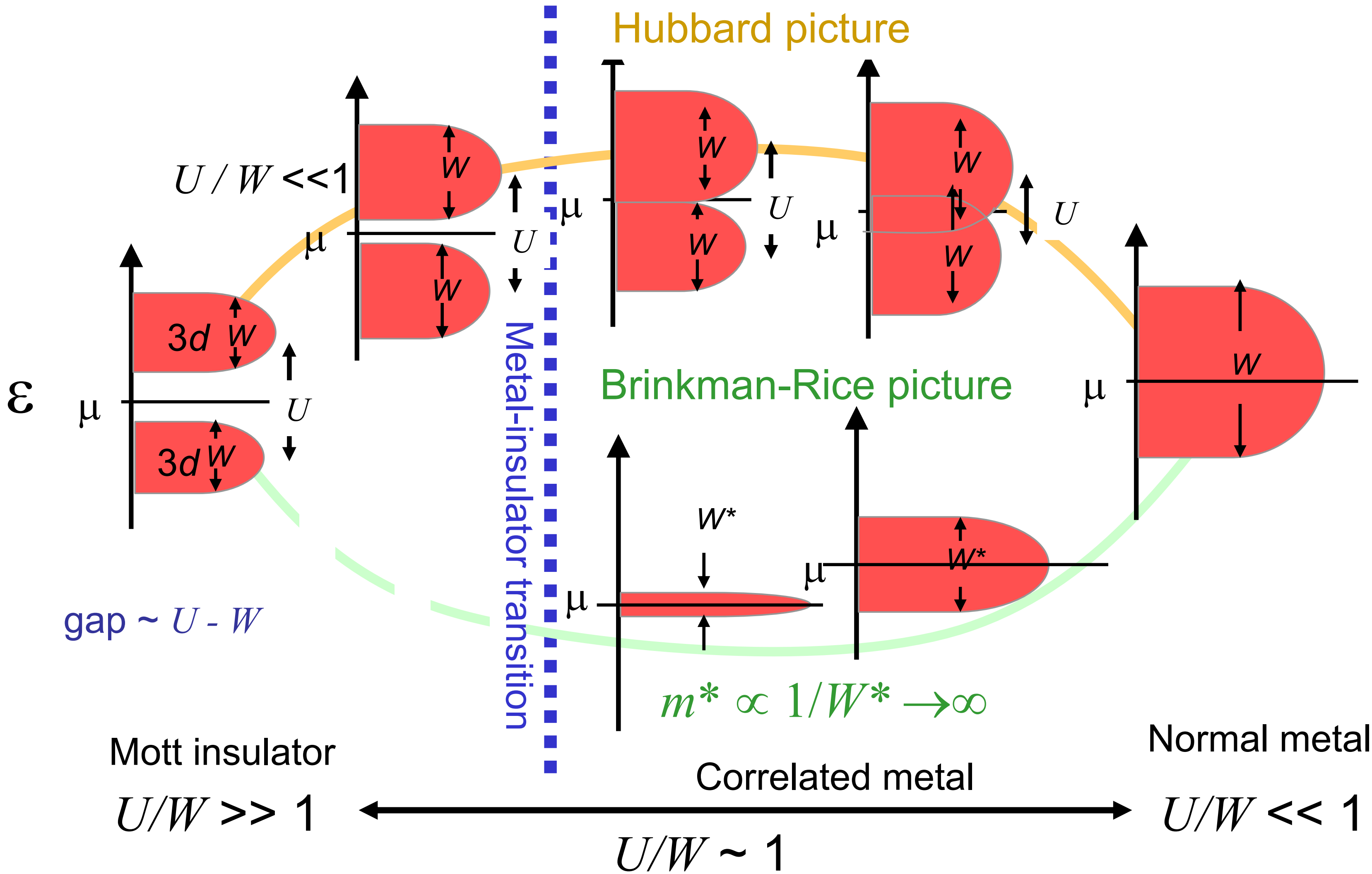

Electronic structure change across bandwidth-controlled metal-insulator transition

Dynamical mean-field theory (DMFT) calculation

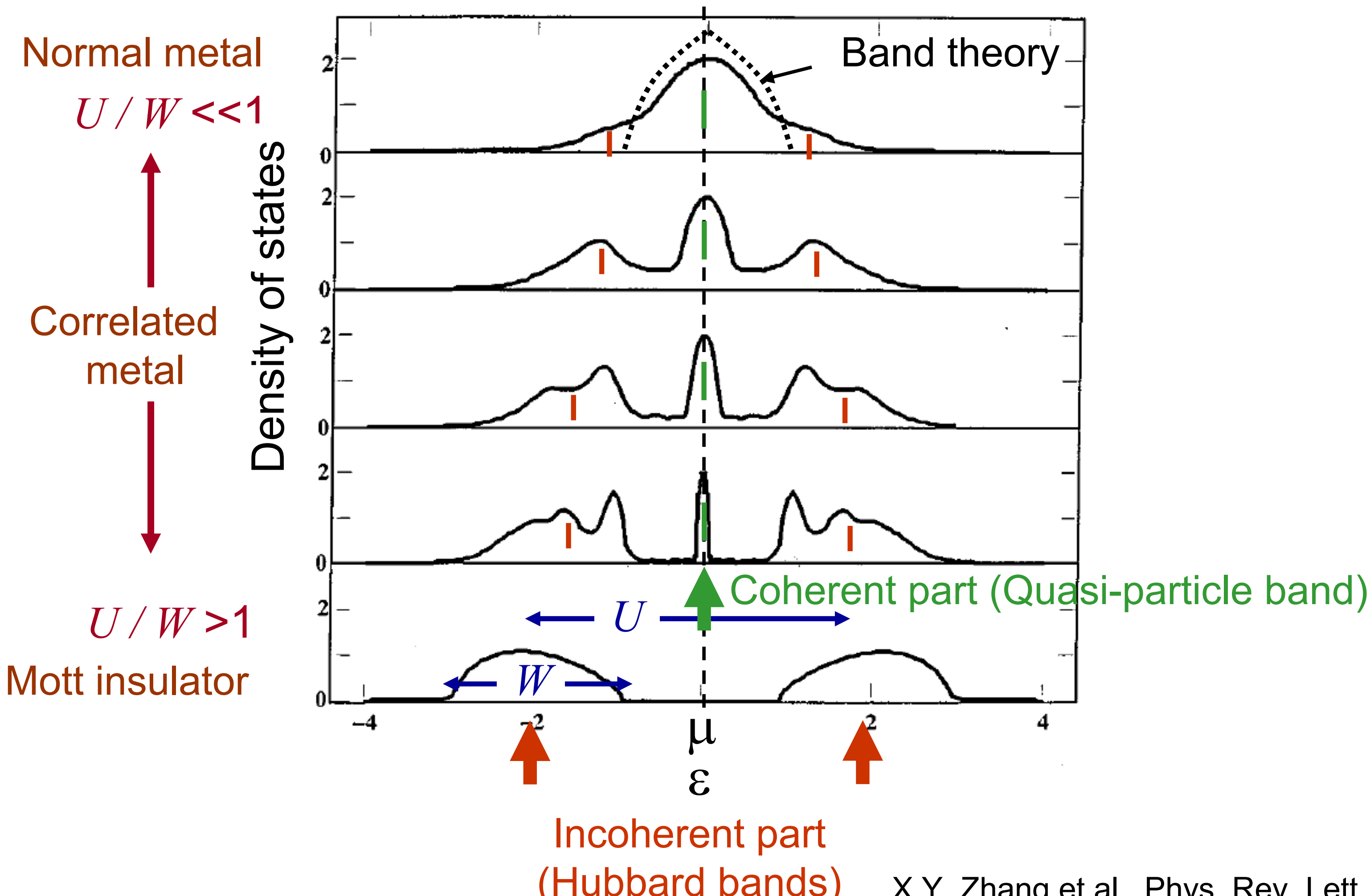

X.Y. Zhang et al., Phys. Rev. Lett., 1993

Bandwidth- *versus* filling-controlled in Mott-Hubbard systems

Perovskite structure

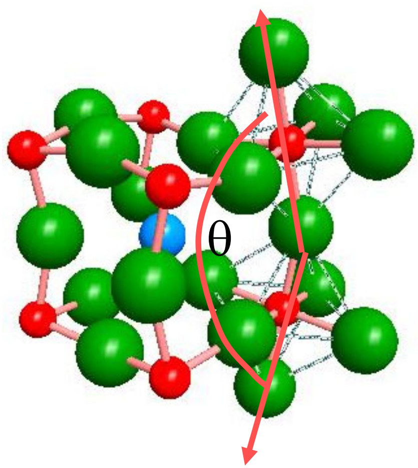

$W \propto \cos^2\theta$

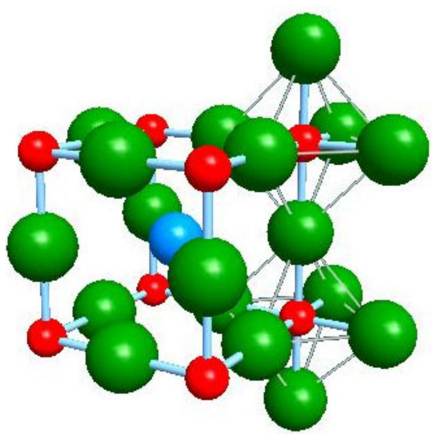

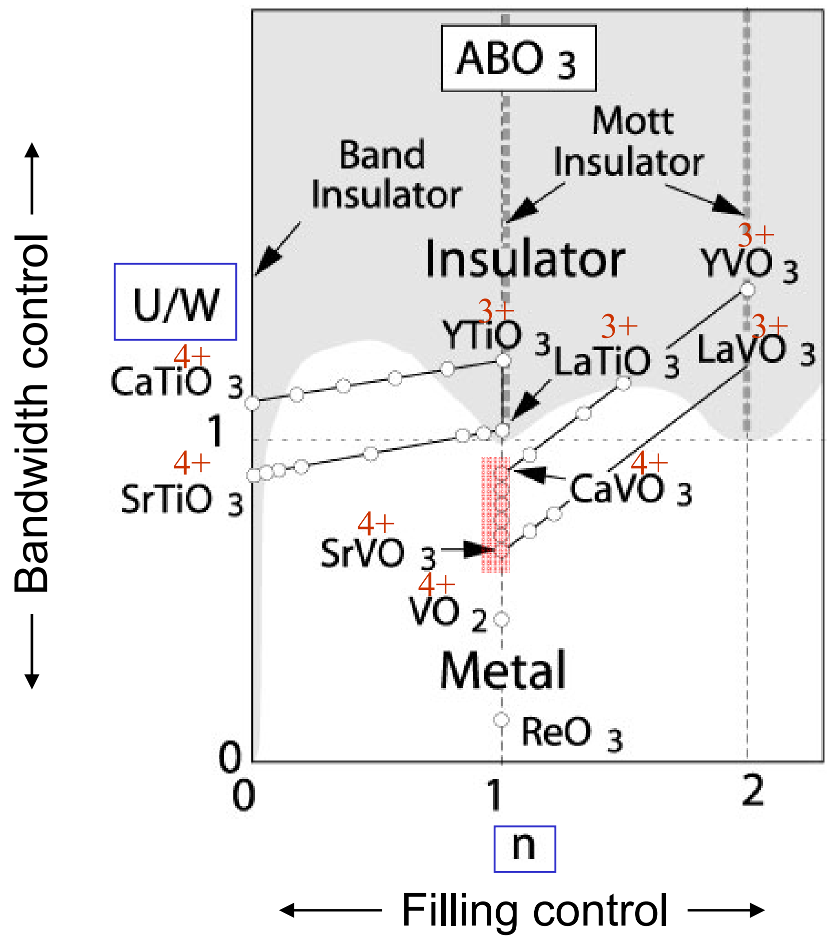

Electronic structure change across bandwidth-controlled metal-insulator transition

Photoemission spectra of $Ca_{1-x}Sr_xVO_3$(d^1)

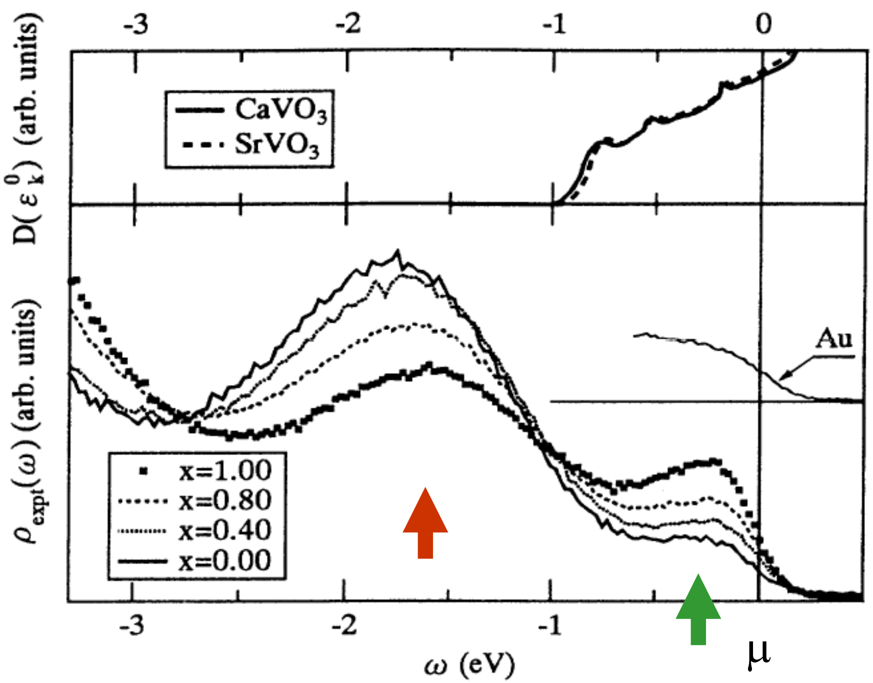

Incoherent part

Coherent part

DMFT calc.

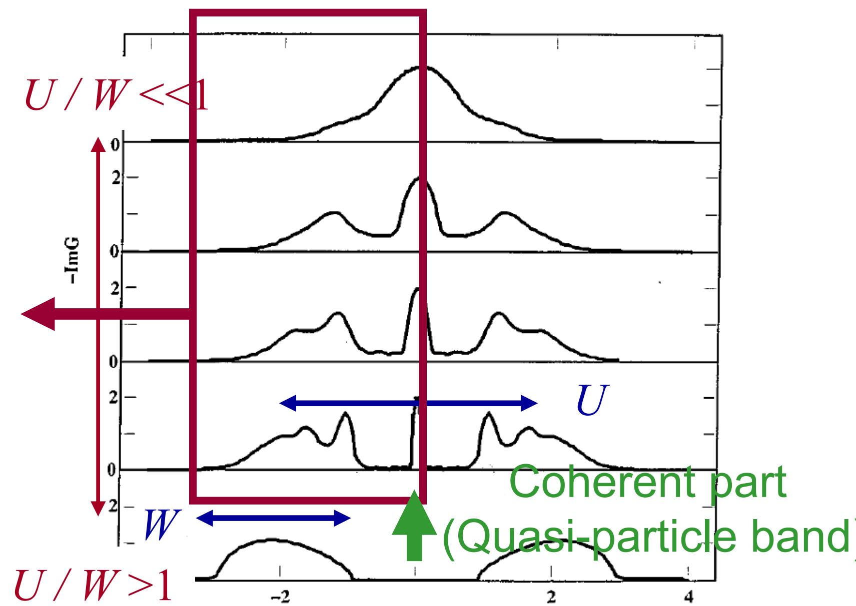

ε

Incoherent part
(Hubbard bands)

H.I. Inoue et al., Phys. Rev. Lett. 1995

Bandwidth- *versus* filling-controlled in Mott-Hubbard systems

Perovskite structure

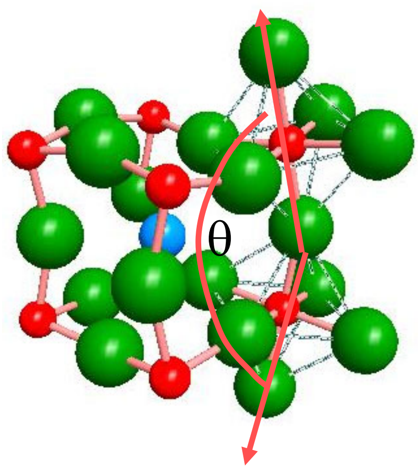

$W \propto \cos^2\theta$

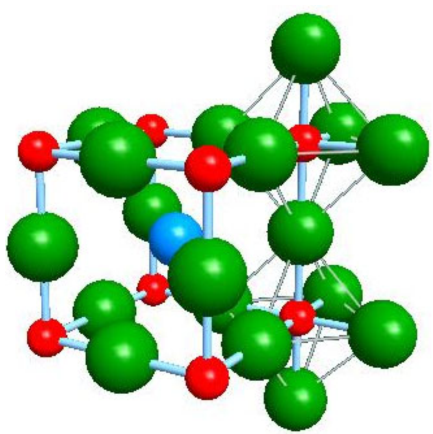

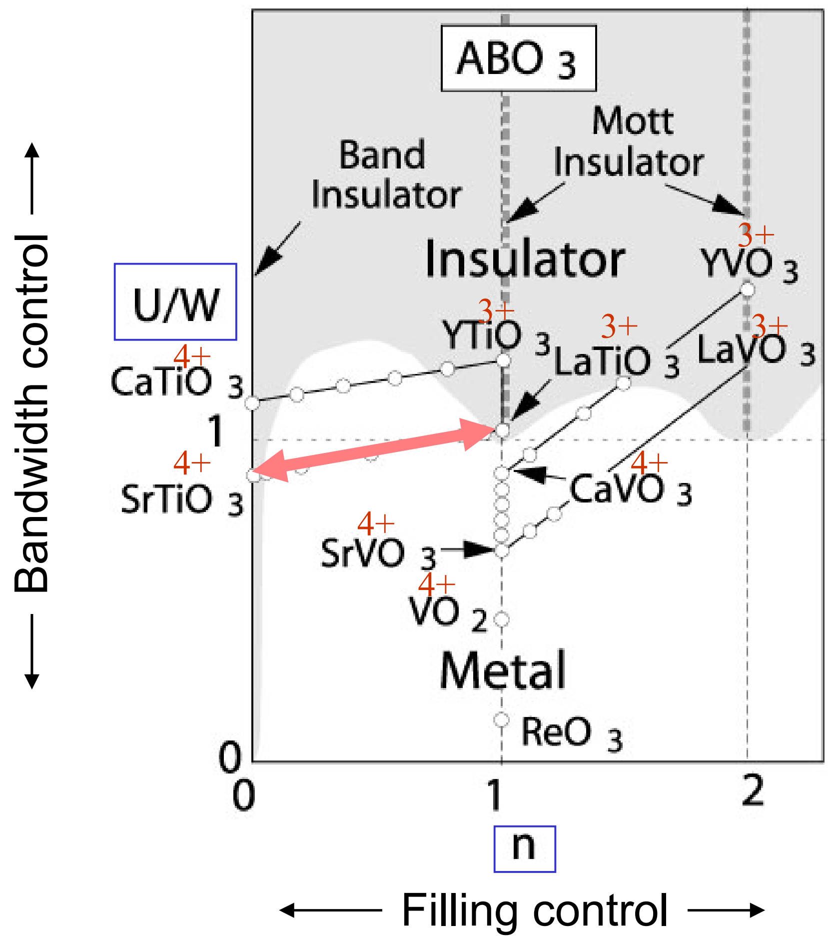

Filling-controlled Mott-Hubbard system $La_{1-x}Sr_xTiO_3$

Electronic specific heat &
Pauli-paramagnetic suseptibiulity

Kodowaki-Woods relationship

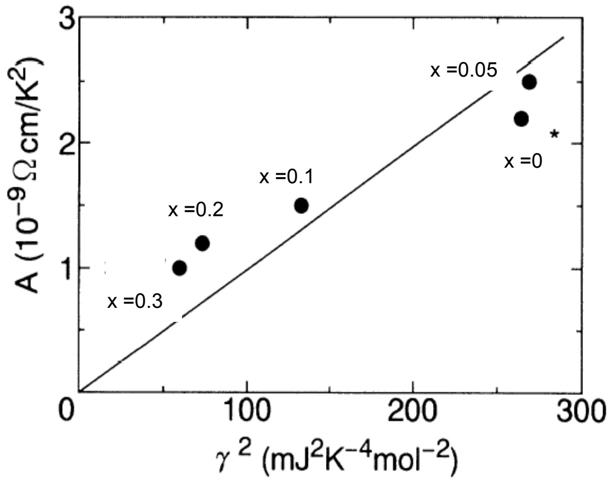

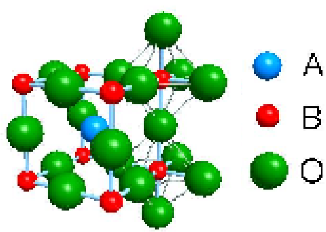

Y. Tokura et al. PRL '93

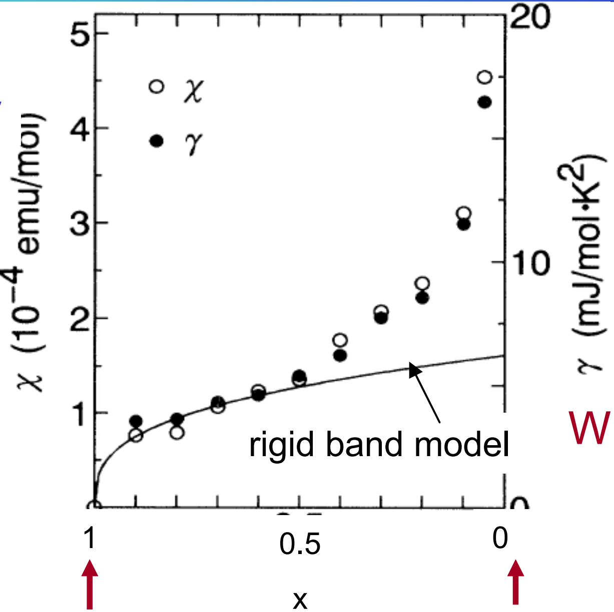

Wilson ratio:
$\chi/\gamma \sim 2$

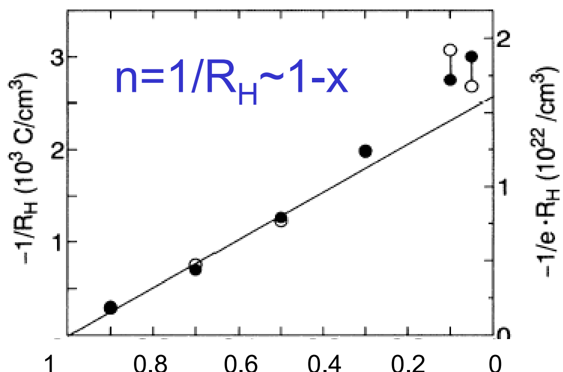

1 ← x → 0

$SrTiO_3$
d^0

$LaTiO_3$
d^1 Mott insulator

Perovskite-type transition-metal oxdies

Bandwidth control

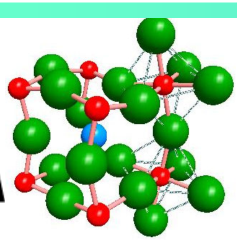

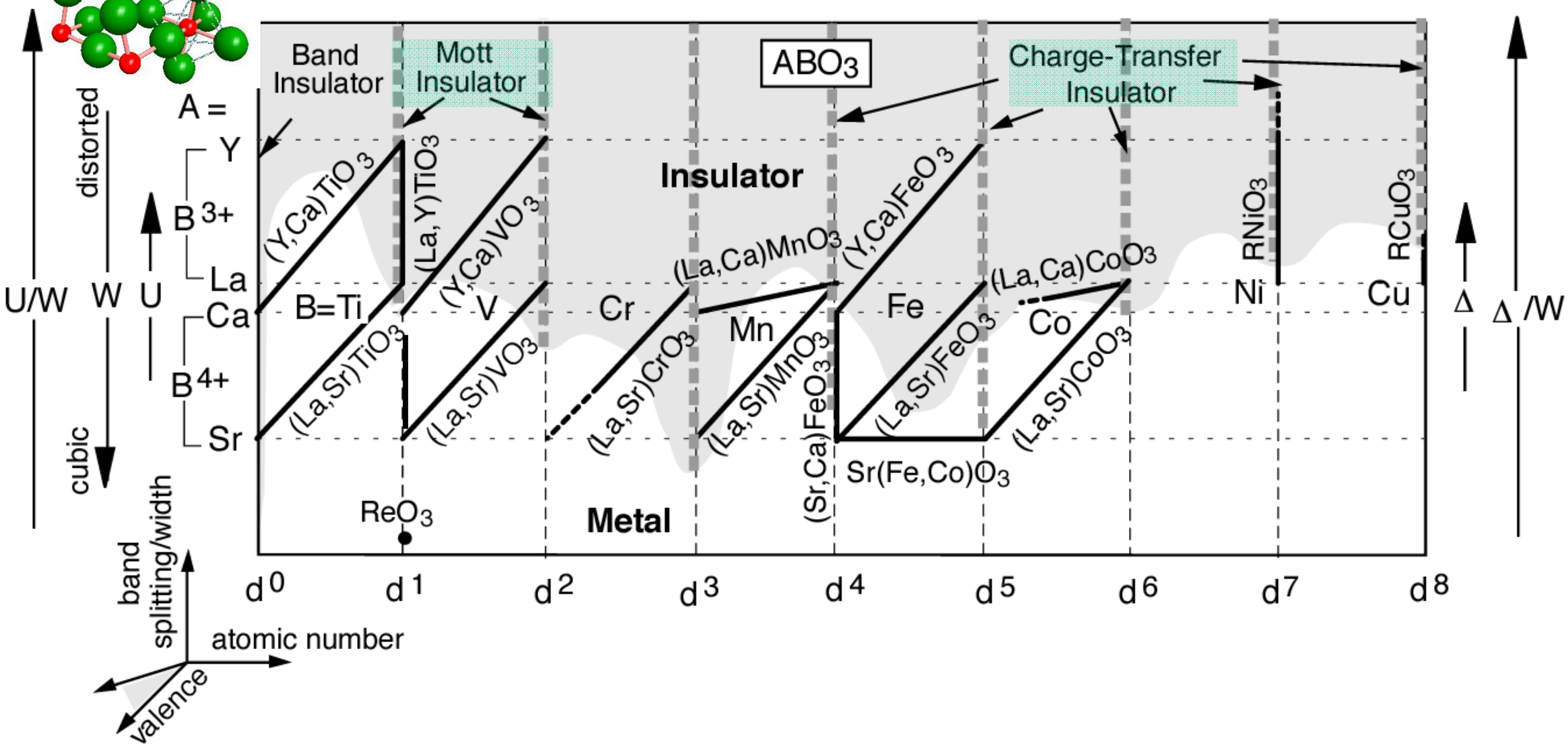

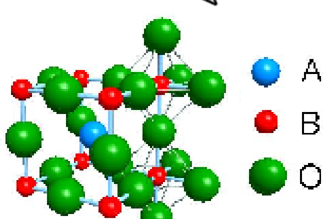

Filling control

M. Imada, A. Fujimori and Y. Tokura, Rev. Mod. Phys. '98

Zaanen-Sawatzky-Allen diagram

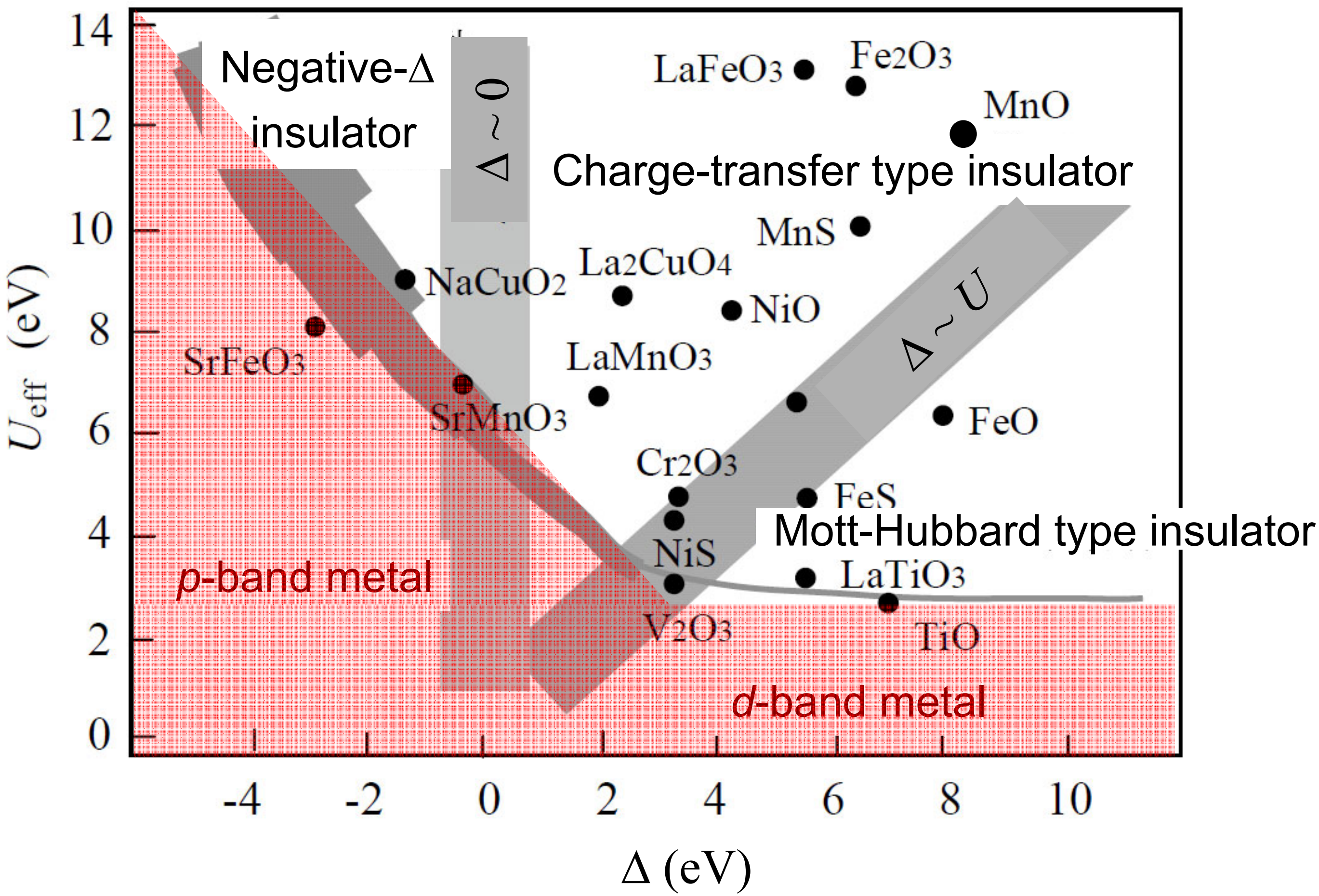

J. Zaanen, G.A. Sawatzky and J.W. Allen, PRL '85

Metal-insulator transition through collapse of charge-transfer gap – Bandwidth control

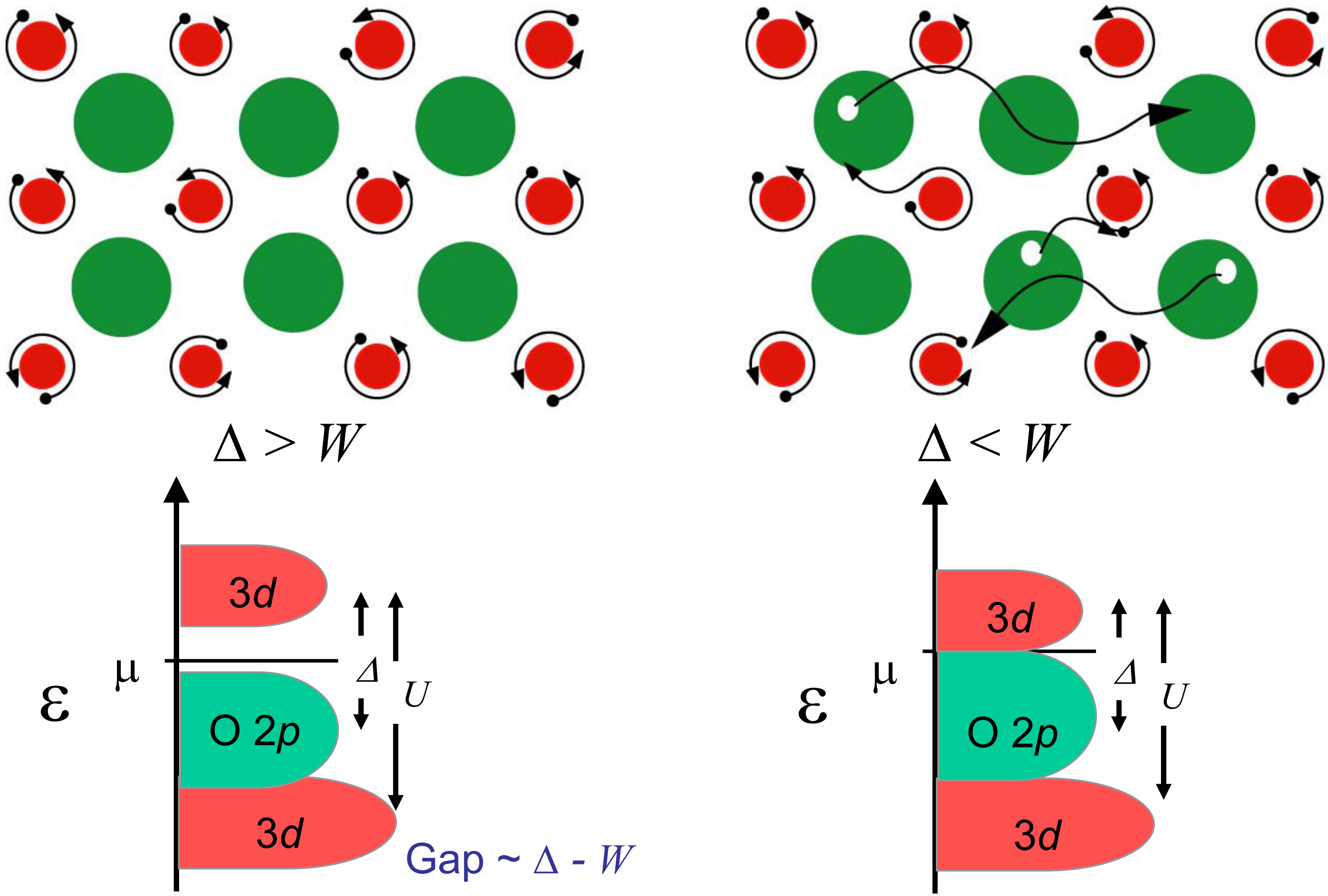

Metal-insulator transition through carrier doping into charge-transfer insulator

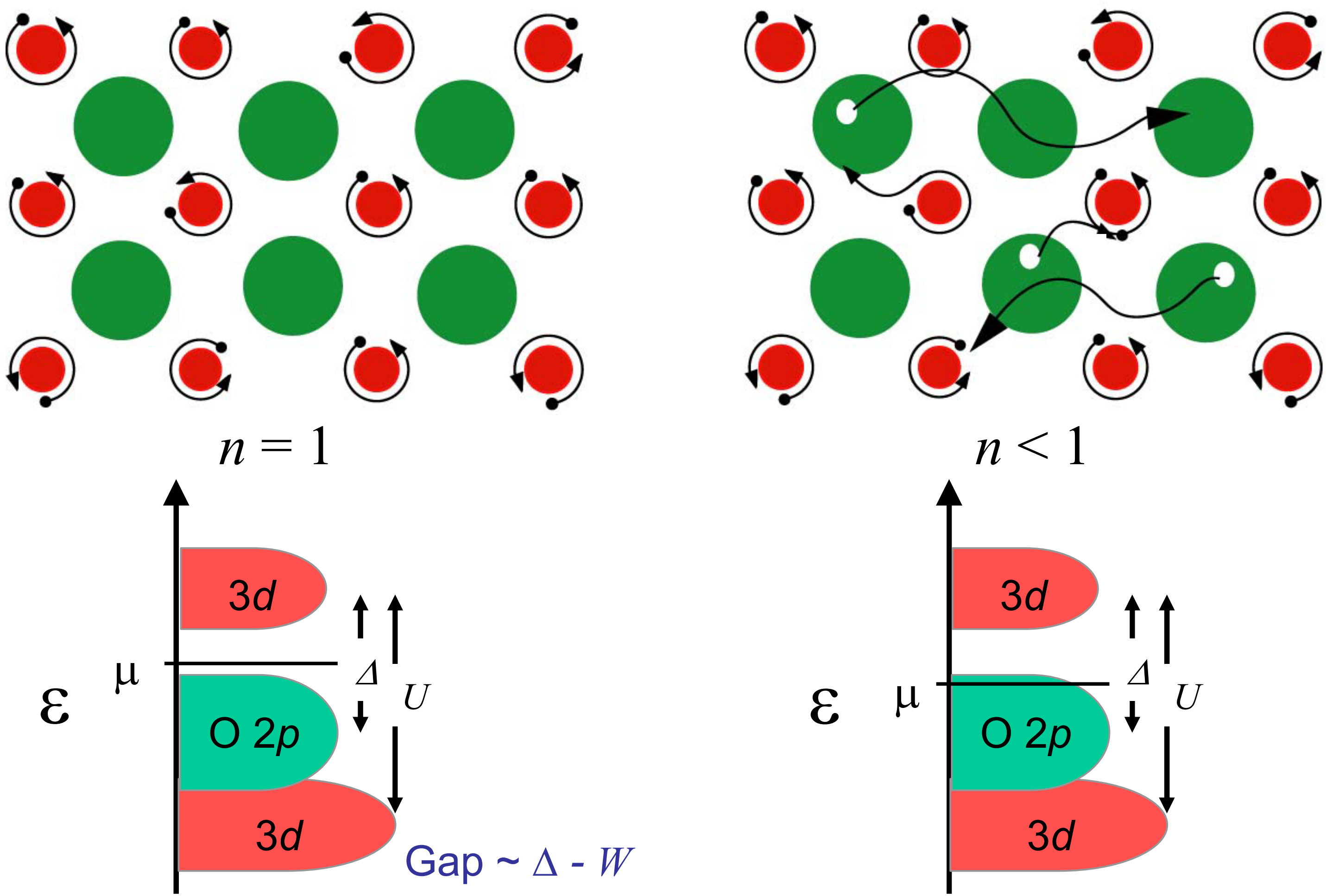

Perovskite-type transition-metal oxdies

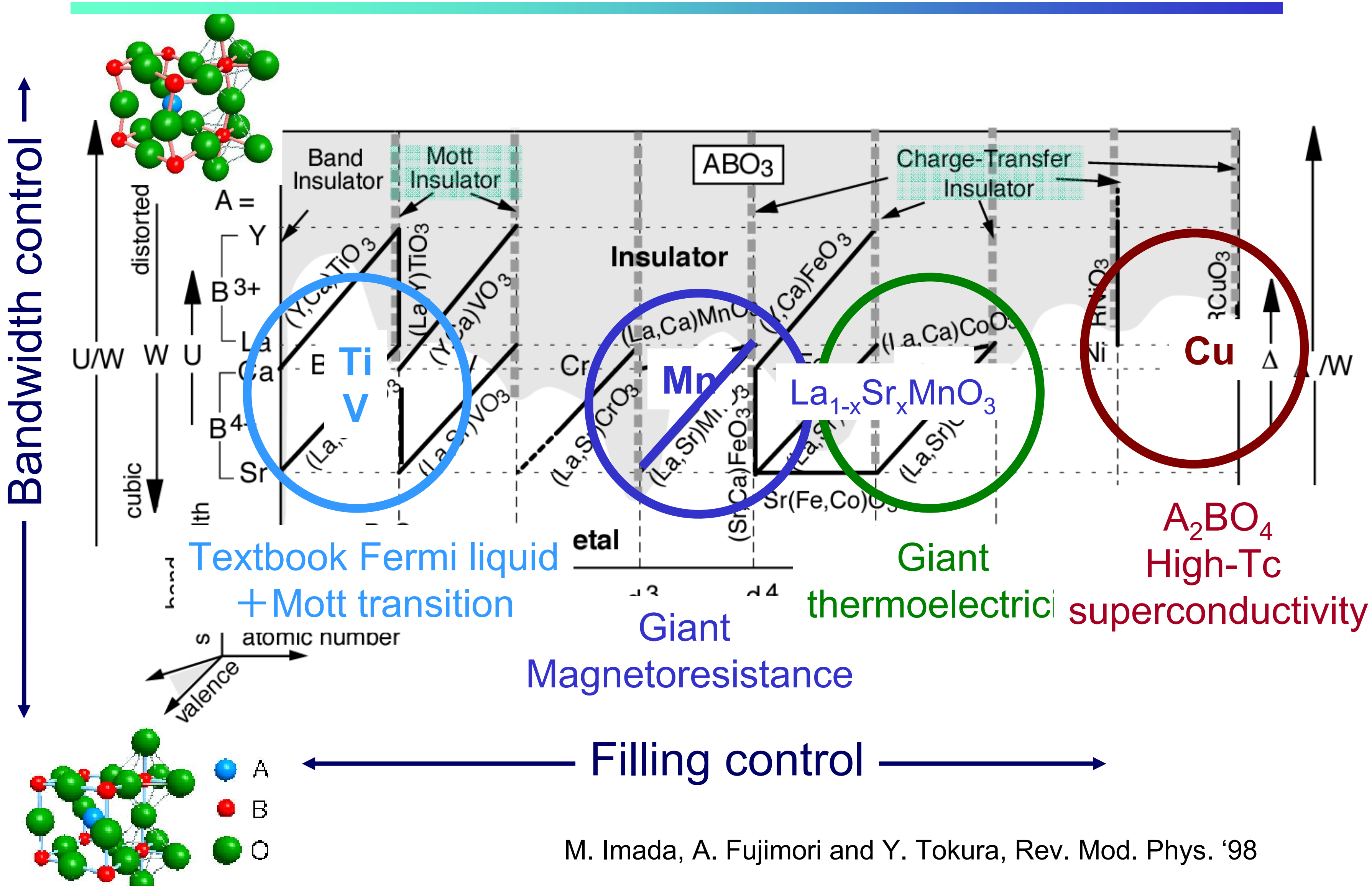

M. Imada, A. Fujimori and Y. Tokura, Rev. Mod. Phys. '98

Perovskite-type Mn oxdies

Electronic structure of Mn ion

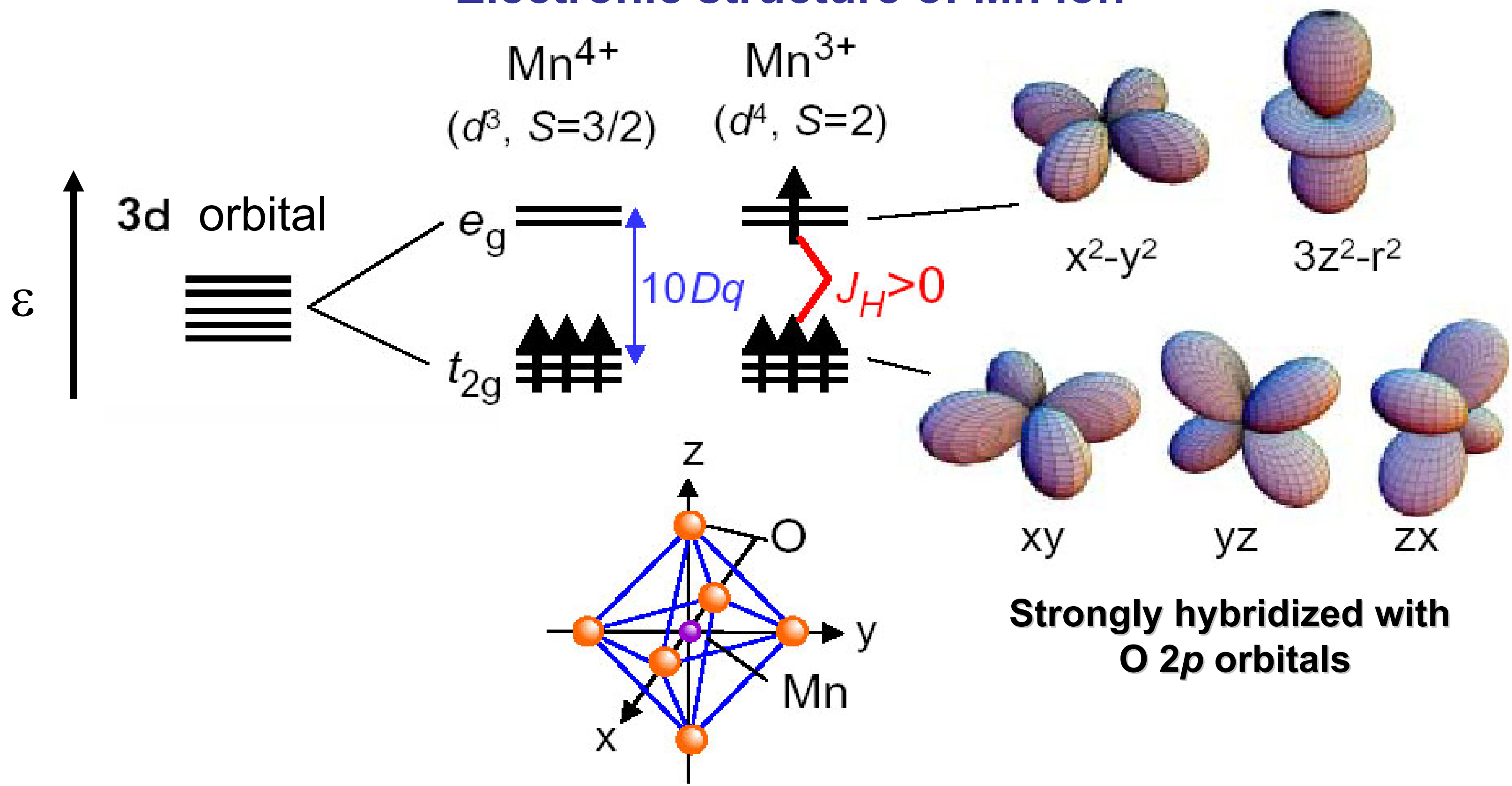

Strongly hybridized with O 2*p* orbitals

MnO_6 octahedron

Y. Tokura

If Hund coupling $3J_H$ > Cryst. field $10Dq$ → high-spin state

Double exchange model for magneto-resistance in Mn oxdies

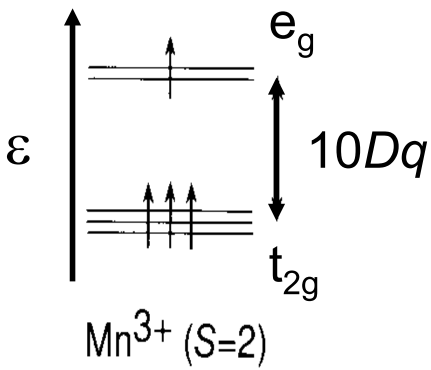

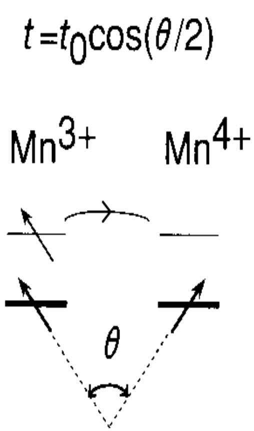

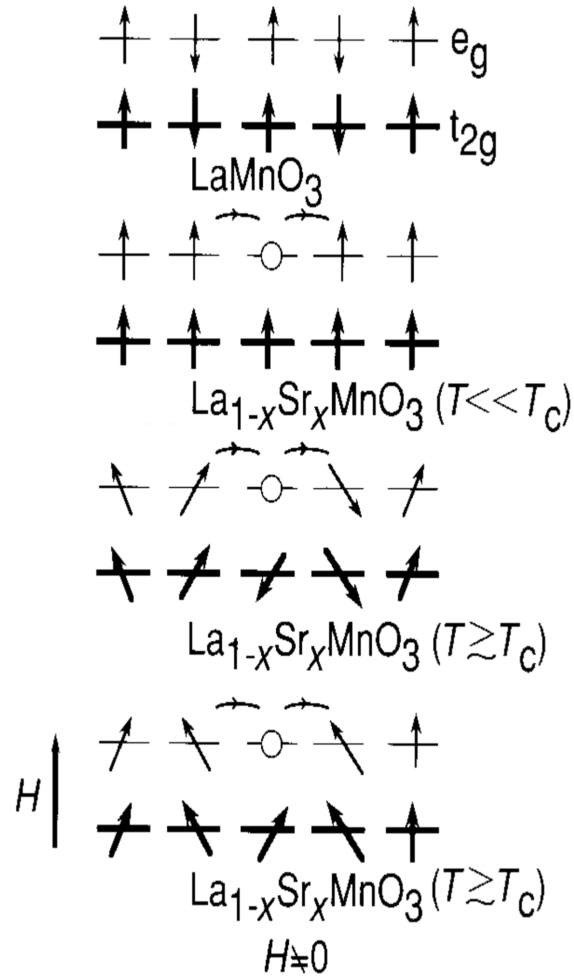

$$\mathcal{H}_{DE} = \mathcal{H}_t + \mathcal{H}_{Hund},$$

$$\mathcal{H}_t = -t \sum_{\substack{\langle ij \rangle \\ \sigma}} (c_{i\sigma}^{\dagger} c_{j\sigma} + \text{H.c.}),$$

$$\mathcal{H}_{Hund} = -J_H \sum_i \vec{S}_i \cdot \vec{\sigma}_i,$$

$\vec{S}_i$; e_g spin

$\vec{\sigma}_i$; t_{2g} spin

J_{H}: Hund coupling constant

Colossal magnetoresistance of Mn oxdies

$La_{1-x}Sr_xMnO_3$

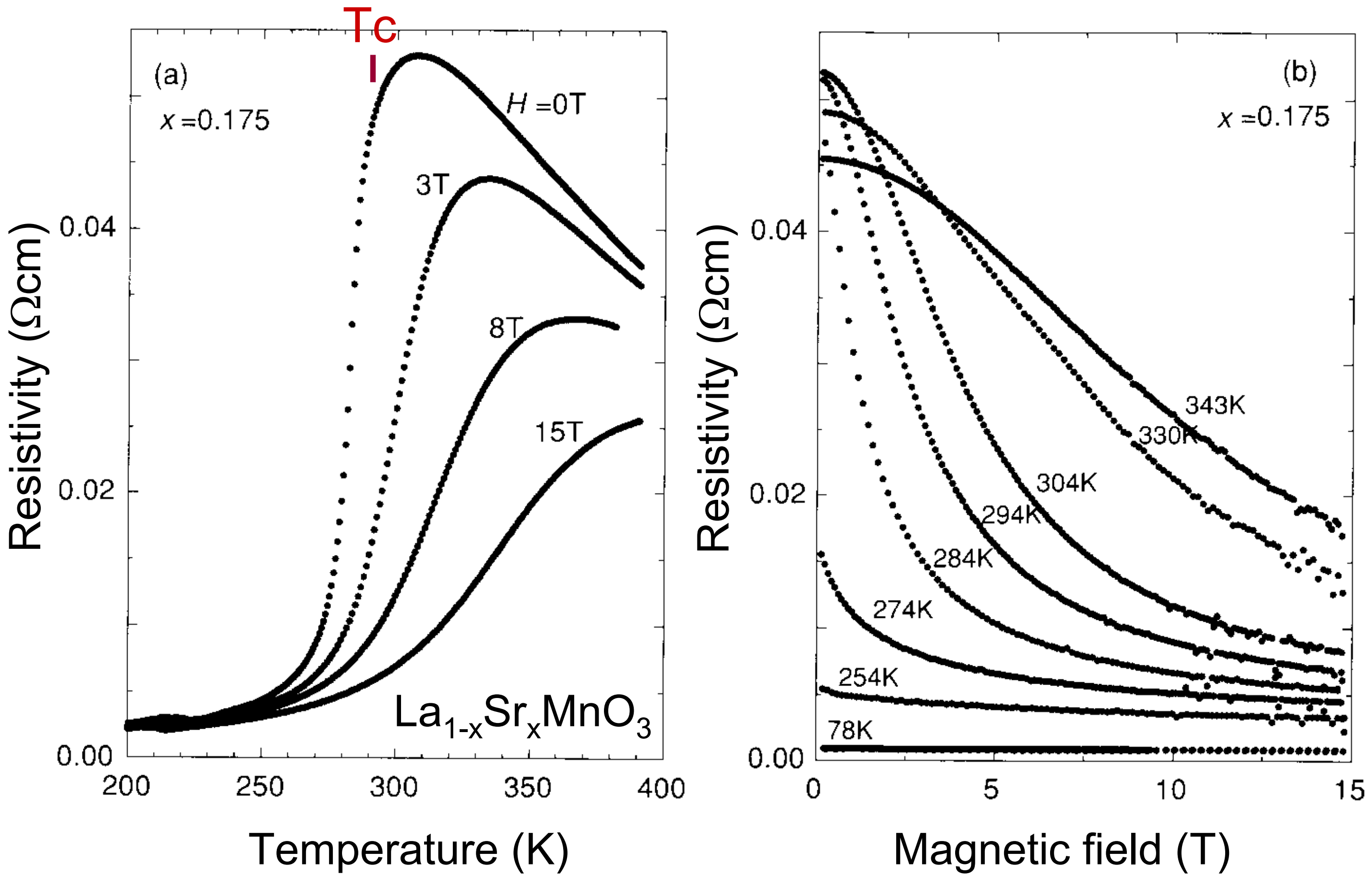

Y. Tokura et al., J. Phys. Soc. Jpn. '94

Perovskite-type transition-metal oxdies

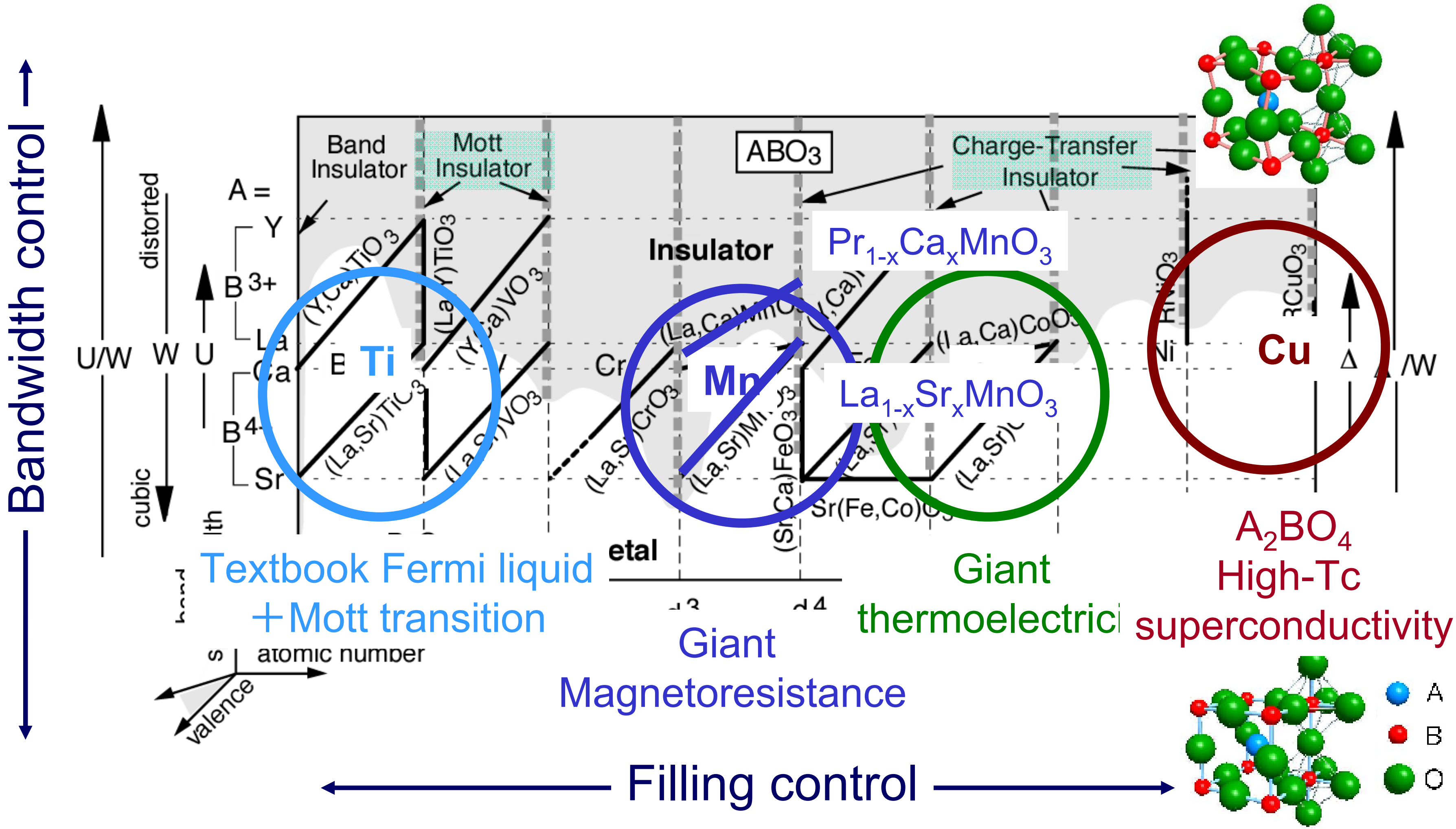

M. Imada, A. Fujimori and Y. Tokura, Rev. Mod. Phys. '98

Spin-charge-orbital ordering in perovskite-type Mn oxdies

$Pr_{1-x}Ca_xMnO_3$

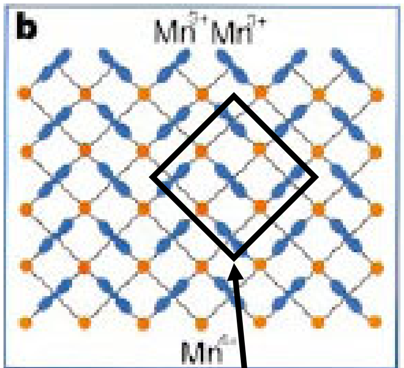

x=0.5

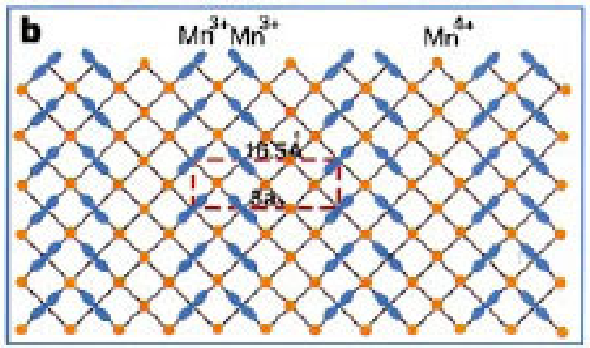

x=0.67

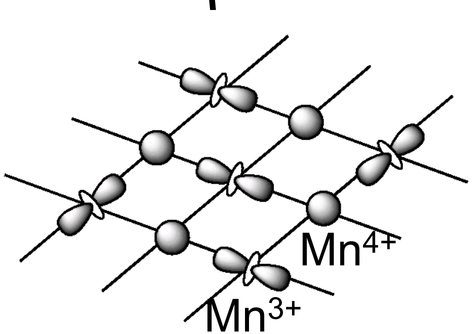

Jahn-Teller distortion of MnO_6 octahedron

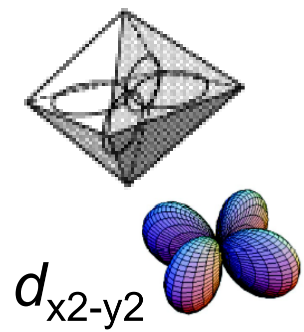

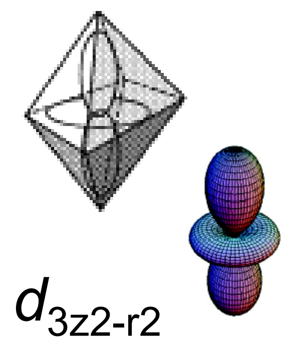

Even bigger magnetoresistance in narrow-band Mn oxdies

Magneto-resistance

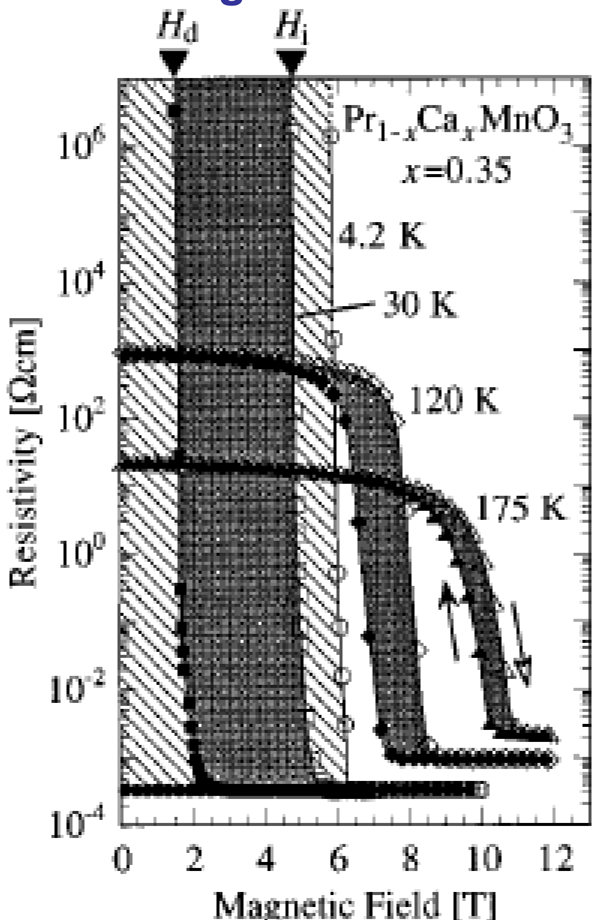

Resistance drop by electric field

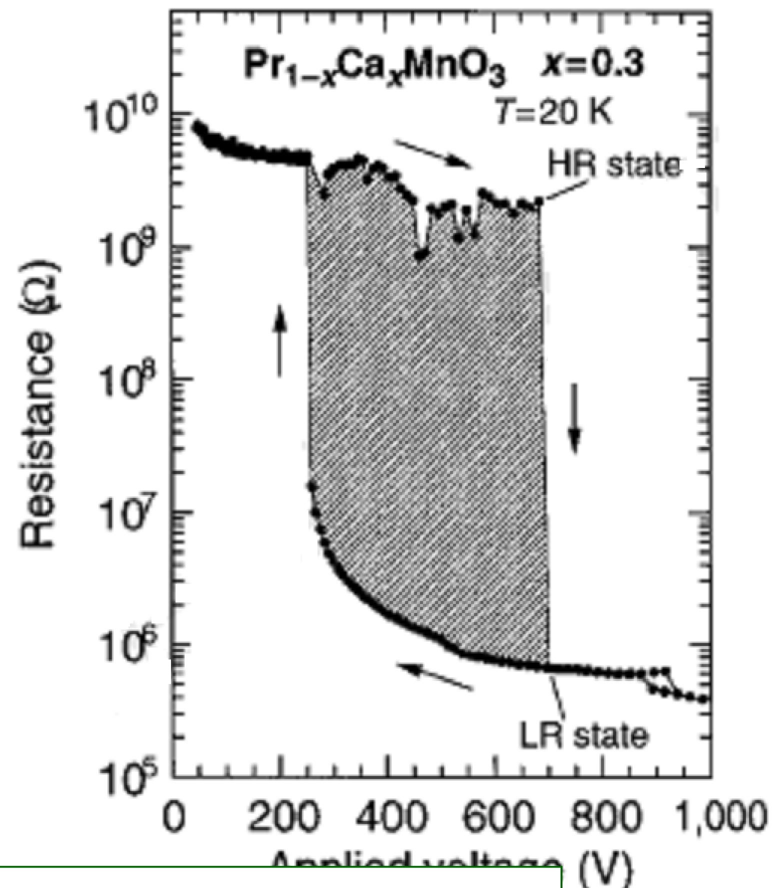

Metal-insulator transition induced by *H* or *E*

Y. Tomioka et al., Phys. Rev. B 1996

A. Asamitsu et al., Nature 1997

Fabrication and characterization

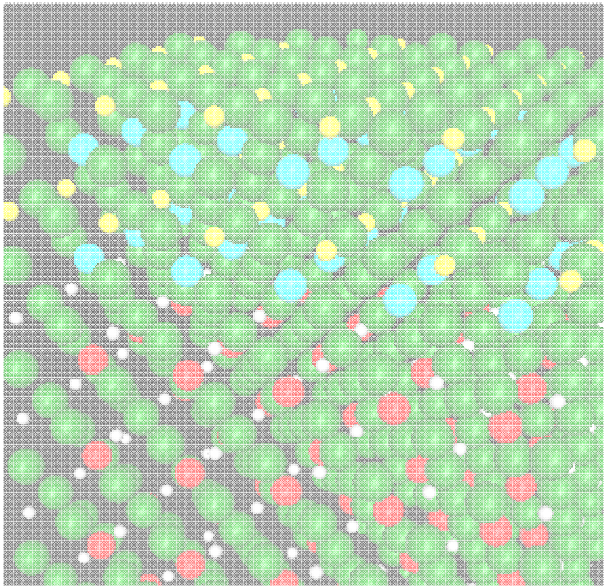

MBE using pulsed laser deposition (PLD)

PLD system

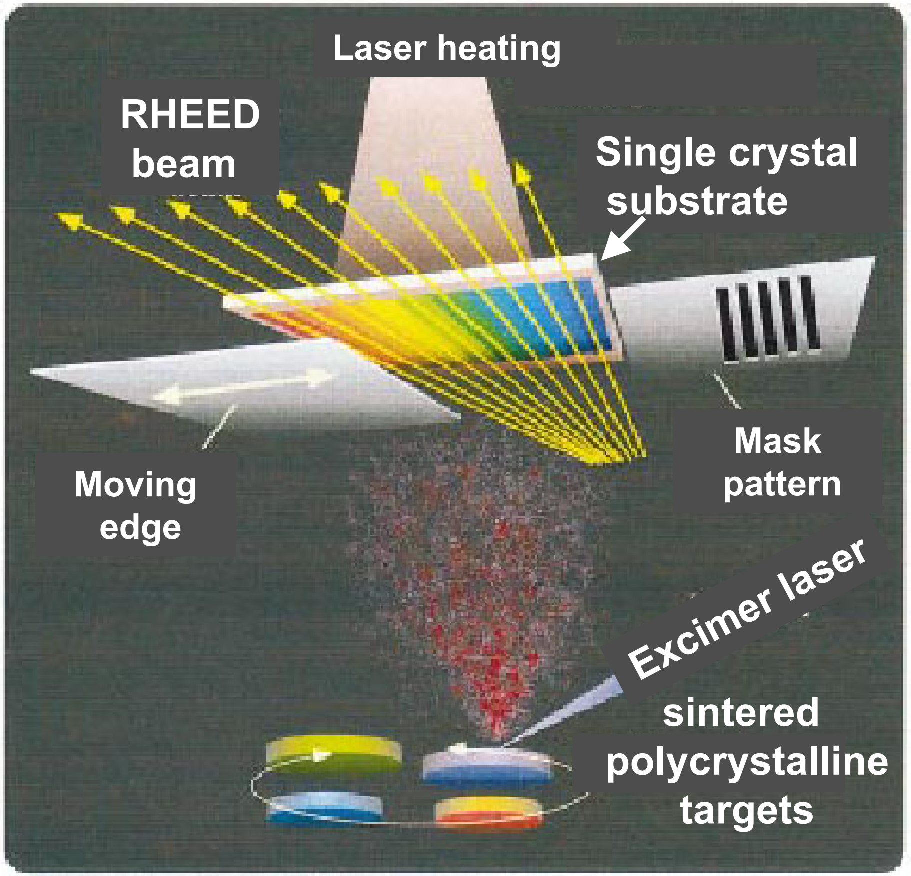

Monitoring RHEED oscillations

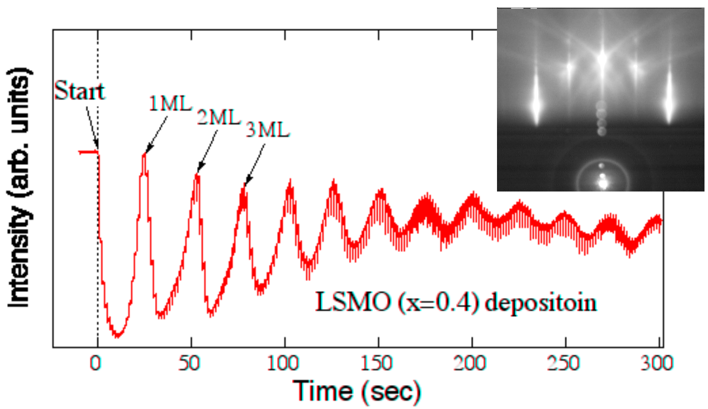

T. Ohnishi et al., APL ’01.

Characterization of epitaxially grown thin film on $SrTiO_3(001)$ substrate

Atomic force microscope (AFM)

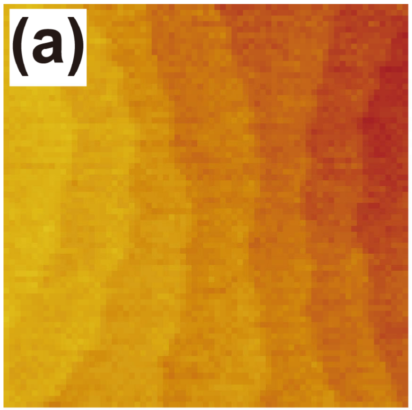

Transmission electron Microscopy (TEM)

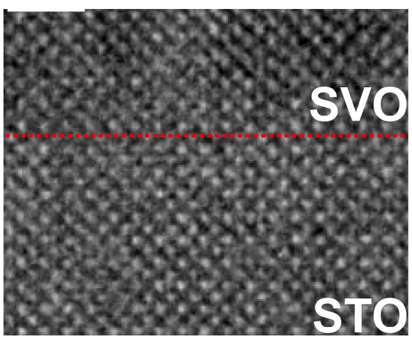

Reciprocal space mapping of XRD pattern

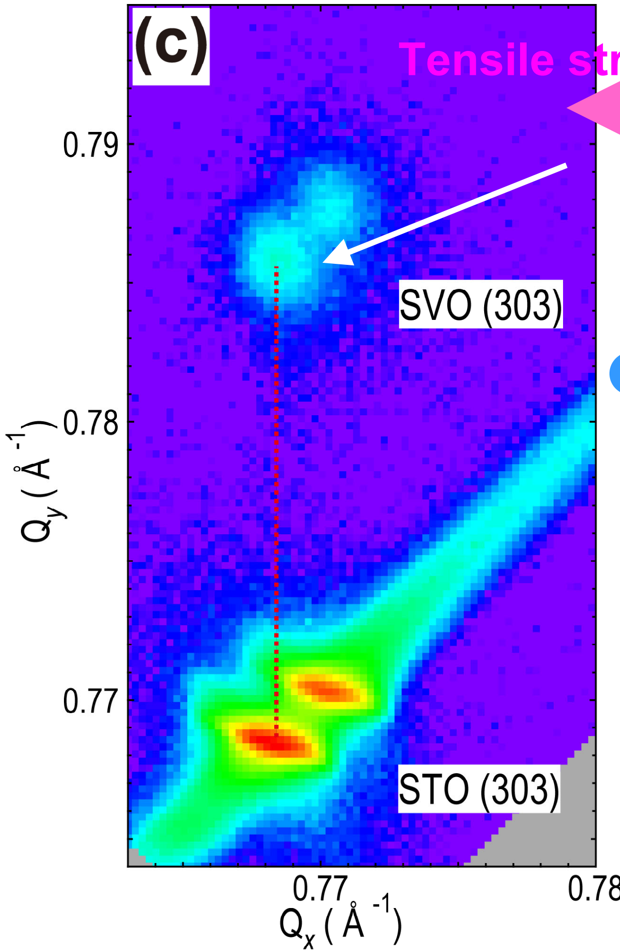

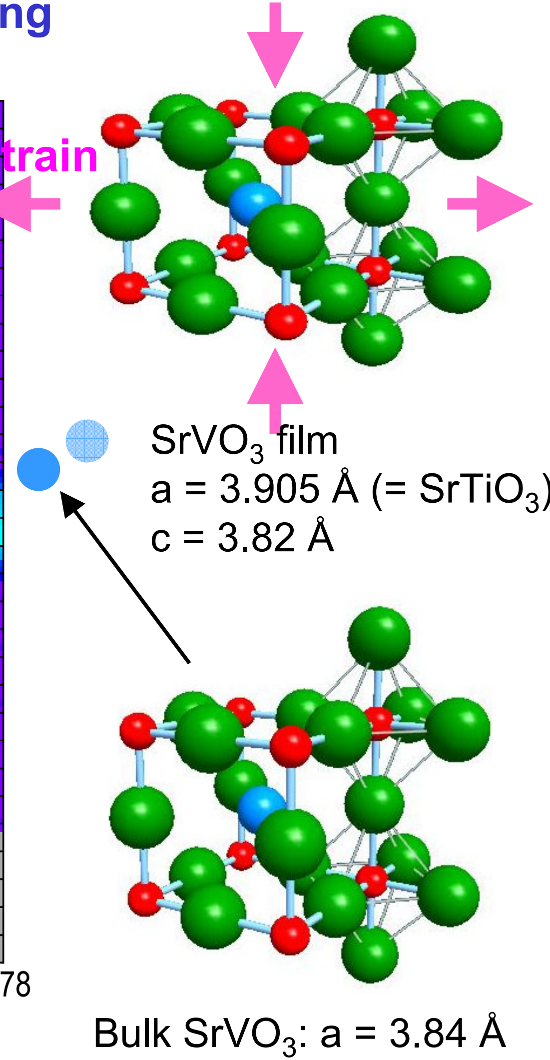

K. Yoshimatsu et al.

Characterization of epitaxially grown superlattice on $SrTiO_3(001)$ substrate

$[(LaMnO_3)_{11.8} / (SrMnO_3)_{4.4}]_6$ superlattice

TEM image

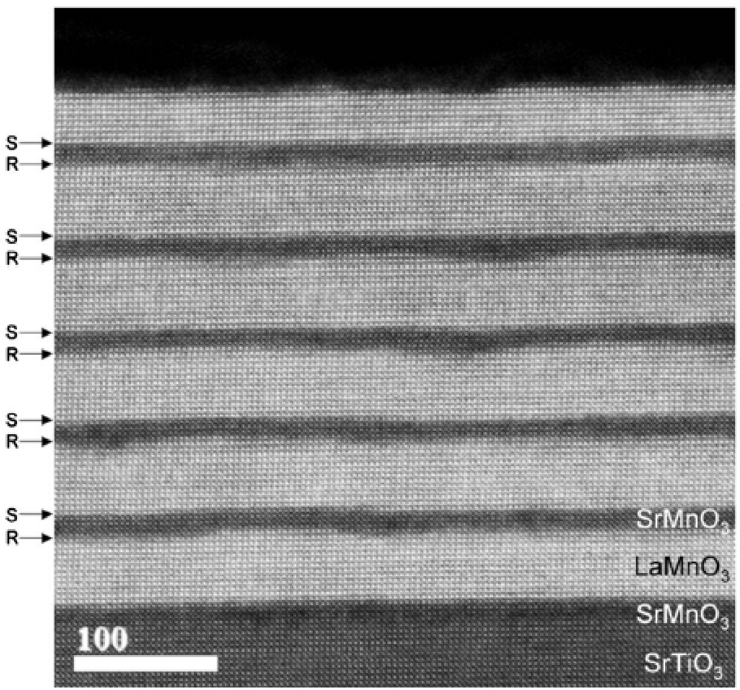

X-ray reflection

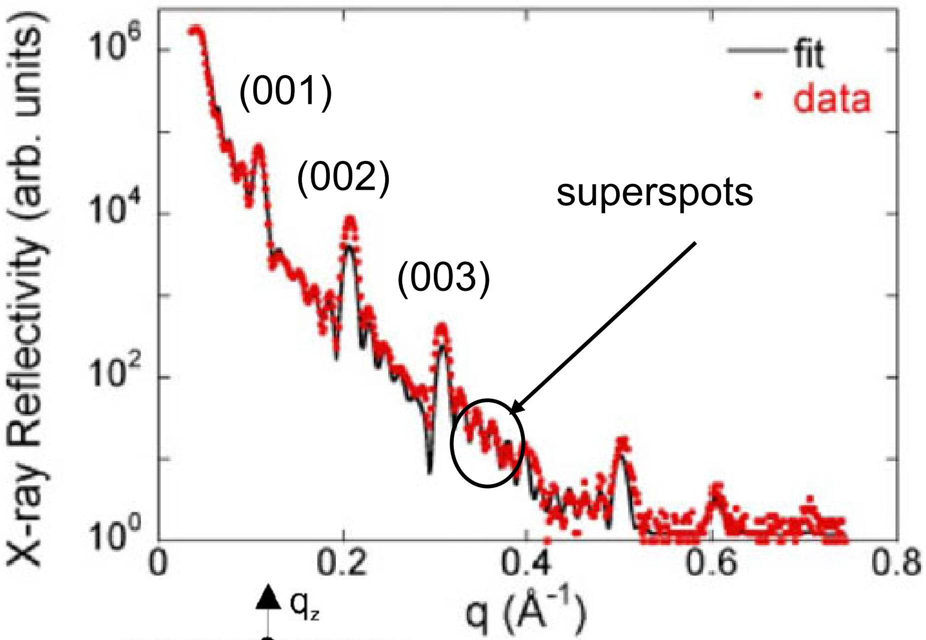

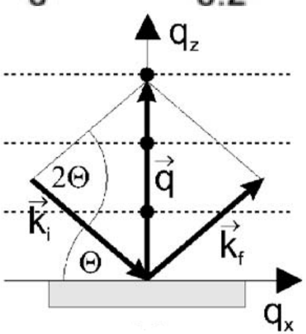

S.J. May et al. PRB ’08

Soft x-ray scattering from $[(LaMnO_3)_m/(SrMnO_3)_{m'}]_n$ superlattice

X-ray scattering (reflectivity)

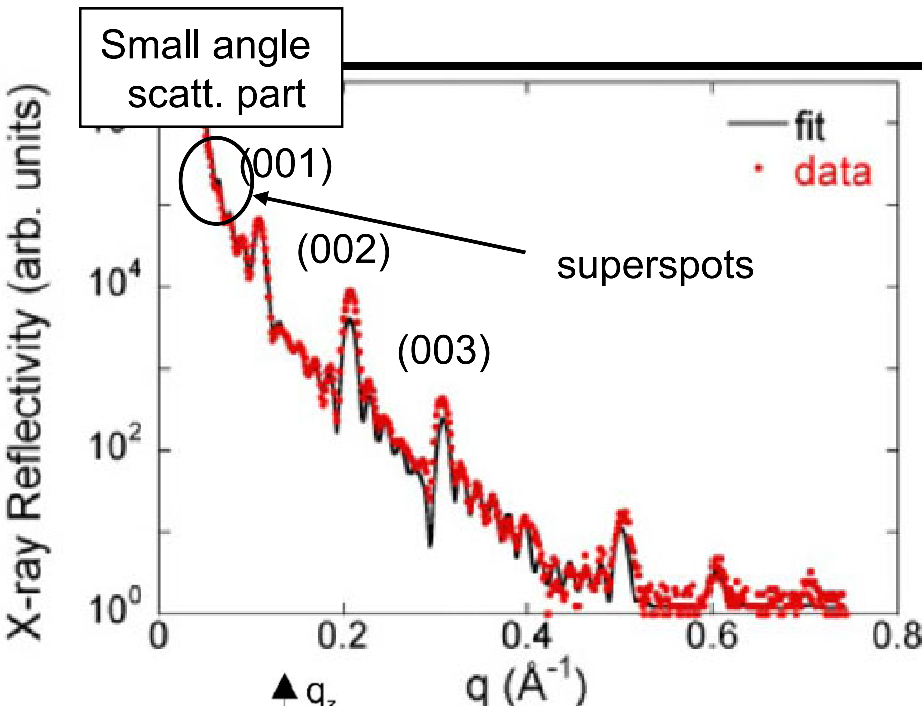

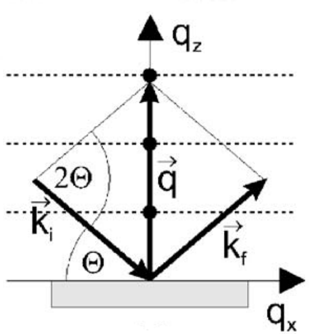

S.J. May et al. PRB '08

Soft X-ray scattering

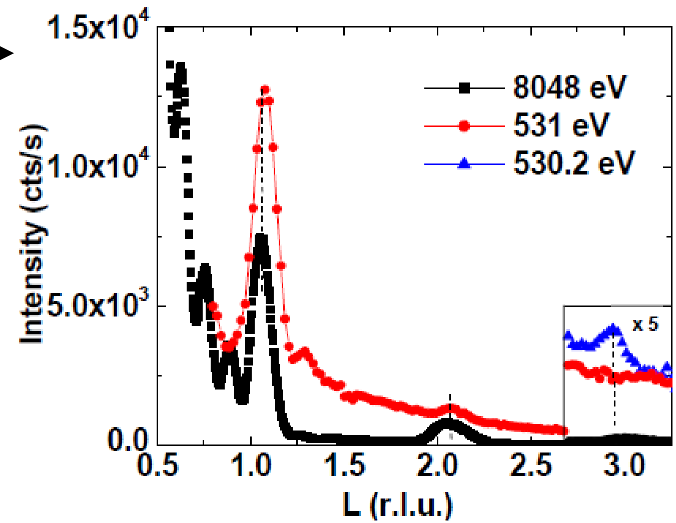

$S(003) = 2f_{int} - f_{LMO} - f_{SMO}$

(003) (in units of 1/m+m'):
visible only at O 1*s* edge
→ O 2*p* hole doping only at interface.

S. Smadici et al.,. PRL '07

In-situ ARPES measurement system of PLD-grown oxide thin films

AFM image

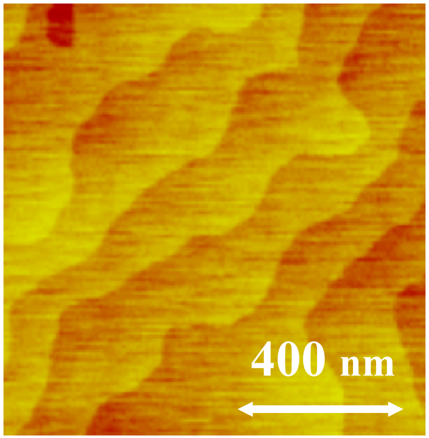

LEED

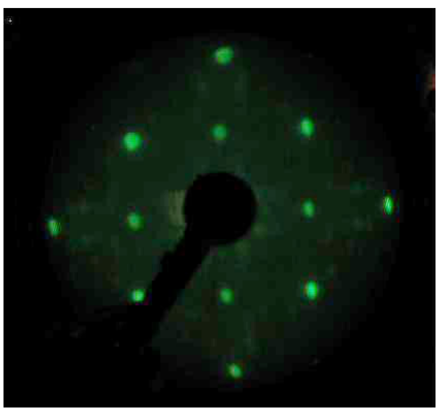

Combined photoemission-laser MBE system

Oshima-Kumigashira group

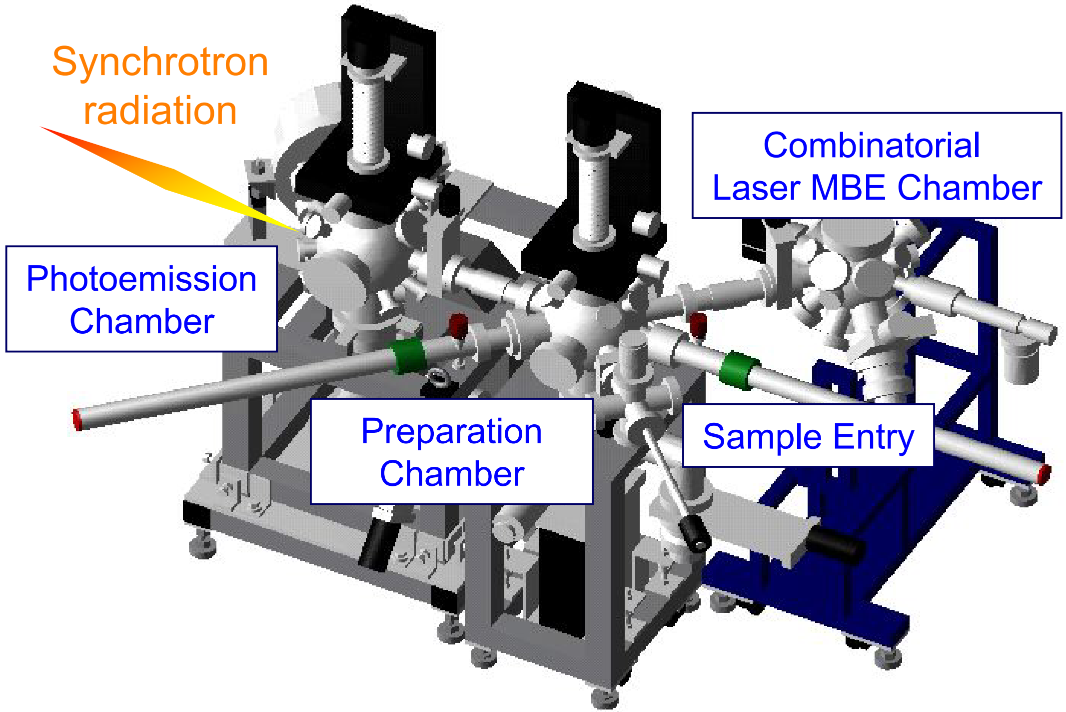

Photon Factory BL-1c, BL2c, BL-28

K. Horiba et al., Rev. Sci. Instrum. 74, 3406 (2003).

Photoemission spectroscopy of buried interfaces

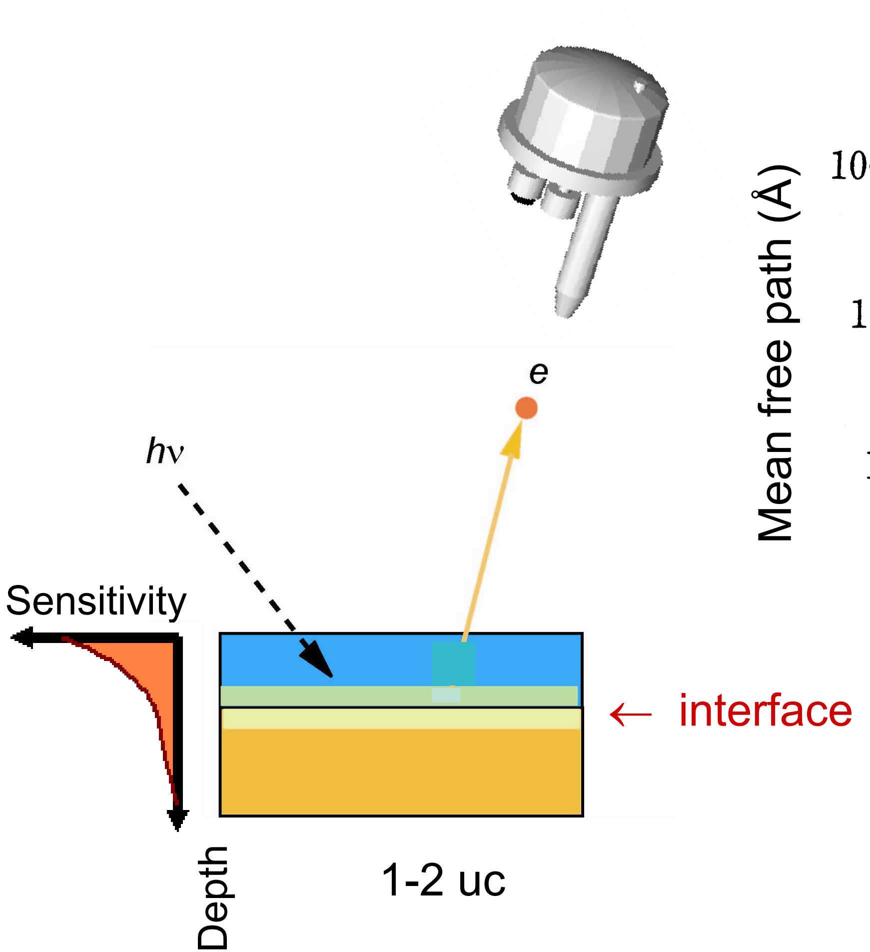

Probing depth of photoelectrons

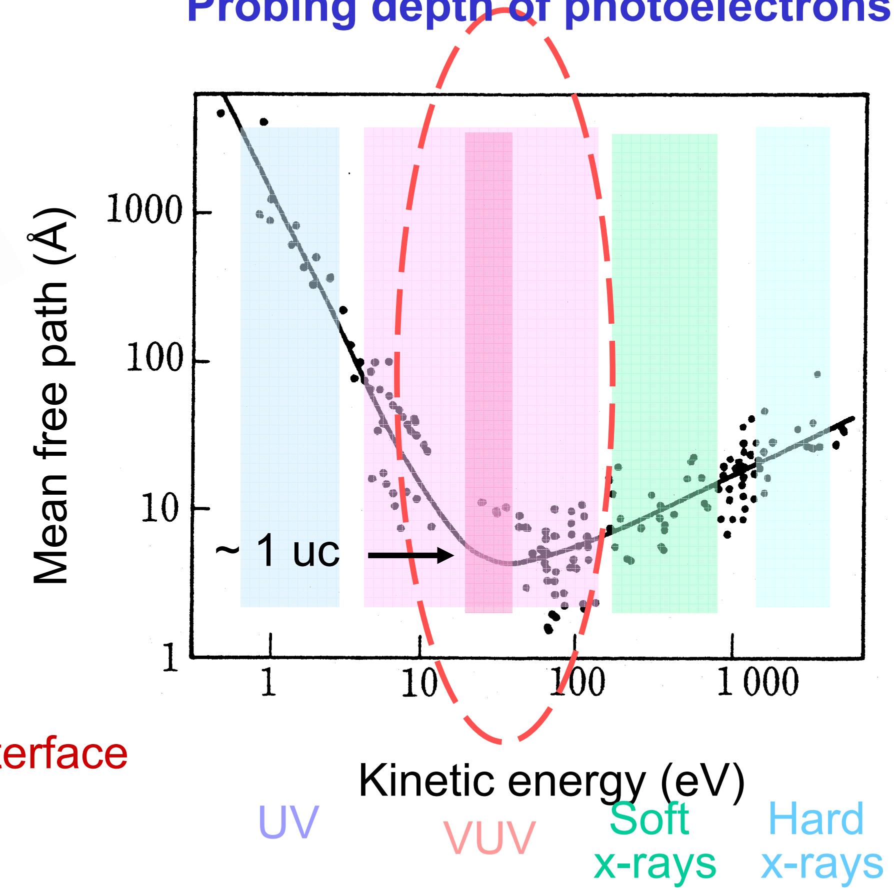

Photoemission spectroscopy of buried interfaces

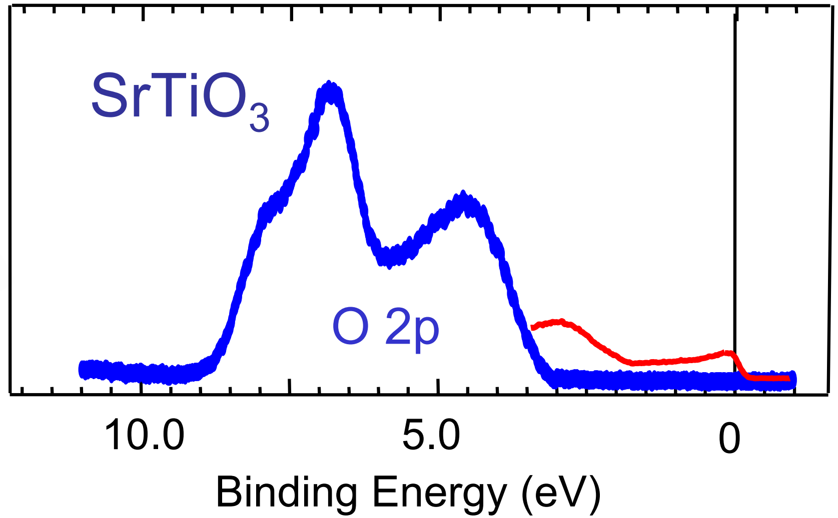

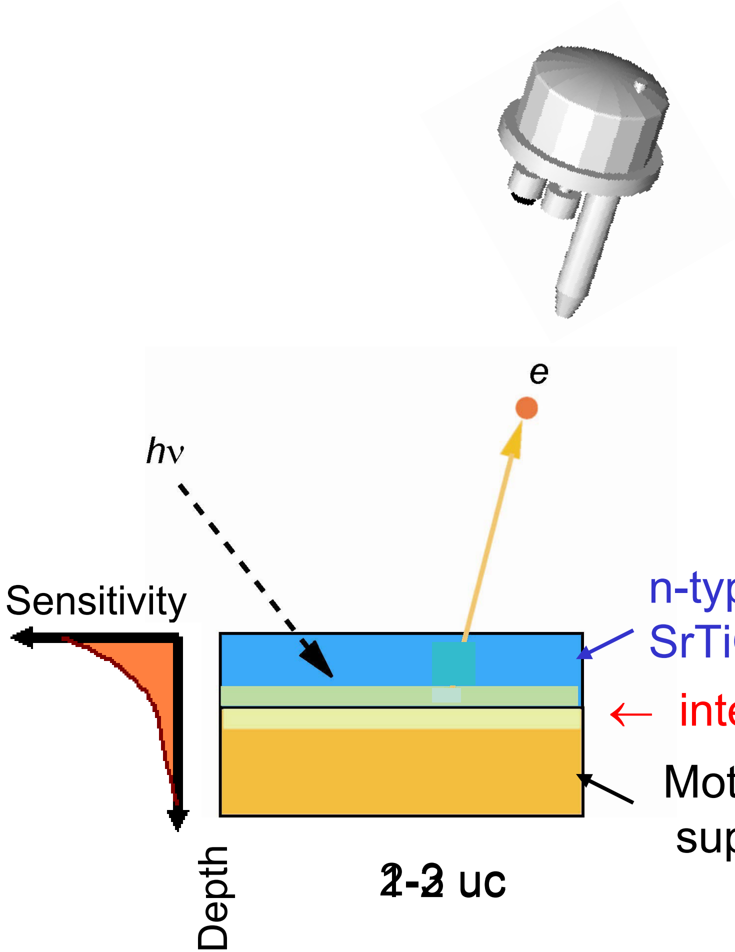

n-type band insulator
SrTiO$_3$, LaAlO$_3$, TiO$_2$, ZnO, etc

← interfacial states

Mott insulator, metal,
superconductor, etc

Photoemission spectroscopy of buried interfaces

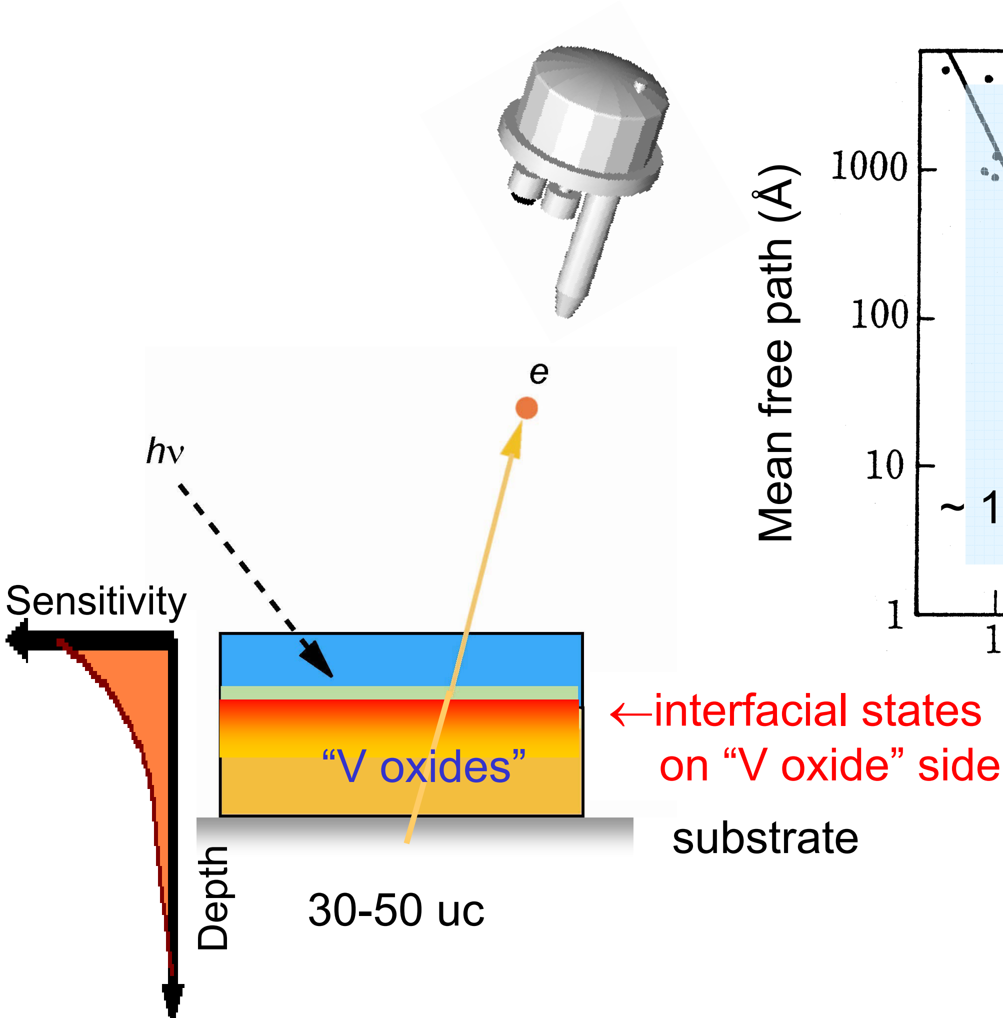

Probing depth of photoelectrons

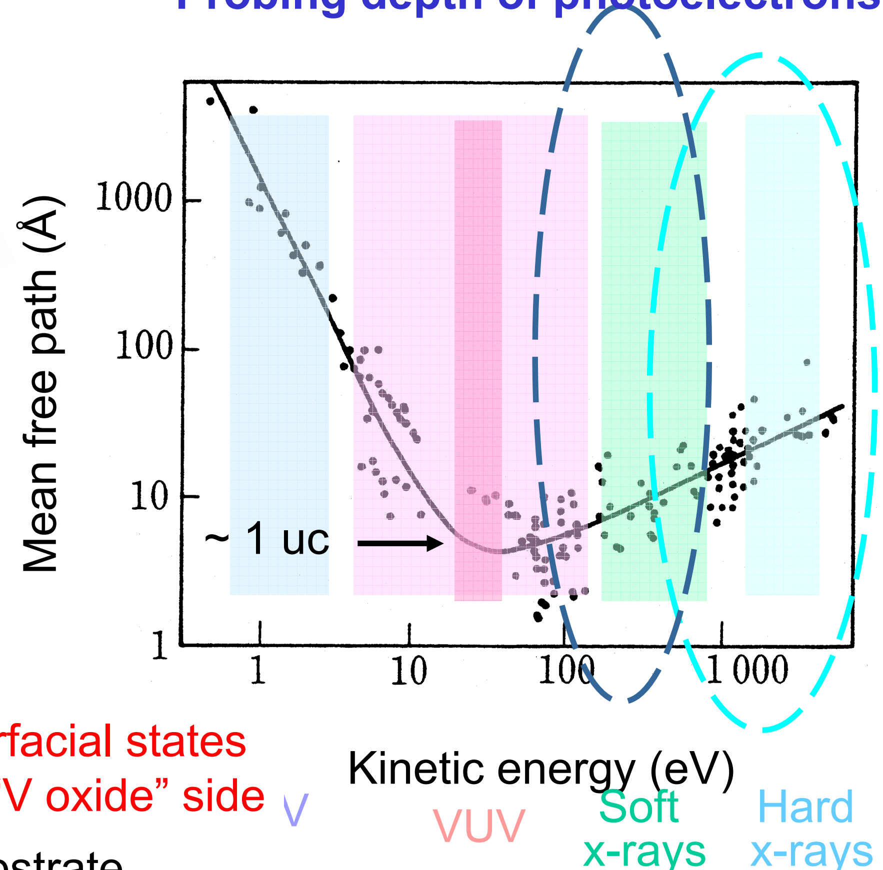

Photoemission spectroscopy of buried interfaces

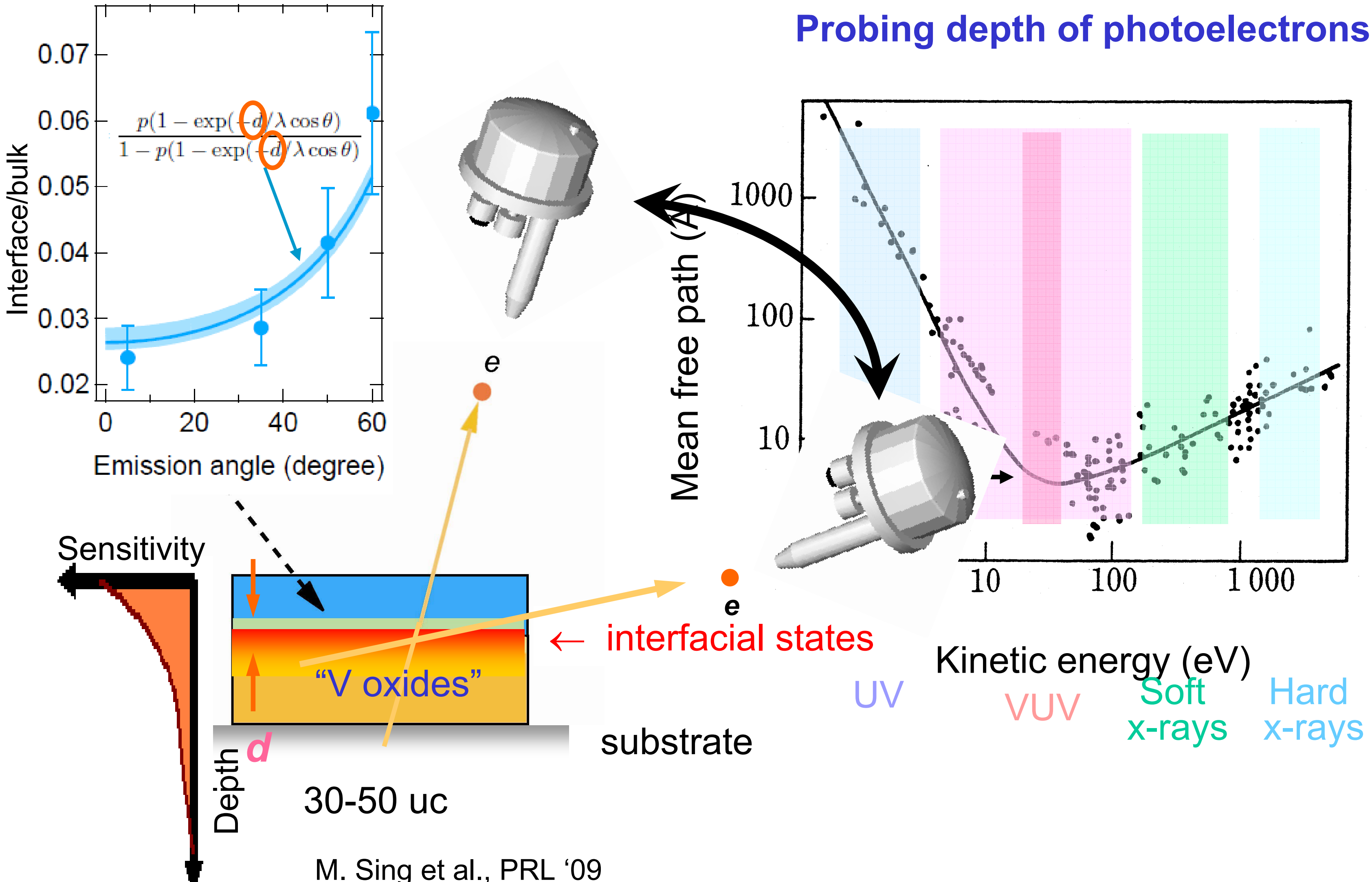

M. Sing et al., PRL '09

Polarized soft x-ray absorption spectroscopy (XAS)

Magnetic circular x-ray dichroism (XMCD)

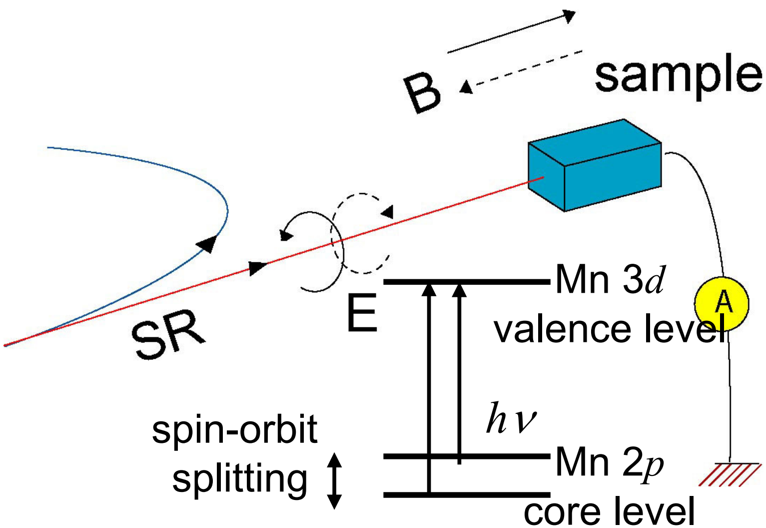

element specific probe

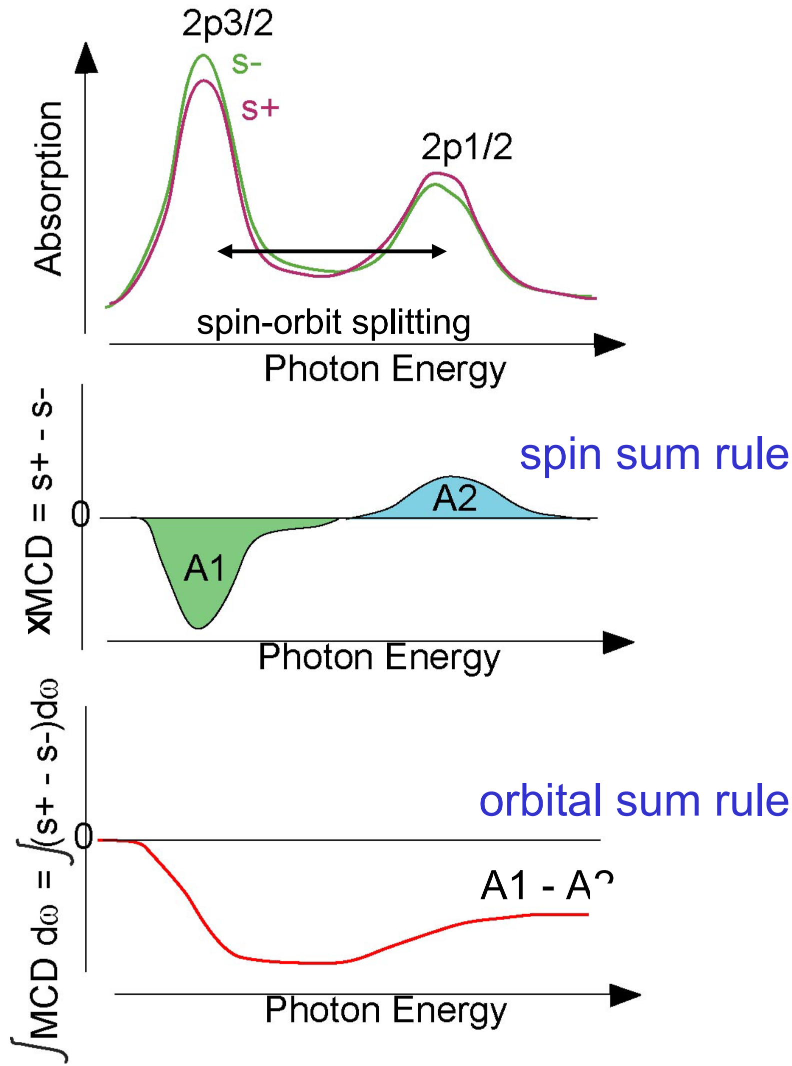

XMCD of buried interfaces

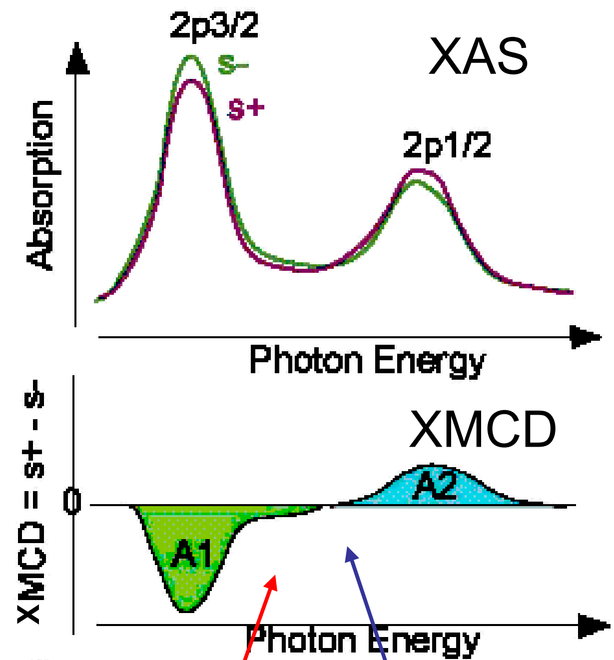

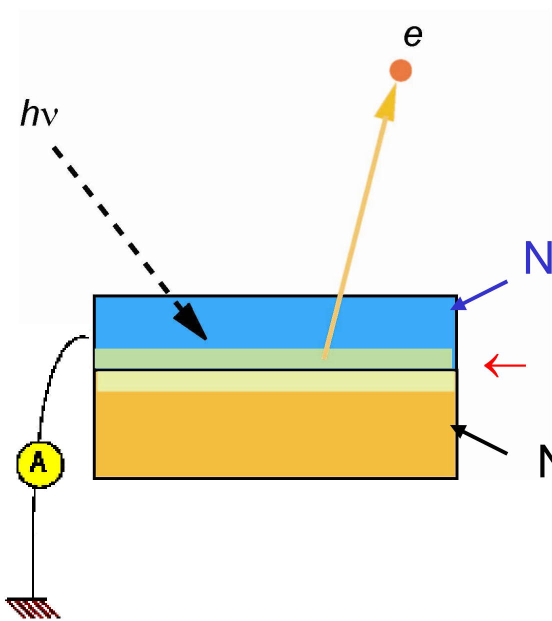

Non-magnetic (Induced magnetism)

← ferromagnetic interface

Non-magnetic or Magnetic

element specific probe

Outline

- Electronic structure of transition-metal oxides
- Fabrication and characterization

- Interfacial electronic structure
- Effects of finite thickness
- Effects of epitaxial strain

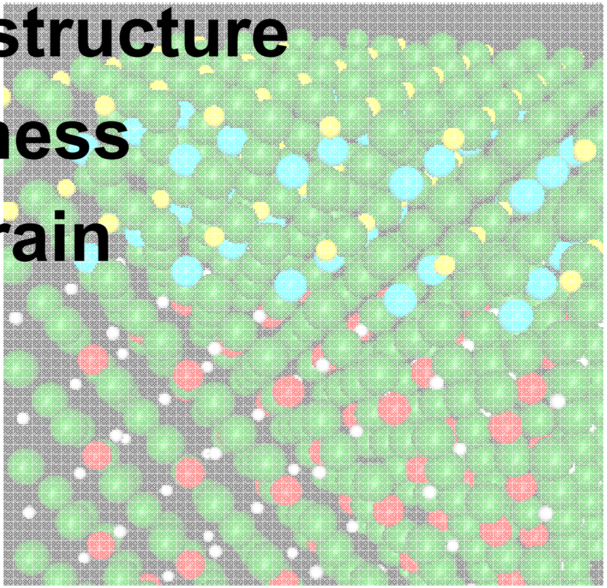

Interfacial electronic structure

Metallic states between two insulators

-States near the Fermi level-

Interfaces

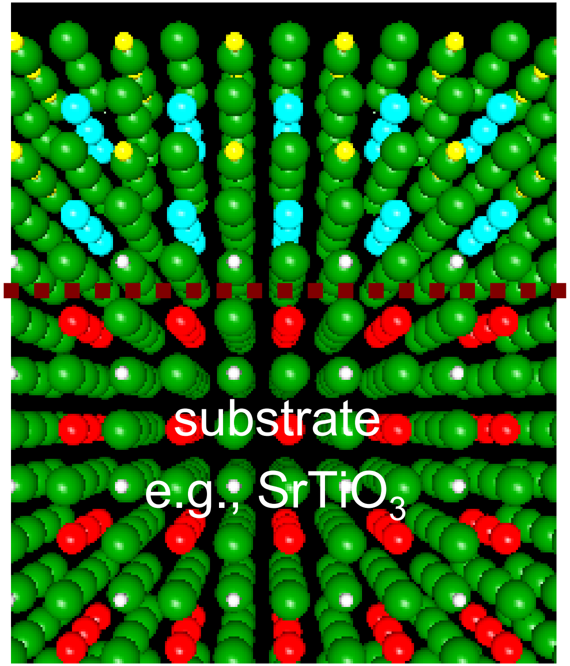

Metallic behavior of interfaces between Mott insulator and band insulator

Perovskite-type oxides ABO_3

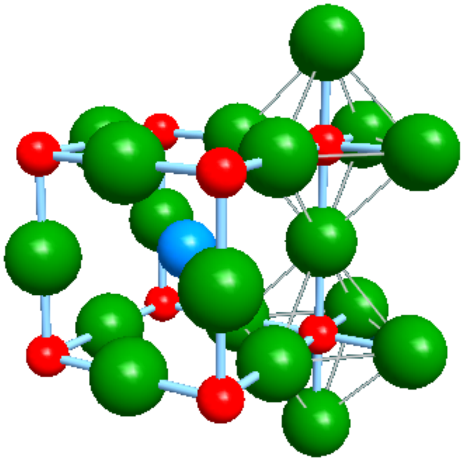

	A	Sr^{2+}	La^{2+}
	B	Ti^{4+} (d^0)	Ti^{3+} (d^1)
	O	O^{2-}	O^{2-}

$SrTiO_3$: d^0 (Ti^{4+}) band insulator

Metallic interfaces !

$LaTiO_3$: d^1 (Ti^{3+}) Mott insulator

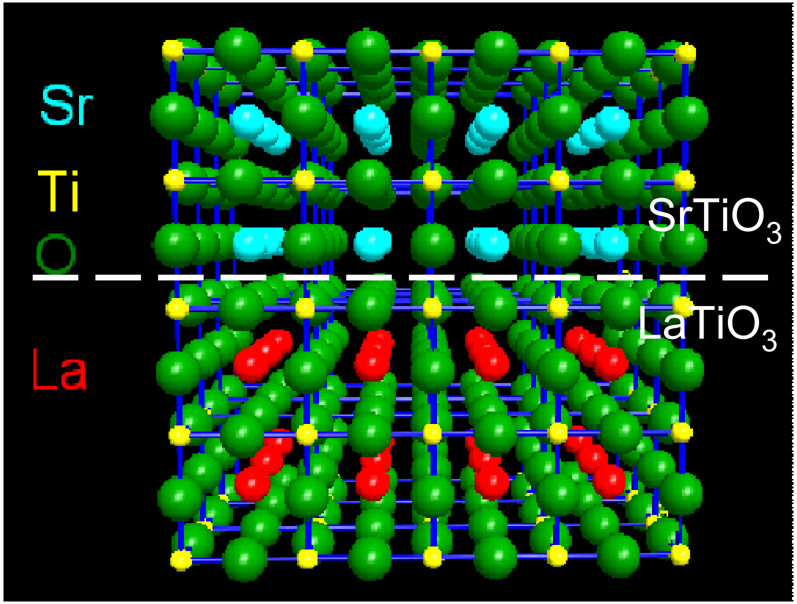

$LaTiO_3$ layers embedded in $SrTiO_3$: Penetration of Ti 3*d* electrons into $SrTiO_3$

$LaTiO_3$: d^1 (Ti^{3+}) Mott insulator
$SrTiO_3$: d^0 (Ti^{4+}) band insulator

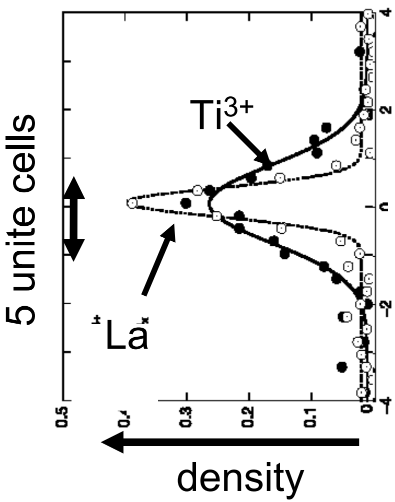

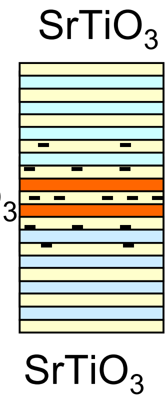

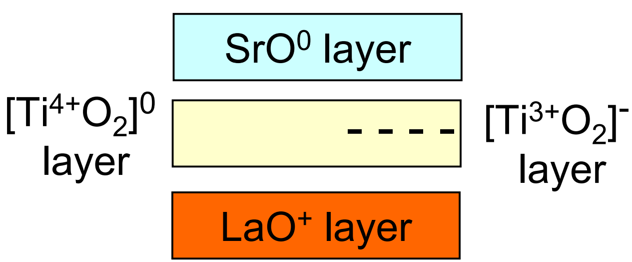

Atomically resolved EELS

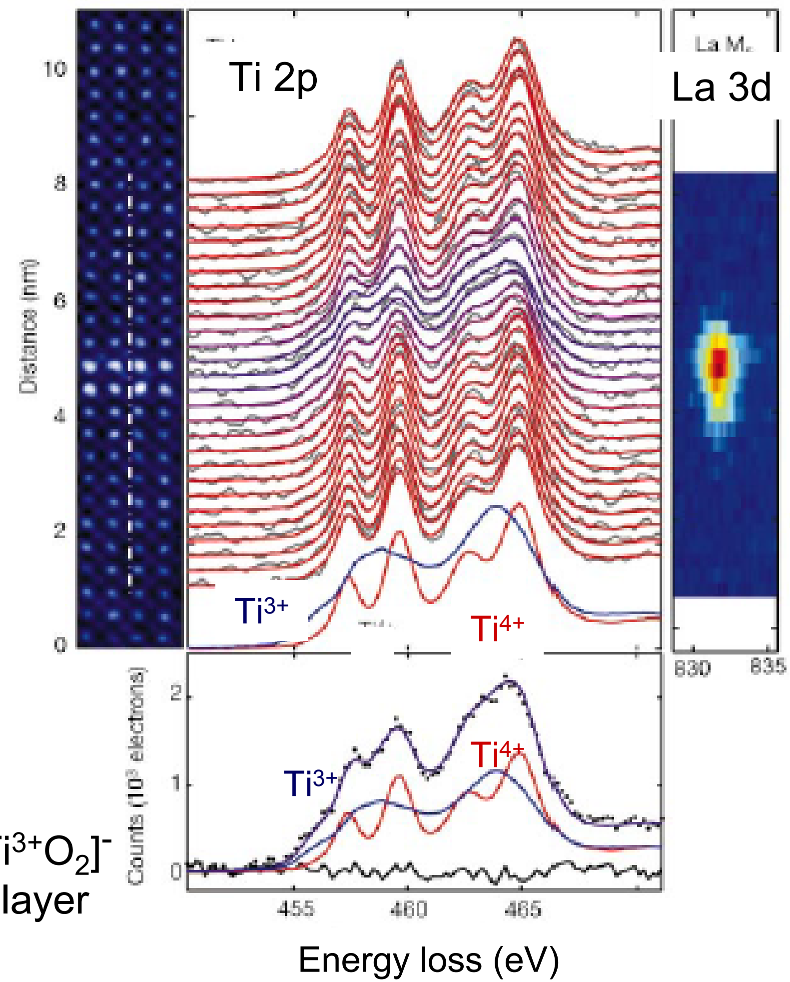

A. Ohtomo et al., Nature '02

Metallic transport of $SrTiO_3/LaTiO_3$ superlattices

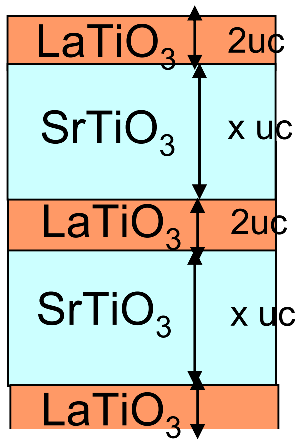

Lattice constant

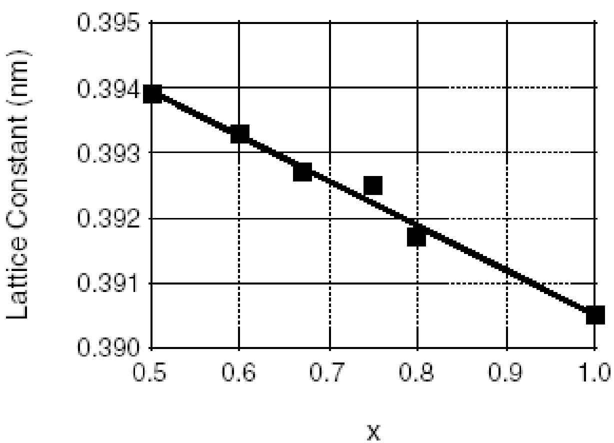

Electrical resistivity

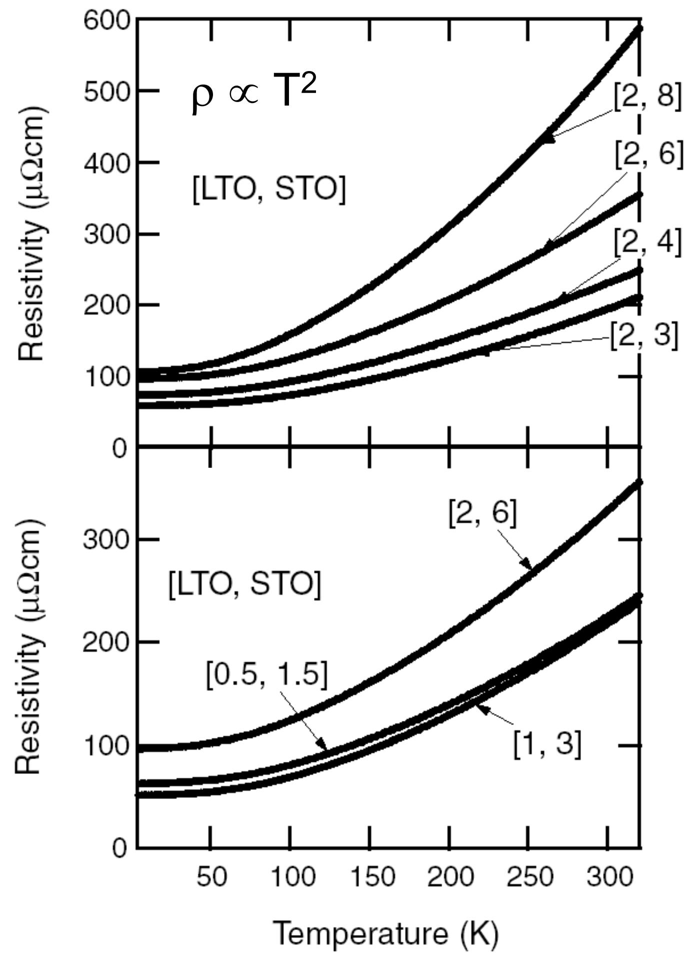

K. Shibuya, M. Lippmaa et al., JJAP '04

Photoemission spectra of $SrTiO_3/LaTiO_3$ interfaces

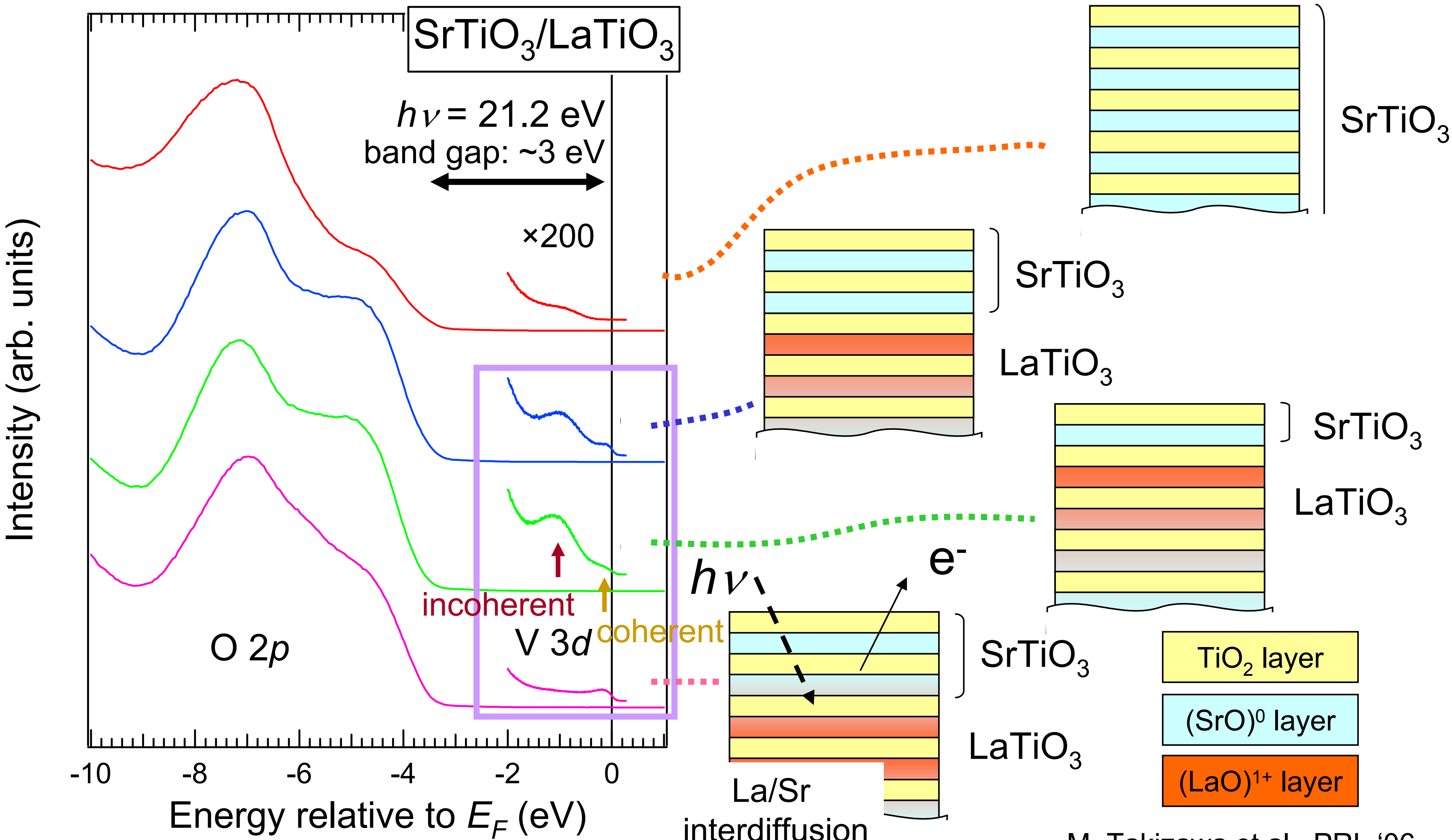

M. Takizawa et al., PRL '06

Photoemission spectra of $SrTiO_3/LaTiO_3$ interfaces

Ti 2*p*-3*d* resonant photoemission

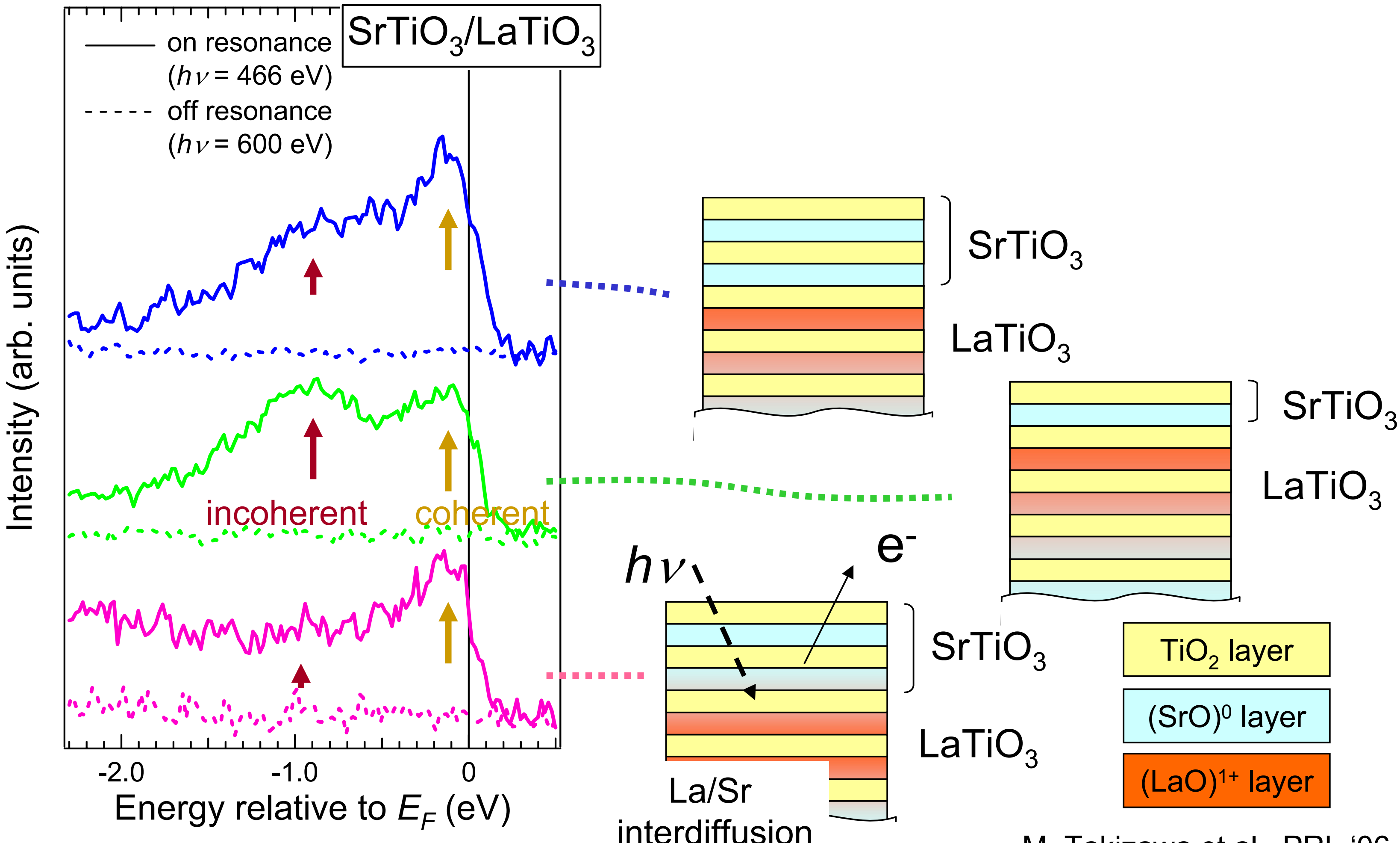

M. Takizawa et al., PRL '06

Metallicity at $SrTiO_3/LaTiO_3$ interfaces resulting from electronic reconstruction

Layer DMFT calculation including long-range Coulomb interaction

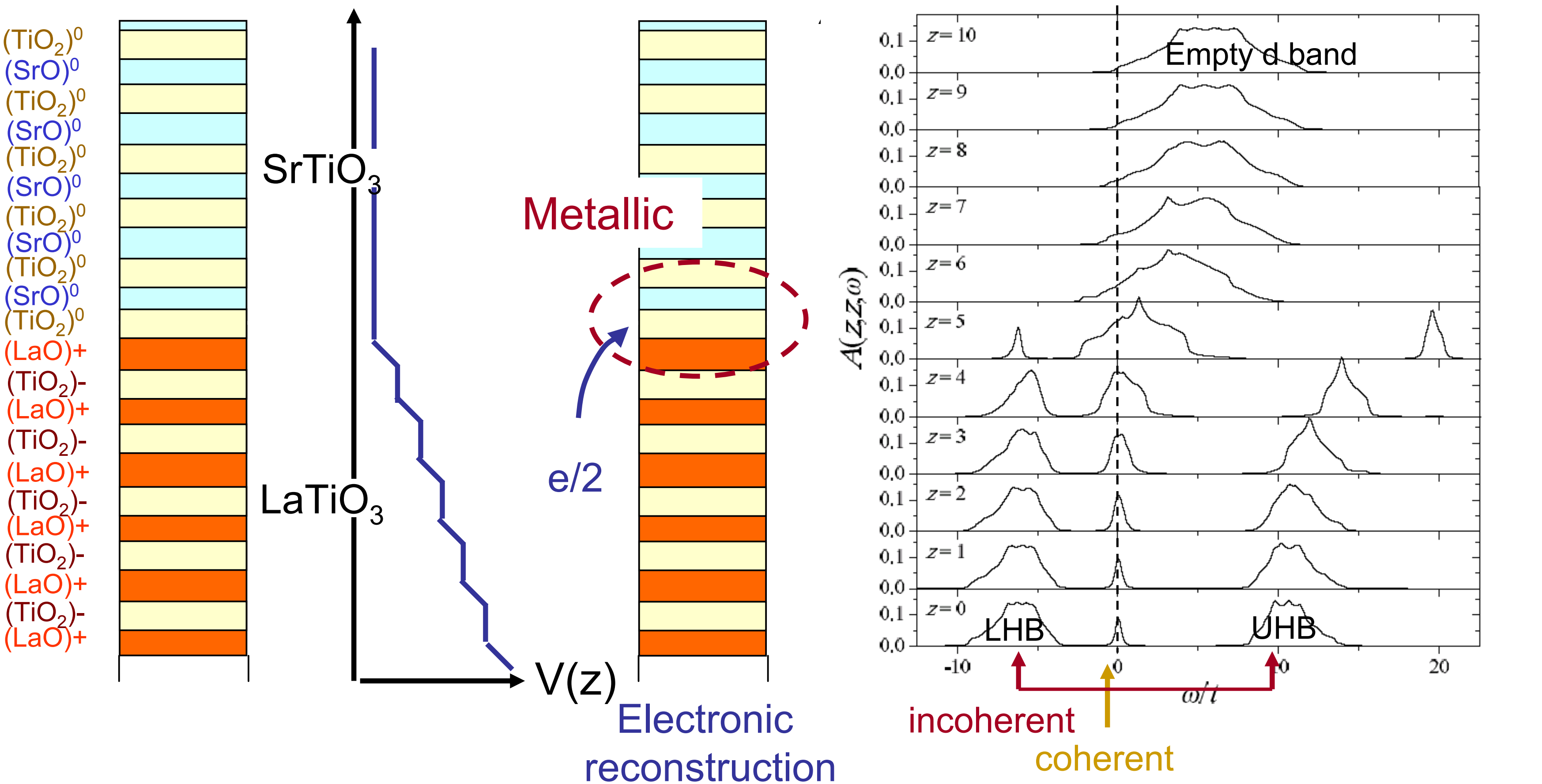

S. Okamoto and A. J. Millis, Nature '04, PRB '04

Interfacial electronic structure

Metallic states between two insulators

-Charge transfer in electronic reconstruction-

Interfaces

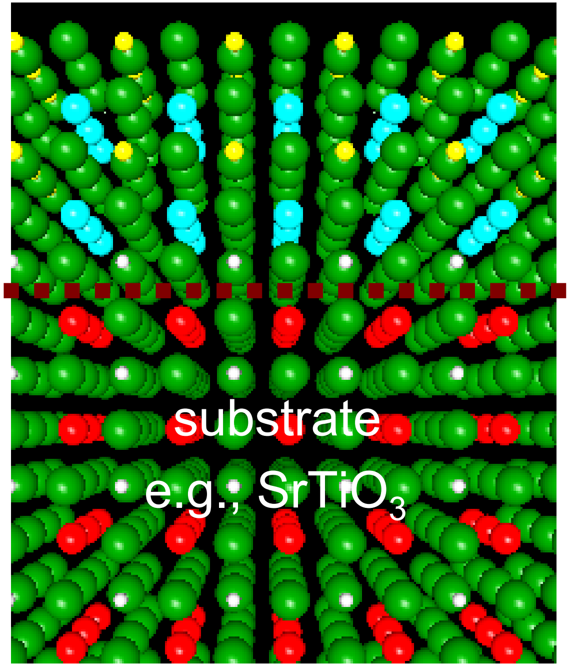

High mobility of *n*-type carriers at interfaces between two band insulators

$LaAlO_3$: band insulator
$SrTiO_3$: band insulator

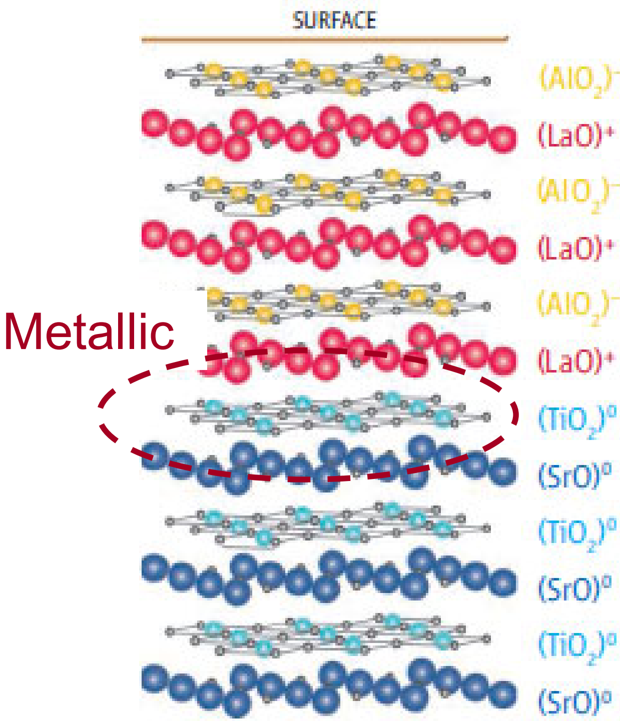

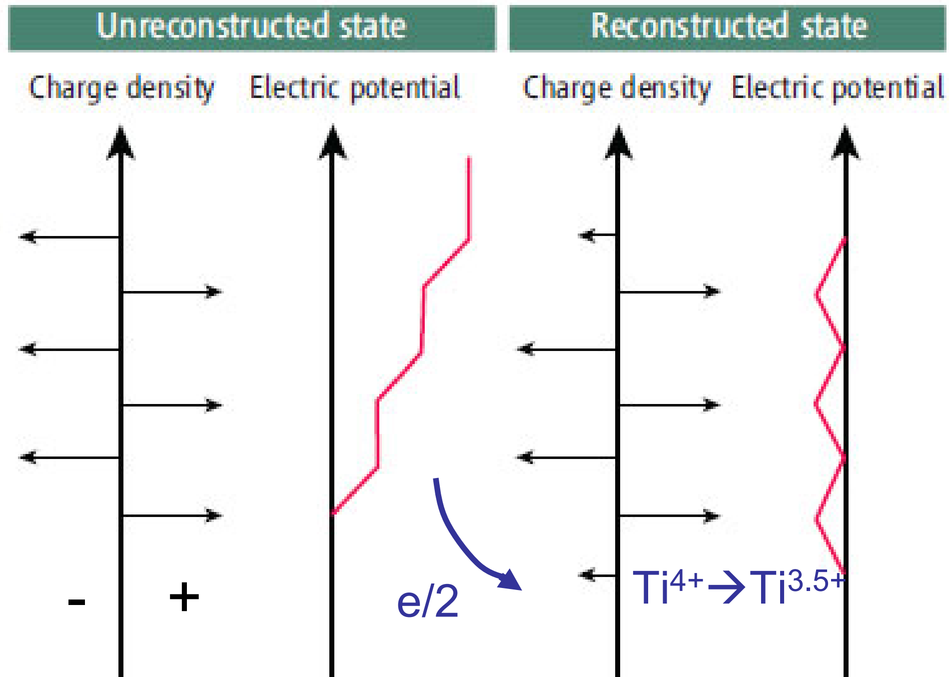

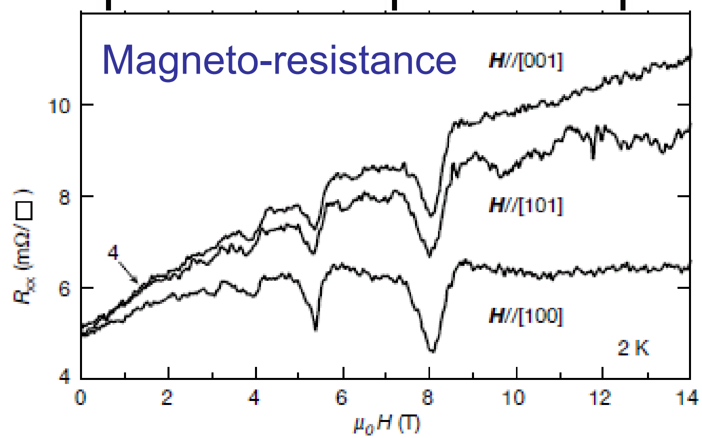

A. Ohtomo and H.Y. Hwang, Nature '04
H.Y. Hwang, Science '07

Critical thickness of ~4 uc for conductivity transition at $LaAlO_3/SrTiO_3$ interface

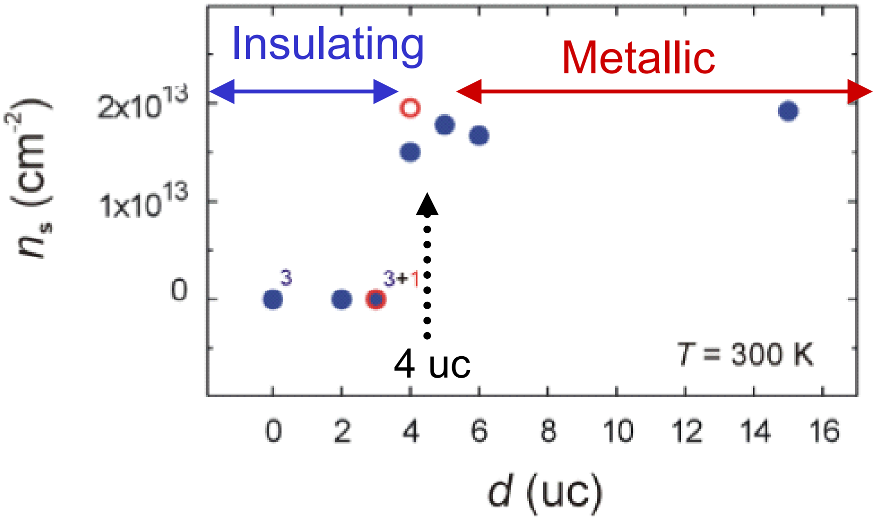

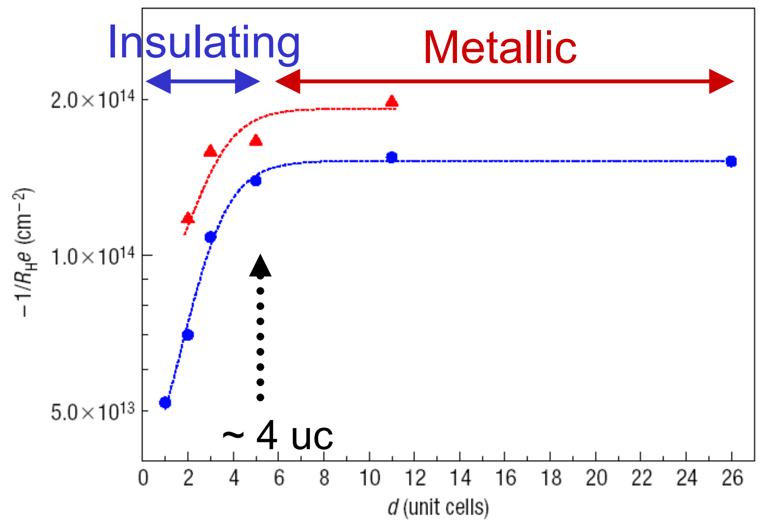

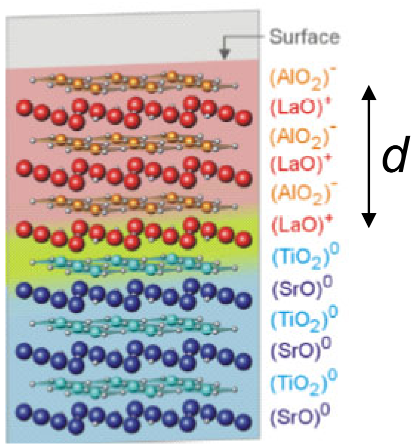

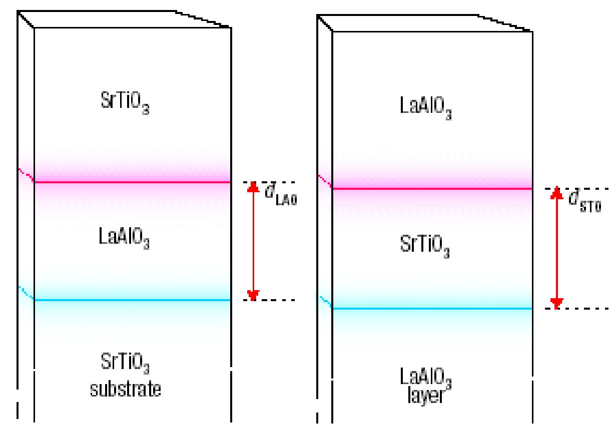

S. Thiel et al., Science '06

M. Huijben et al., Nature Mater.'06

Polar (111) surface of K_3C_{60} and its electronic reconstruction

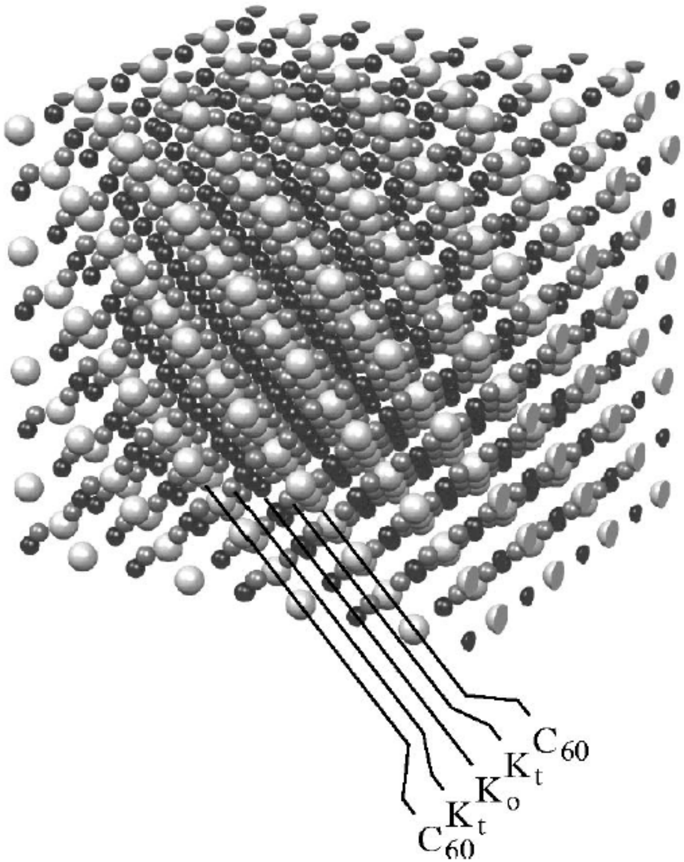

R. Hepster et al., PRB '00

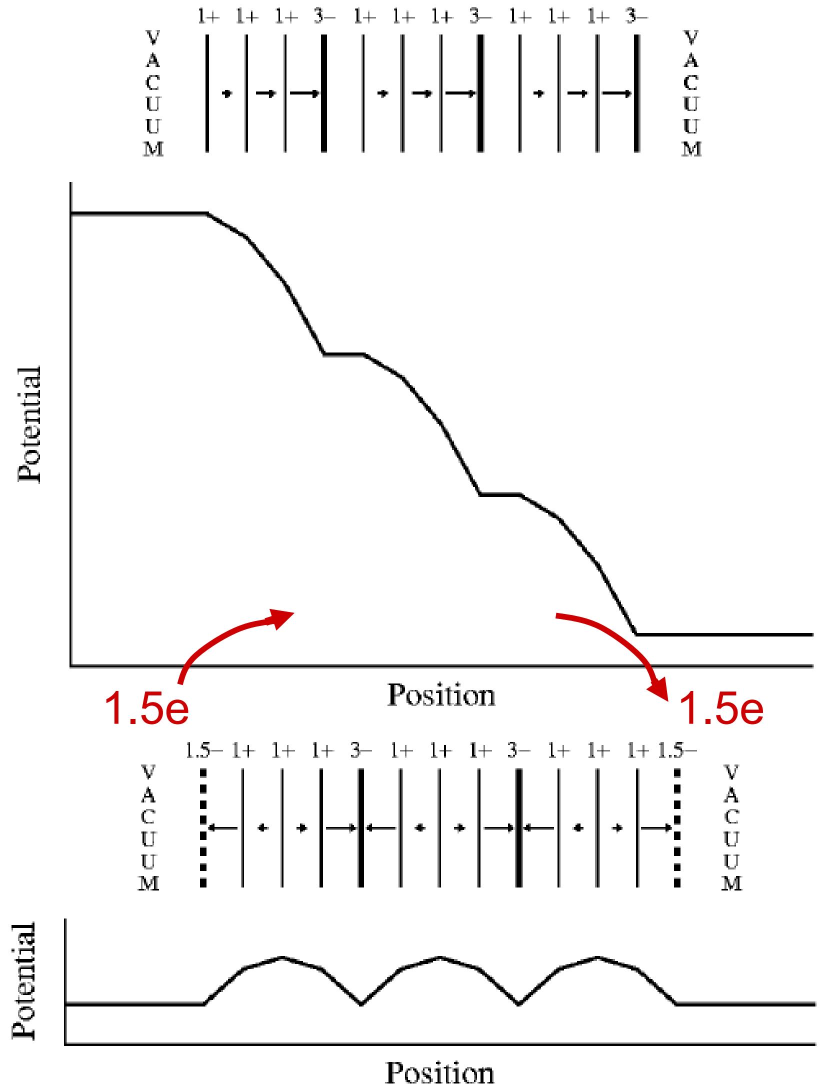

Photoemission spectroscopy of buried interfaces

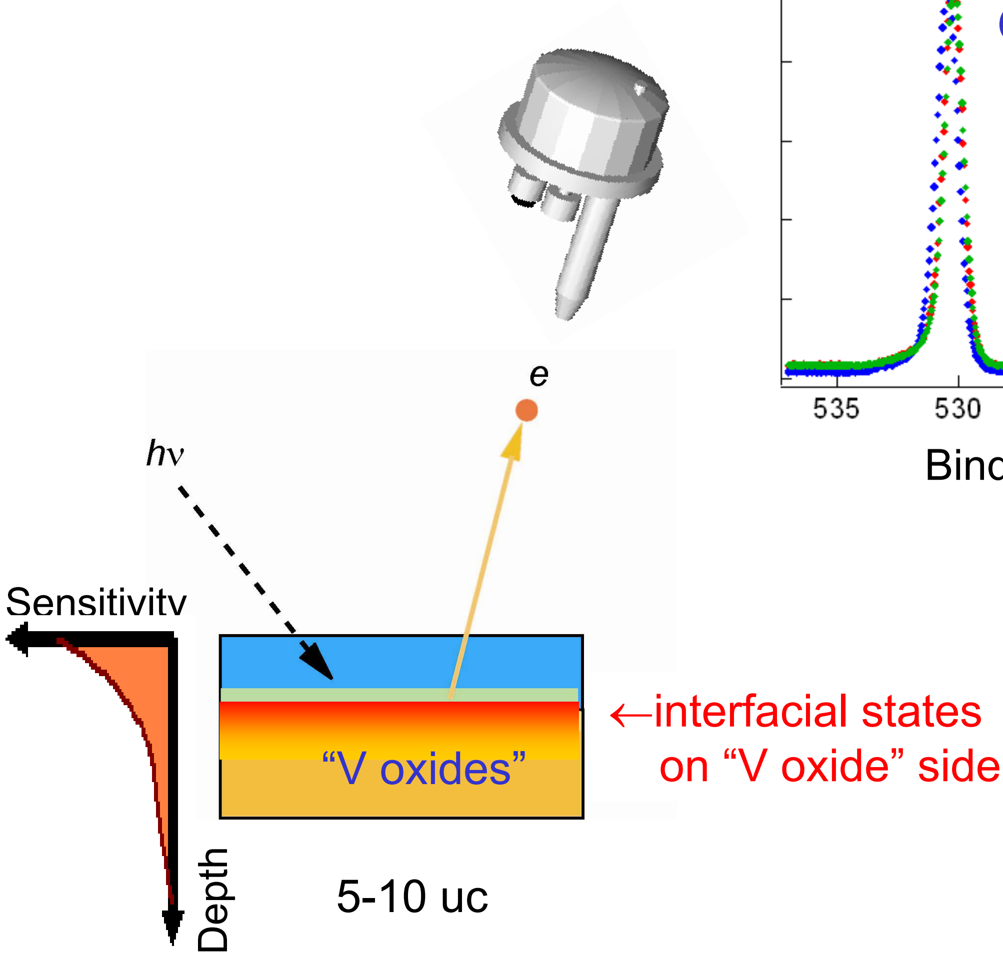

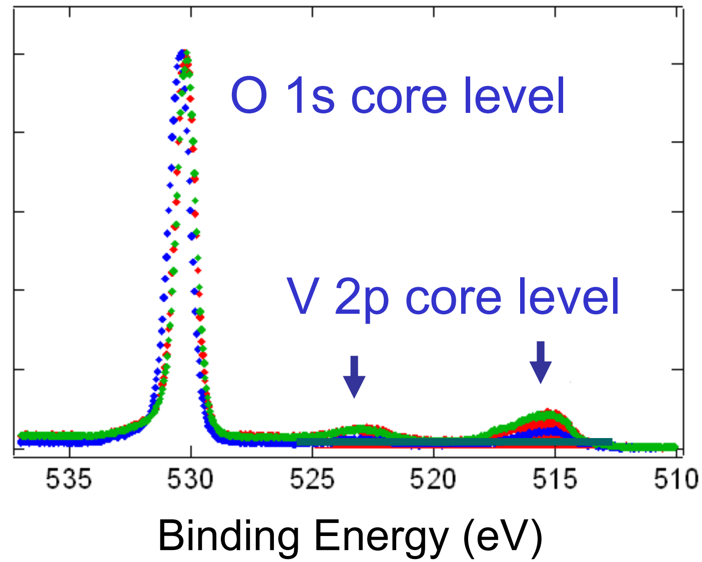

Evidence for Ti^{3+} states at the *n*-type $LaAlO_3/SrTiO_3$ interface

Ti 2*p* core-level spectra

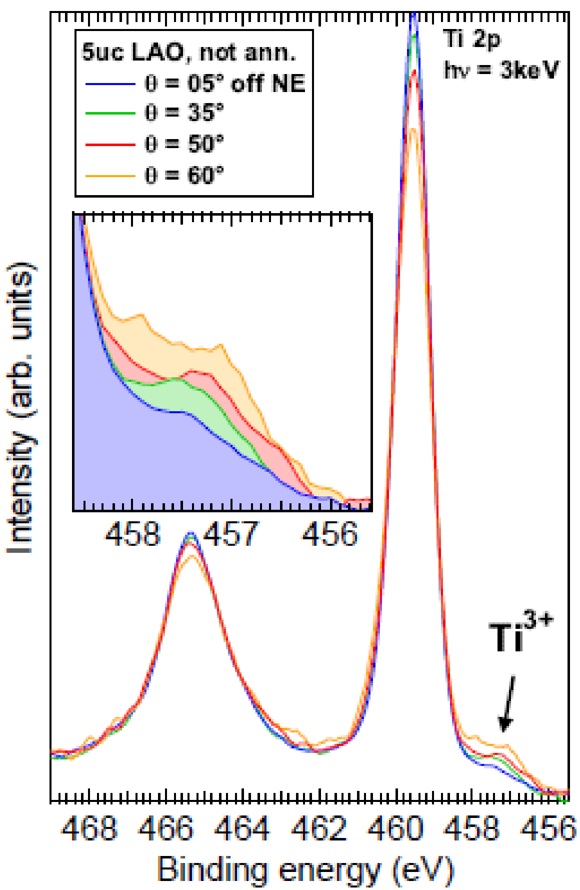

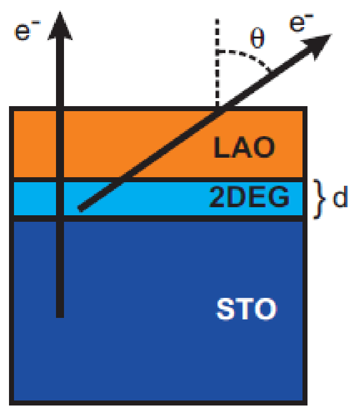

Ti^{3+} intensity

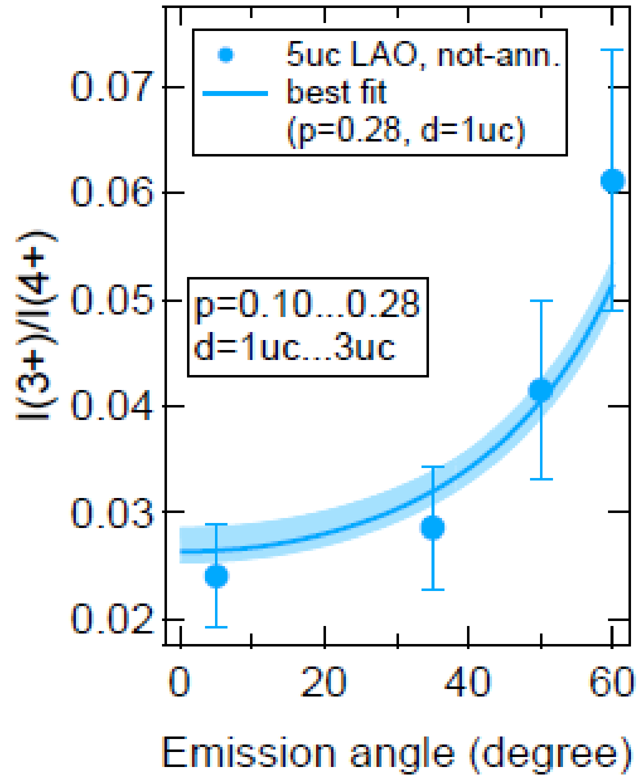

M. Sing et al., PRL ‘09

$LaAlO_3$ overlayer thickness dependence of Ti^{3+} concentration at $LaAlO_3/SrTiO_3$ interface

$LaAlO_3$(x uc)/$SrTiO_3$

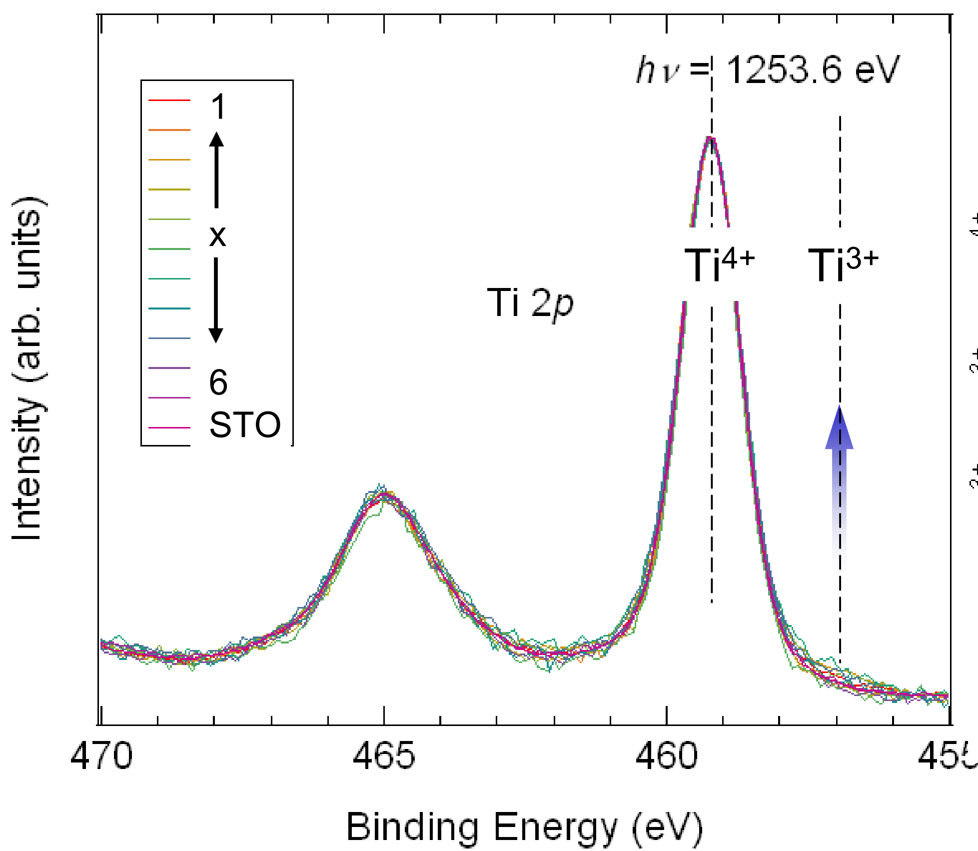

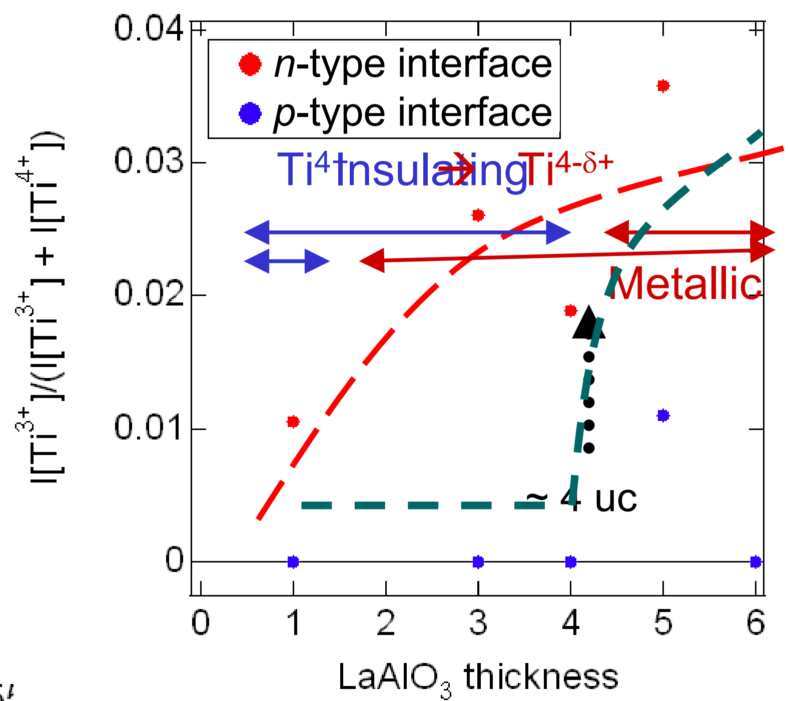

Prepared at 10^{-5} Torr

M. Takizawa et al.

p-type $LaAlO_3/SrTiO_3$ interface

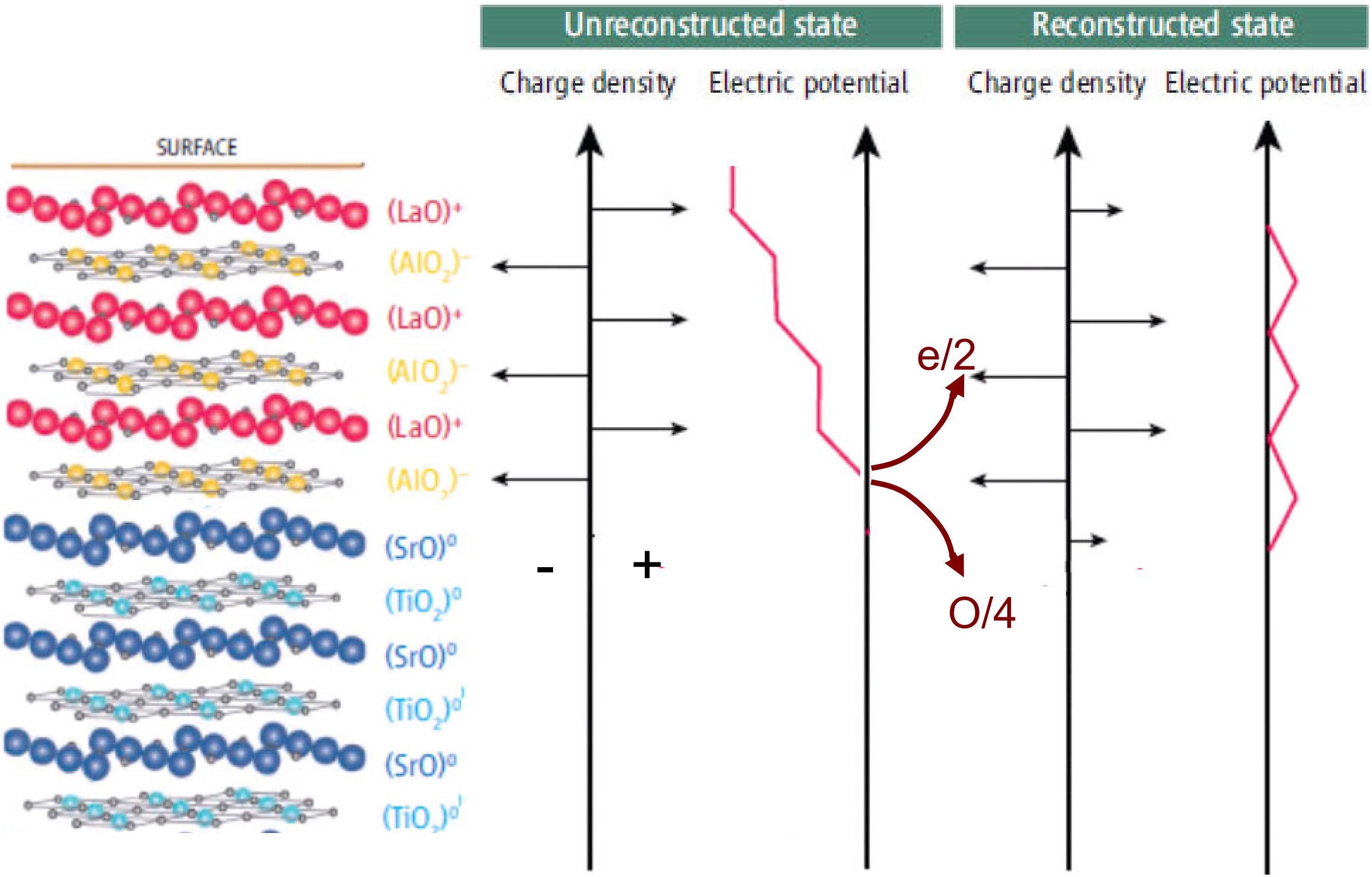

A. Ohtomo and H.Y. Hwang, Nature '04; N. Nakagawa et al, Nat. Mater. '06
H.Y. Hwang, Science '07

$LaAlO_3$ overlayer thickness dependence of Ti^{3+} concentration at $LaAlO_3/SrTiO_3$ interface

$LaAlO_3$(x uc)/$SrTiO_3$

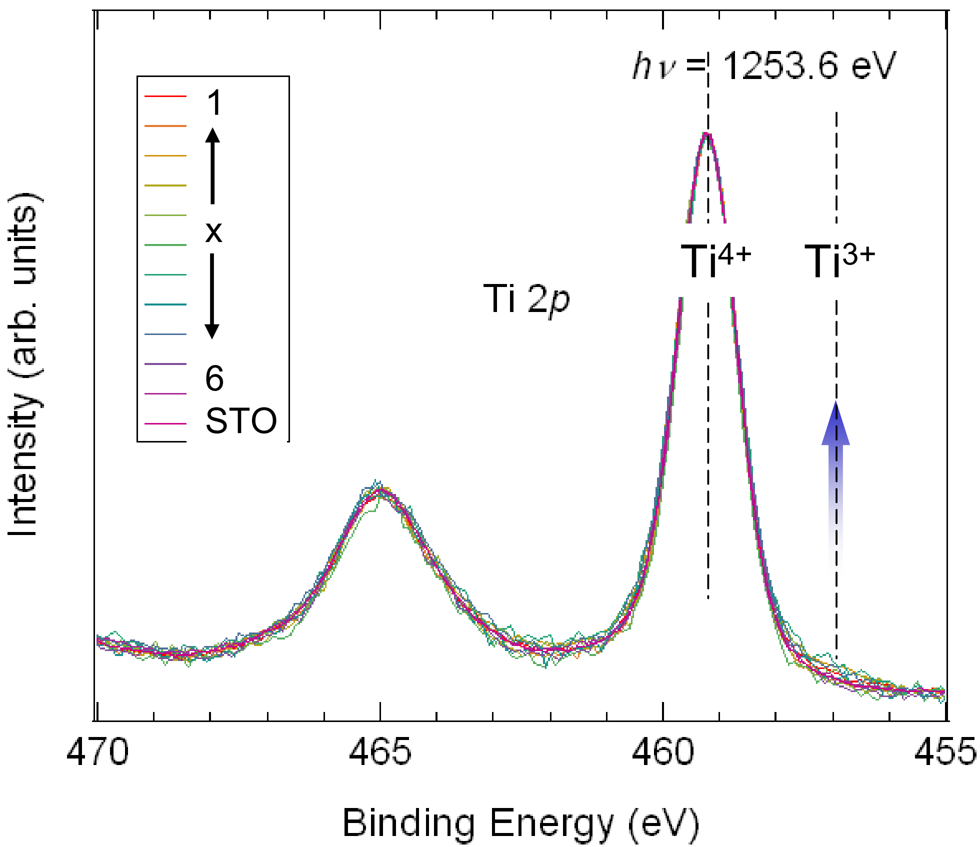

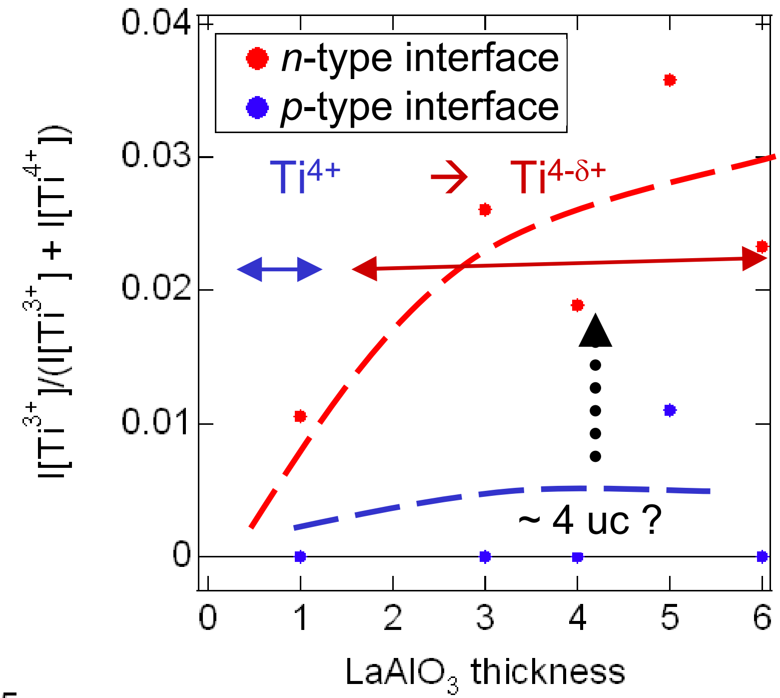

Prepared at 10^{-5} Torr

M. Takizawa et al.

Interfacial electronic structure

Metallic states between two insulators

-Potential change in electronic reconstruction-

Interfaces

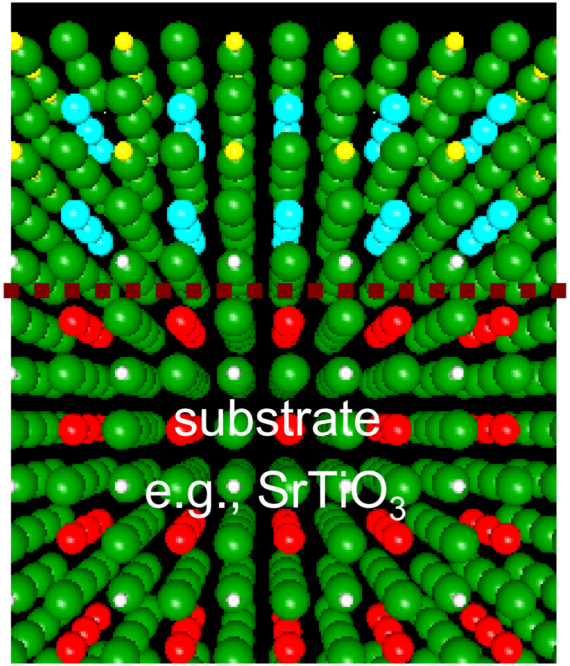

Polar catastrophe model of $LaAlO_3/SrTiO_3$

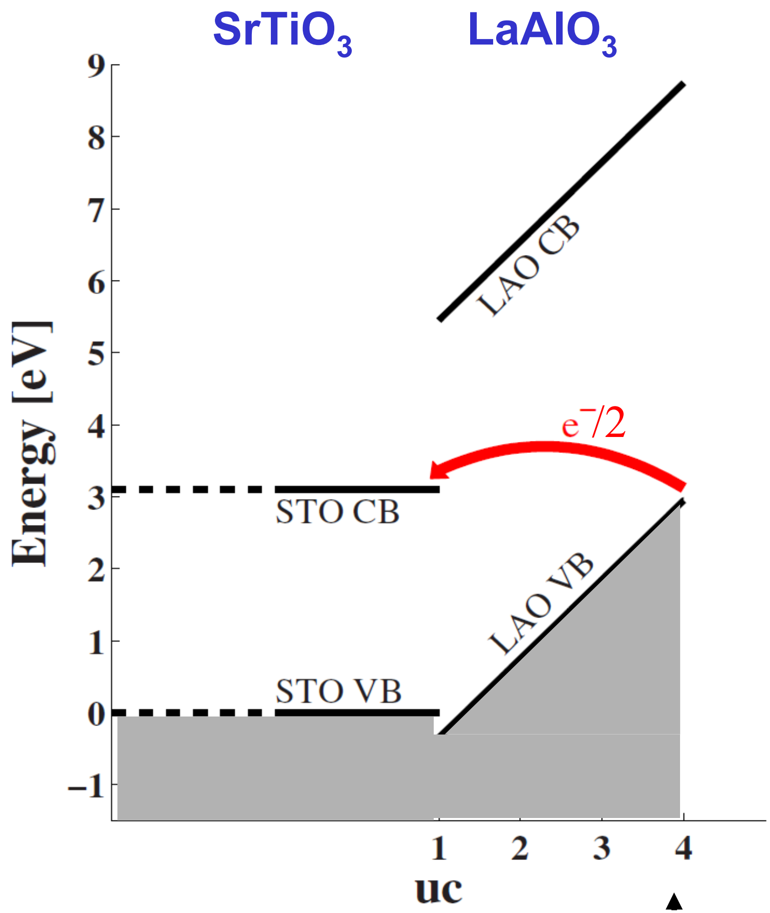

Energy shift?
~1eV/uc

Critical thickness

Y. Segal et al., PRB '09

Probing the potential slope in the $LaAlO_3$ layer of $LaAlO_3/SrTiO_3$

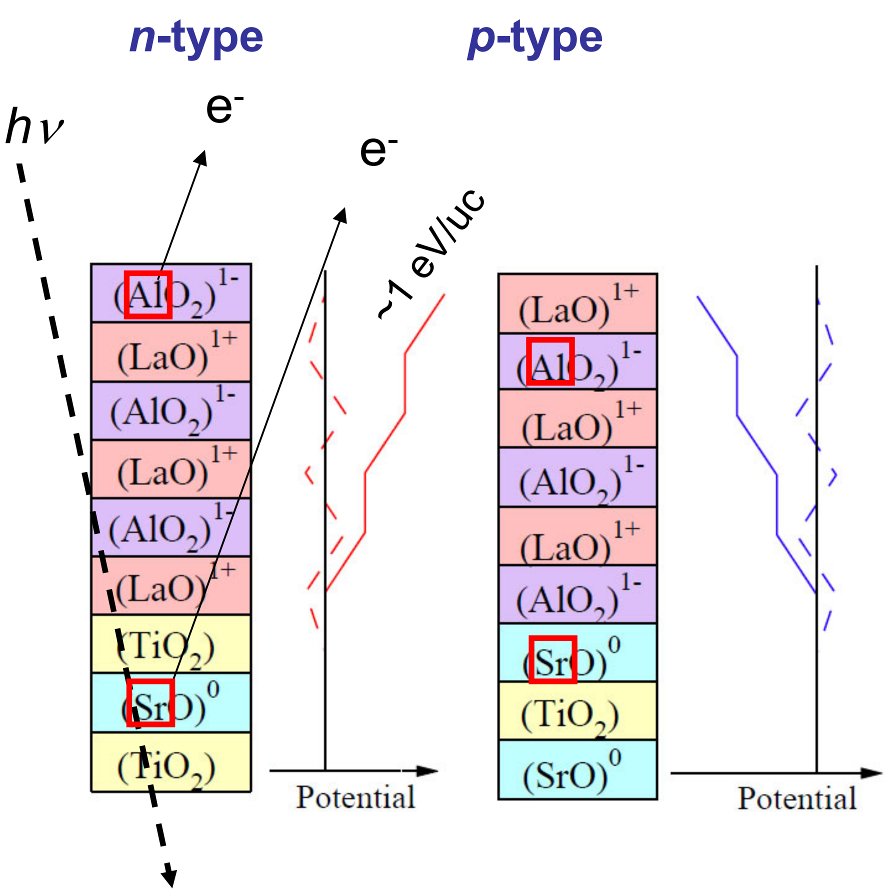

Al 2*p* – Sr 3*d* relative core-level shifts

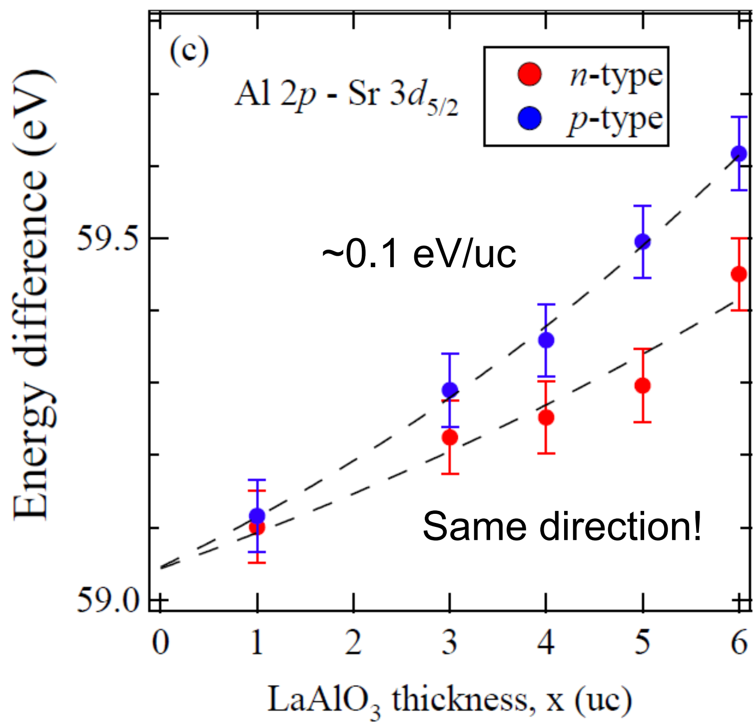

M. Takizawa et al.

Probing the potential slope in the $LaAlO_3$ layer of $LaAlO_3/SrTiO_3$

Polar catastrophe model

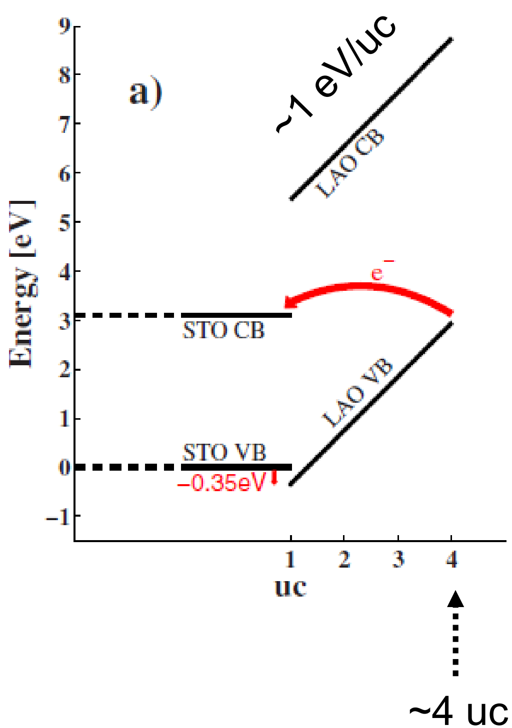

La 3*d* and Al 2*p* core levels referenced to Sr 3*d*

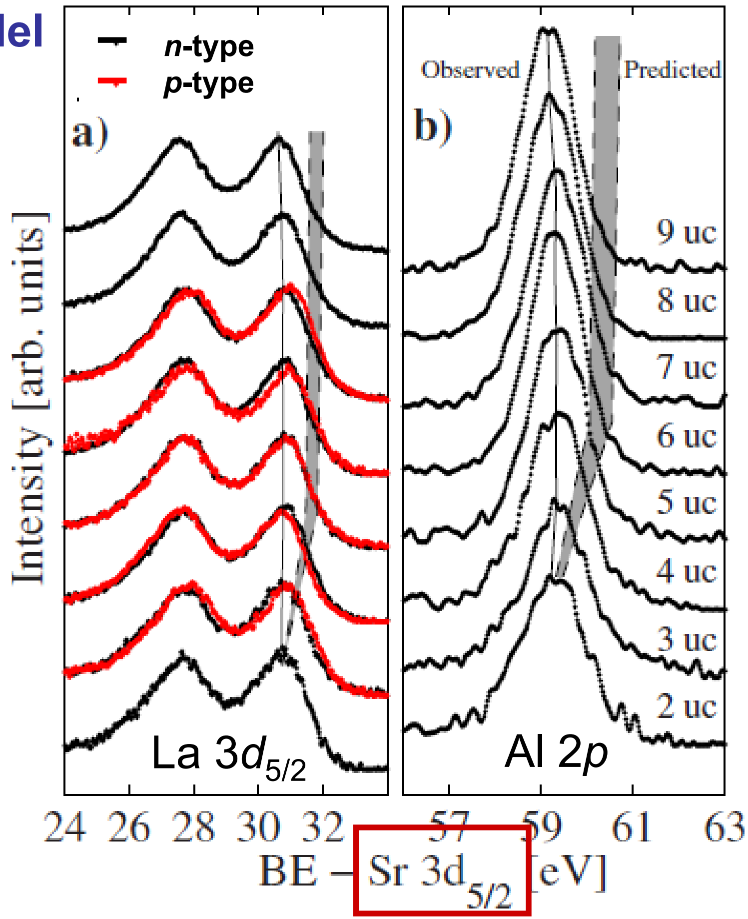

Sr 3*d* – La 4*d* relative core-level shifts

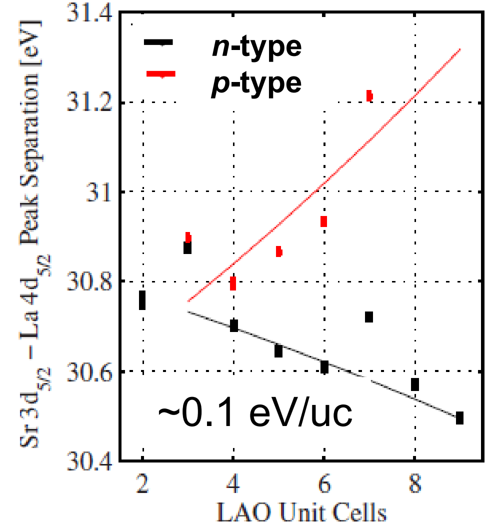

Opposite to the model!

Y. Segal et al., PRB '09

Probing the potential slope in GaN (0001) layers

GaN/AlN(0001)

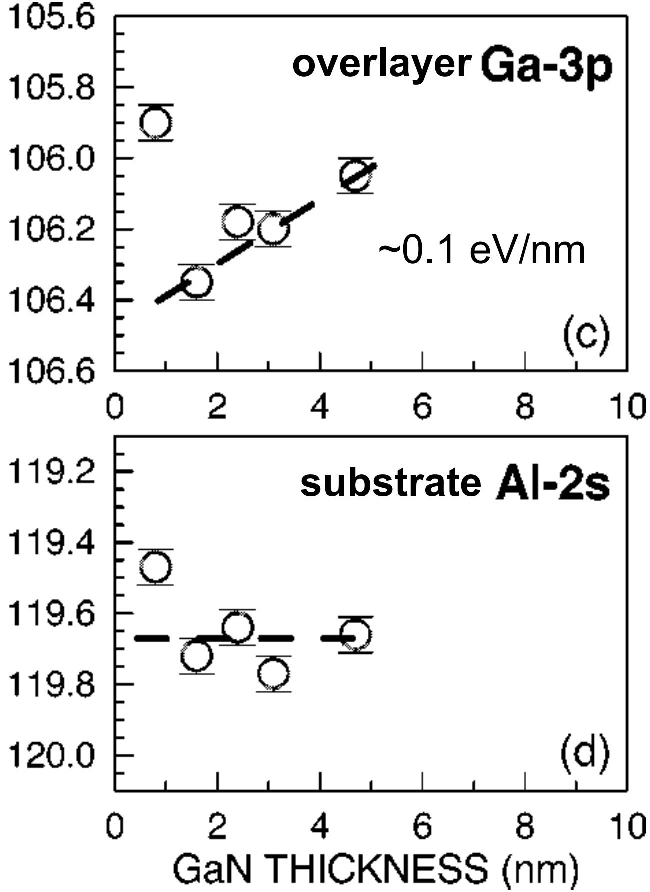

GaN/SiC(0001)

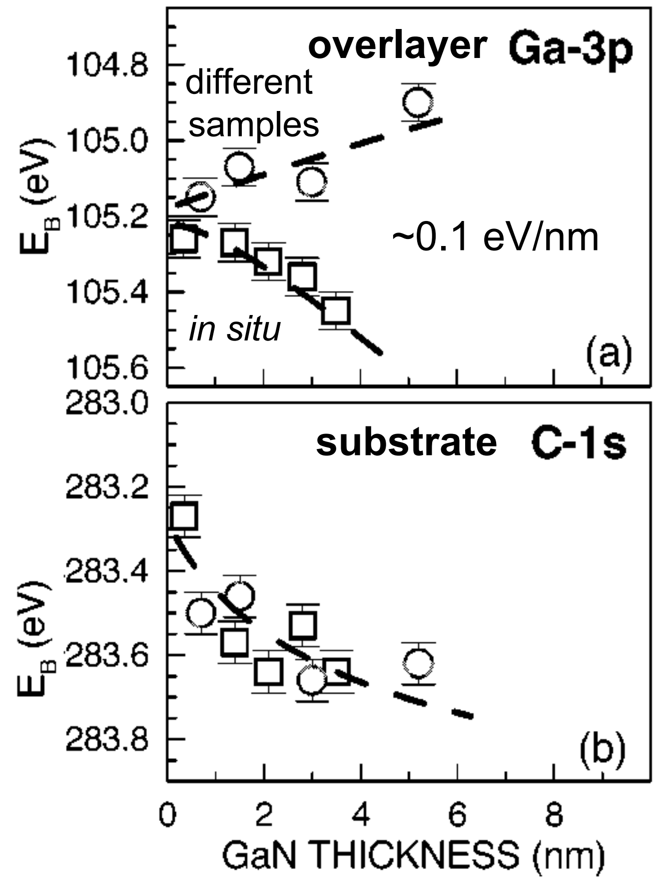

A. Rizzi et al., JVSTB ‘99

Calculated potential in polar GaN/SiC(0001)

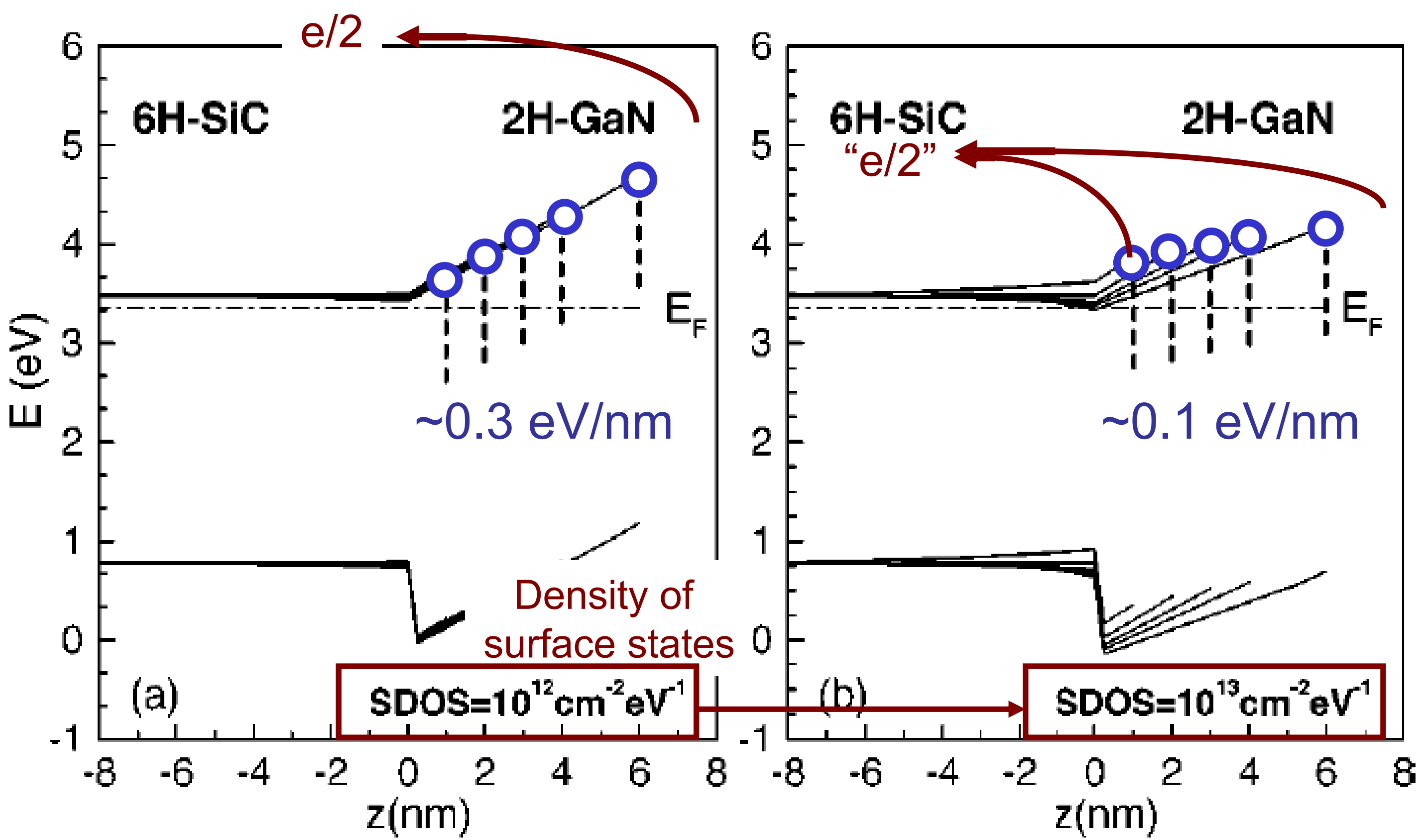

A. Rizzi et al., JVSTB '99

Short summary

- Metallic states between two insulators -

Electronic reconstruction at insulator-insulator interfaces:

- ✓ Charge transfer occurs as expected to avoid the polar catastroph, but the charge transfer starts well below the critical thickness of transport.

- ✓ Potential slope as expected to avoid the polar catastrophe model is much reduced.

- ✓ The above observations can be explained by the gradual reconstruction which starts well below the critical thickness.

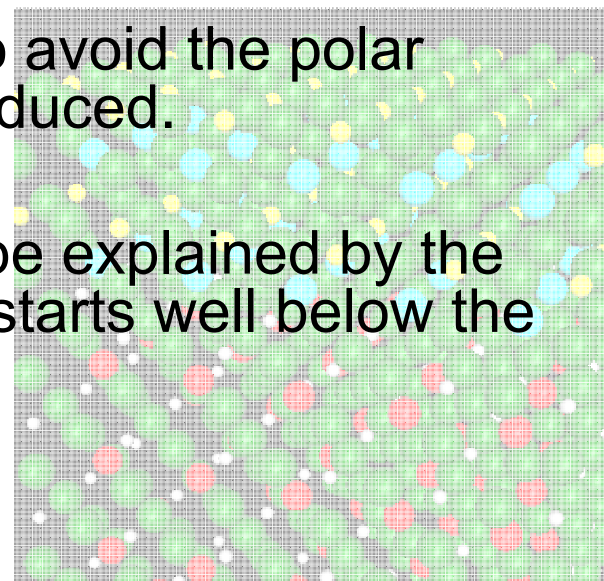

Preparation dependence of carrier distributions at the *n*-type $LaAlO_3/SrTiO_3$ interface

Core-level photoemission

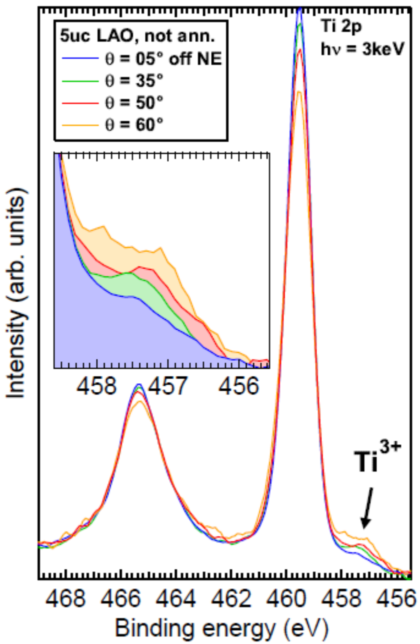

Prepared at 10^{-6} Torr

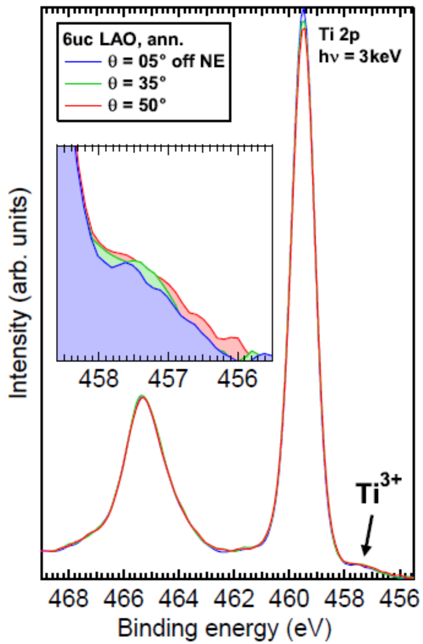

O_2-annealed

M. Sing et al., PRL '09

Cross-sectional AFM

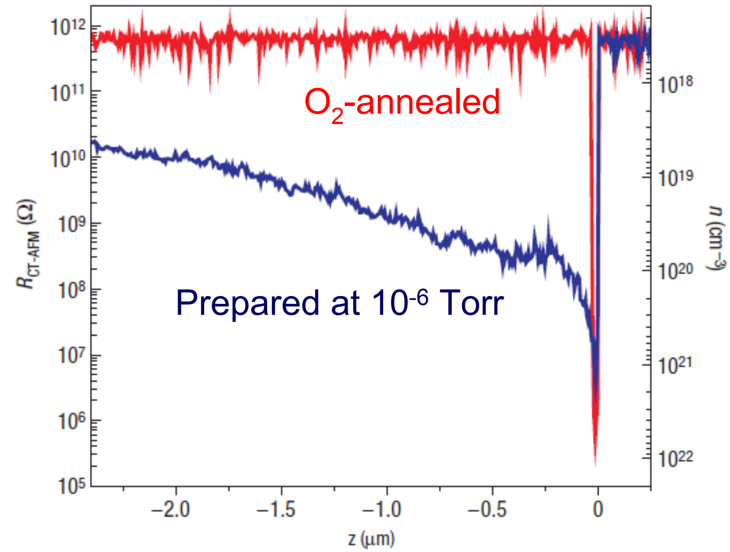

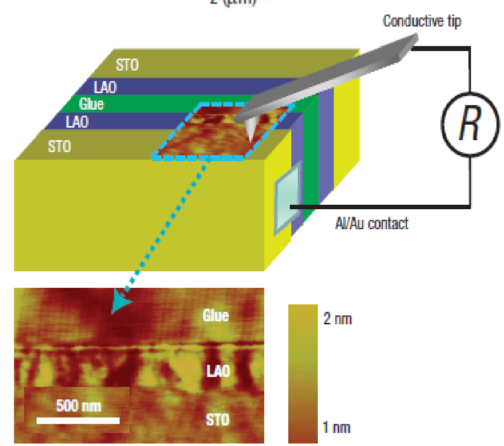

M. Basletic et al., Nat. Phys. '08

Novel physical properties of $LaAlO_3/SrTiO_3$ interfaces

Superconductivity

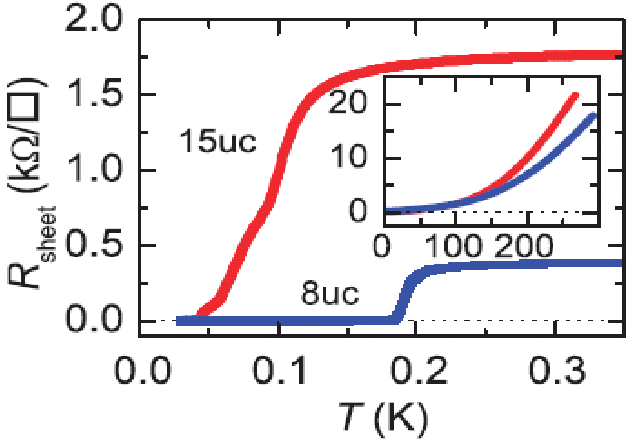

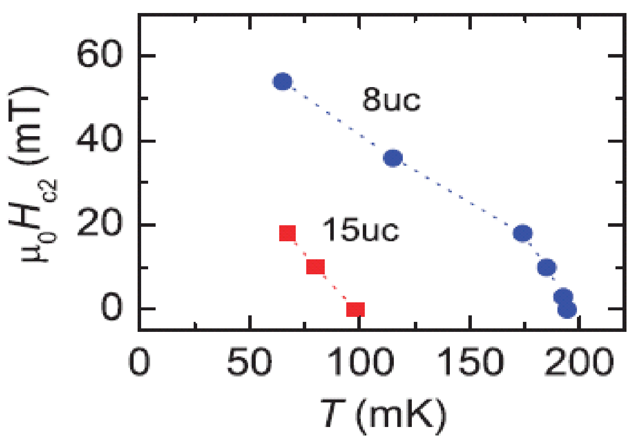

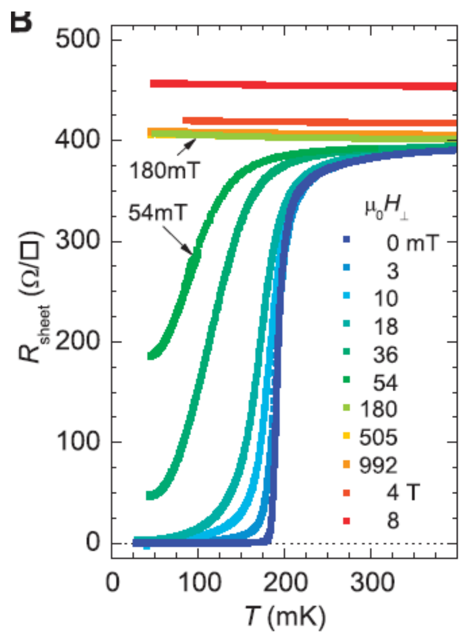

N. Reyren et al. Science '07

Ferromagnetism

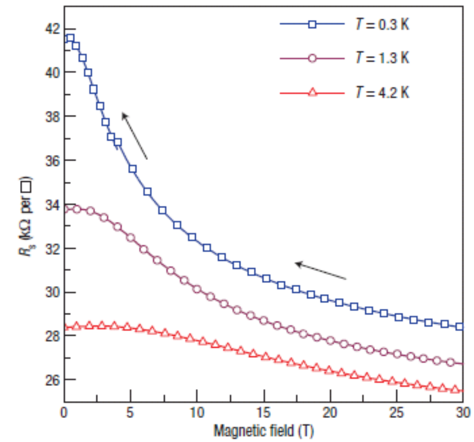

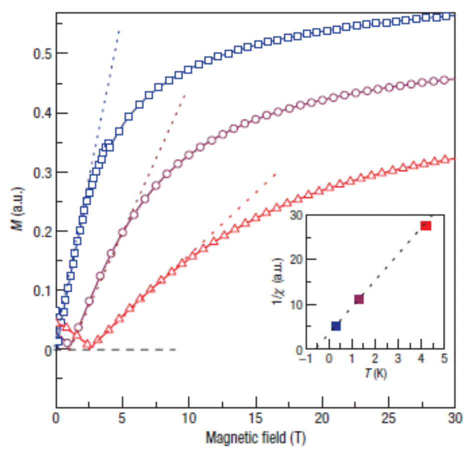

A. Brinkman et al. Nat. Mater. '07
cf: MR by M B. Shalom et al., PRB '09

Gate-voltage control of superconductivity at $LaAlO_3/SrTiO_3$ interface

Resistivity for various gate voltages

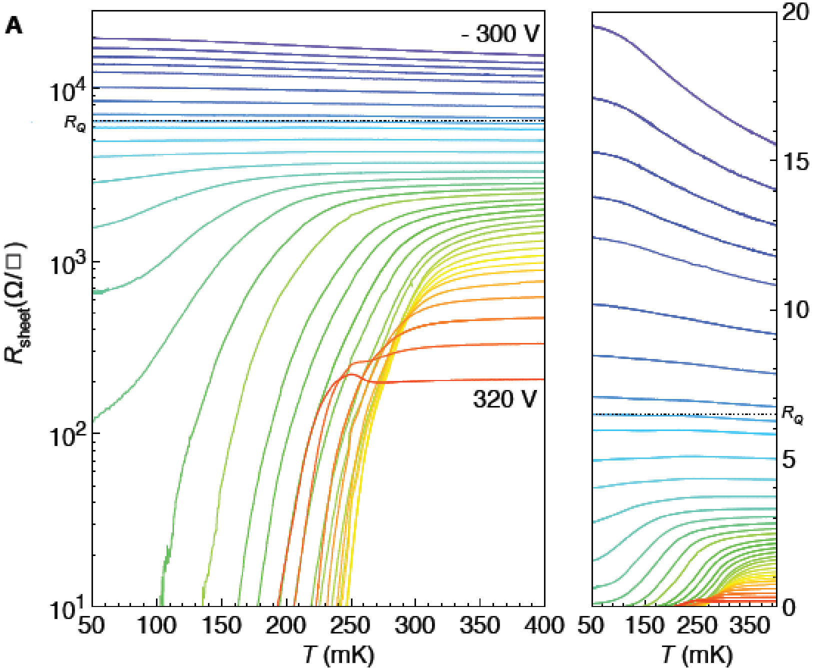

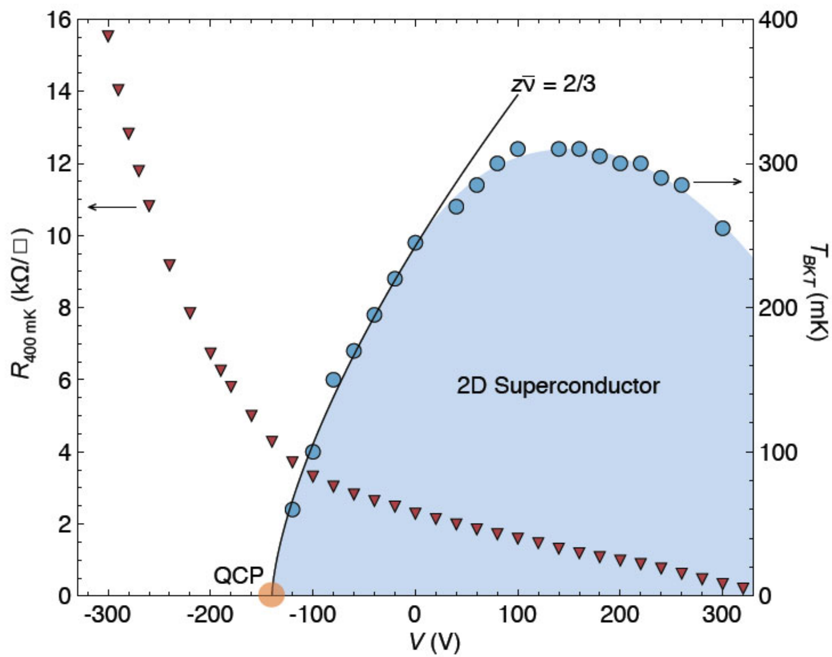

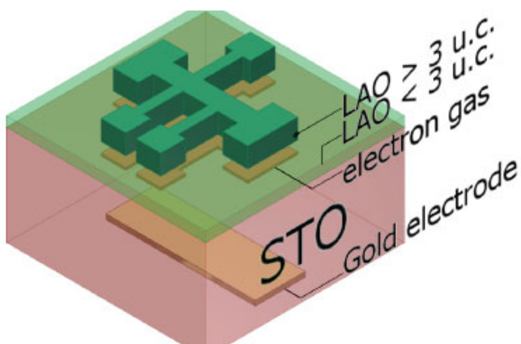

$$T_{BKT} \propto (V - V_c)^{z\bar{\nu}}, \text{ with } z\bar{\nu} = 2/3.$$

A.D. Caviglia et al., Nature '08

Gate-voltage-controlled $LaAlO_3/SrTiO_3$ interface: Filling control or mobility control?

Resistivity for various gate voltages

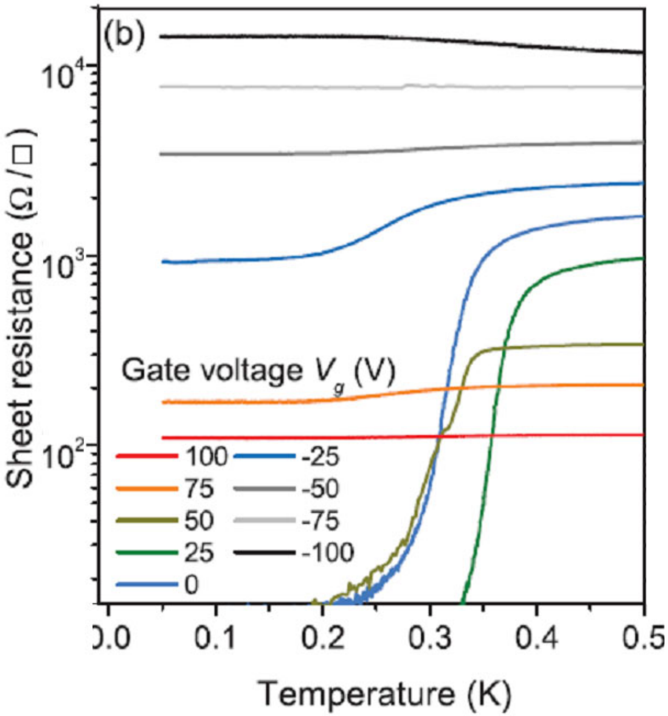

Gate-voltage dependence of carrier density and mobility

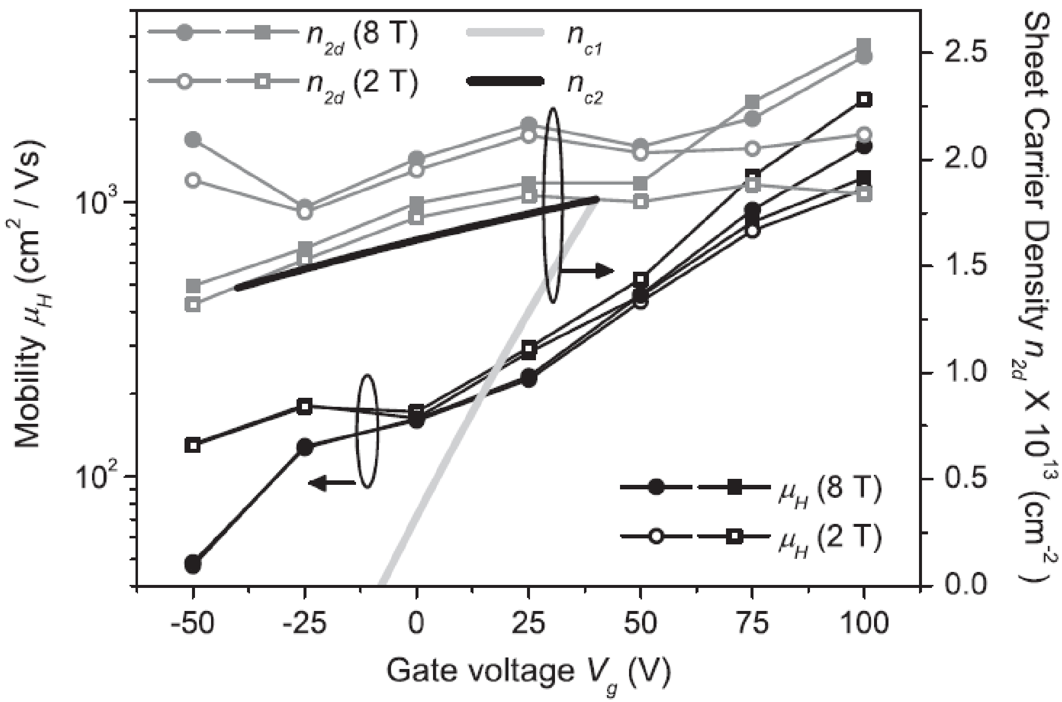

C. Bell et al., PRL '09

Interfacial electronic structure

Ferromagnetism between non-magnetic materials

Interfaces

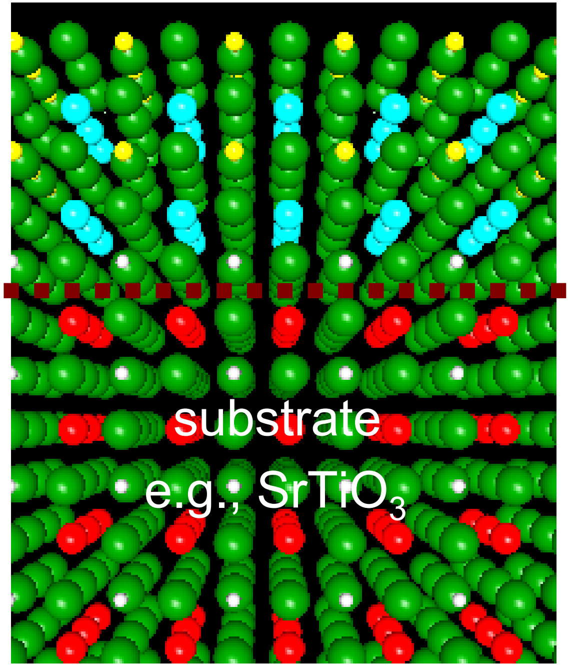

Ferromagnetism in $[(LaMnO_3)_m/(SrMnO_3)_{m'}]_n$ superlattices

Magnetization, resistivity

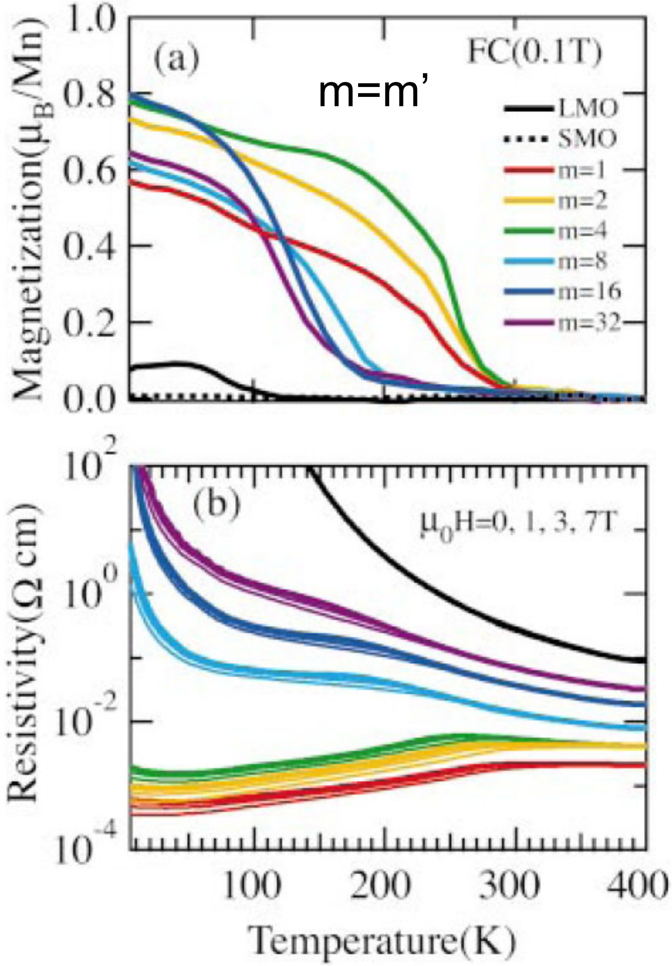

T. Koida et al.,. PRB '02

Polarized neutron reflectivity

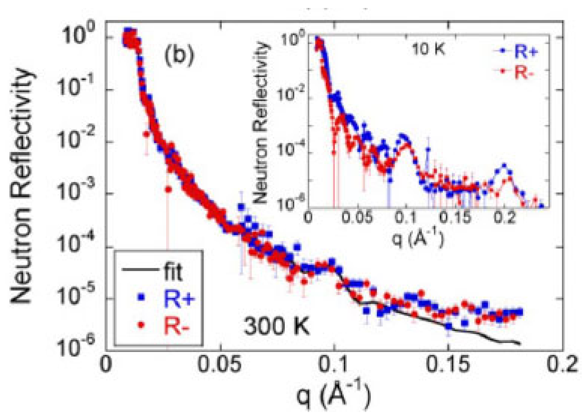

TEM

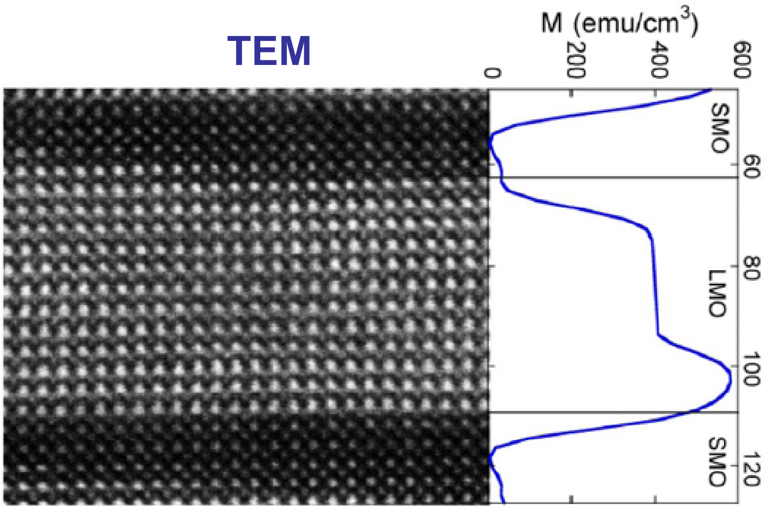

S.J. May et al.,. PRB '08

Soft x-ray scattering from $[(LaMnO_3)_8/(SrMnO_3)_4]_7/SrTiO_3(001)$

STEM image

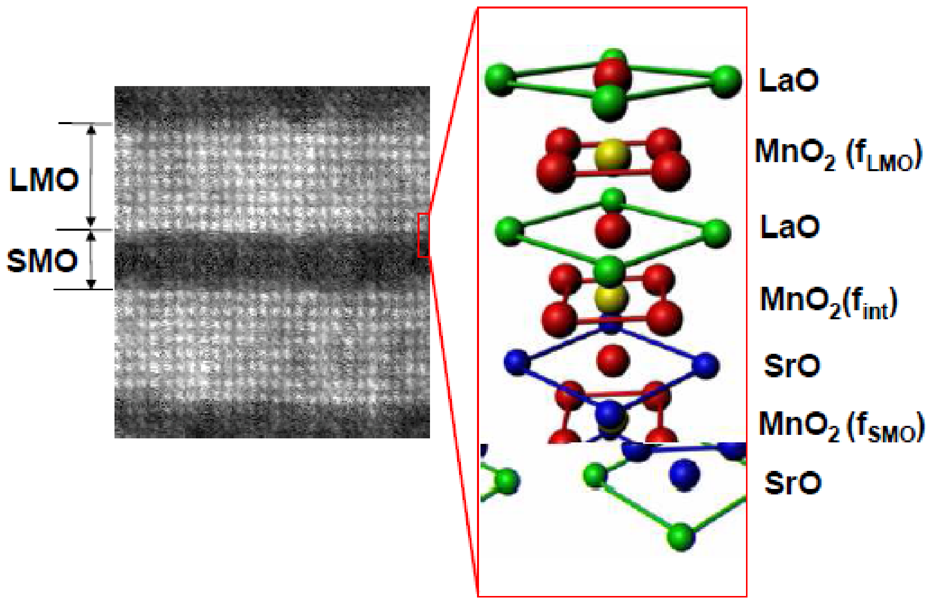

Temperature dependence

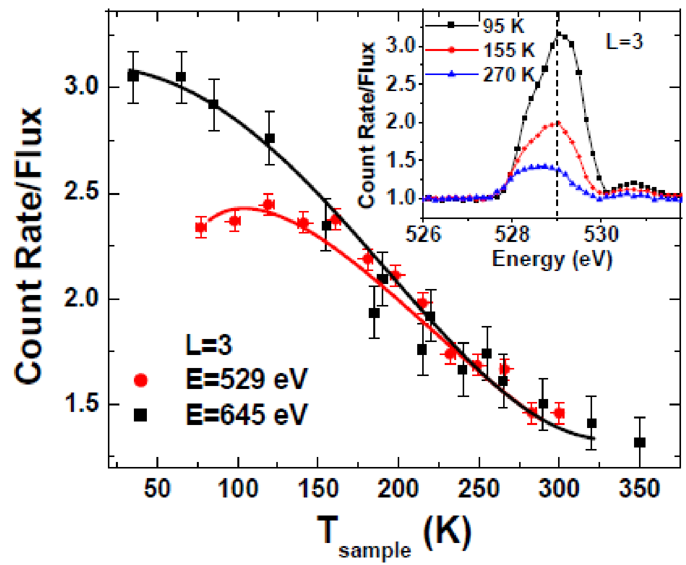

(003) resonance

↕

Metallic behavior

S. Smadici et al.,. PRL ’07
H. Wadati

Ferromagnetism in AF insulator-paramagnetic metal interfaces

$CaMnO_3$: AF insulator
$CaRuO_3$: PM metal

Magnetization

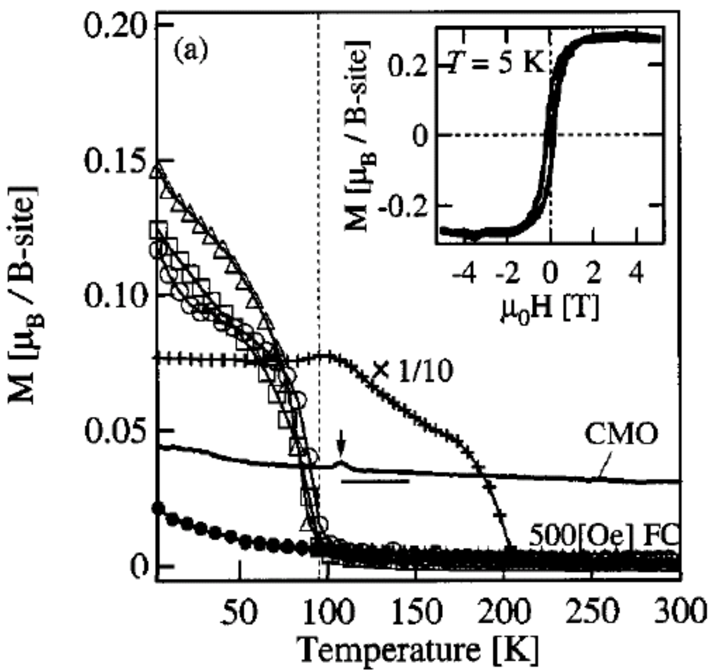

Magnetization and Tc

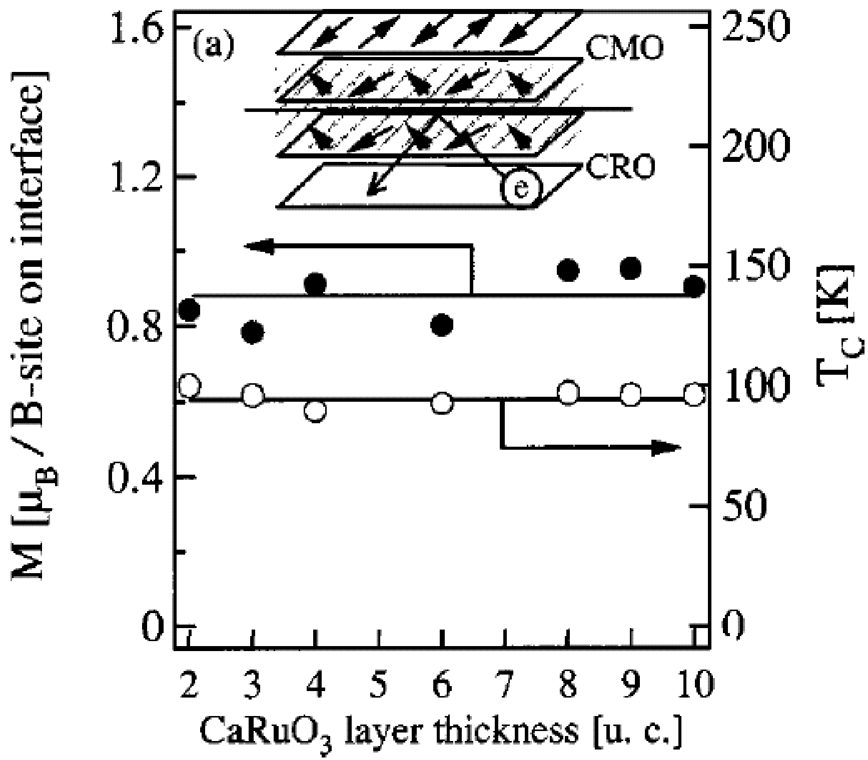

S. Takahashi et al., APL '01

Mn 2*p* and Ru 3*p* XMCD for $CaMn_{1-x}Ru_xO_3$ thin films

XMCD spectra

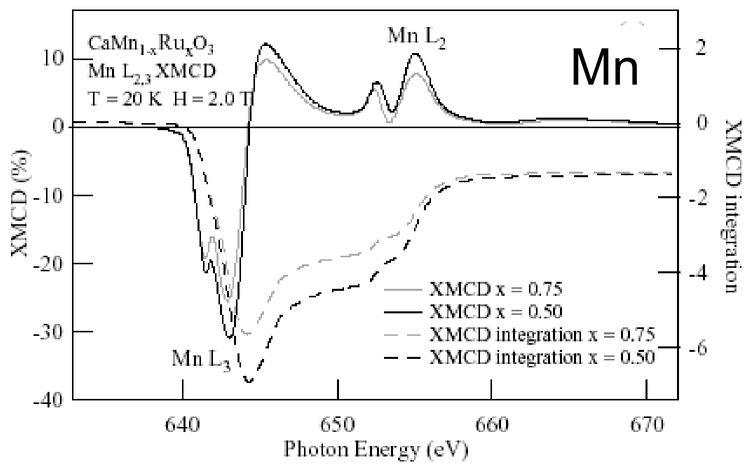

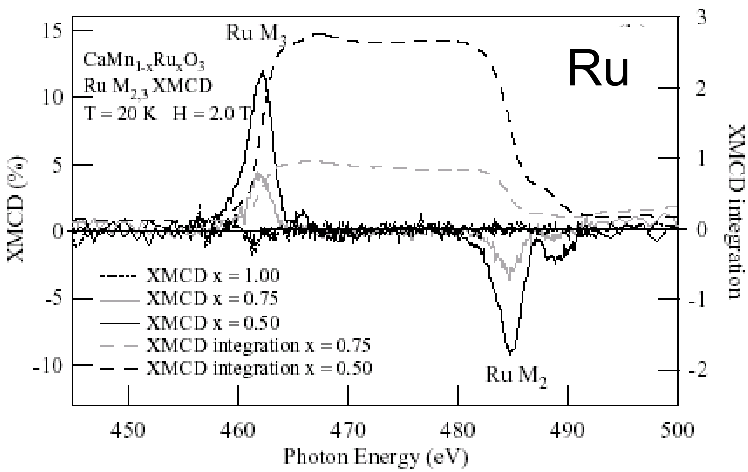

K. Terai et al. PRB '08

Magnetic moments on Mn and Ru

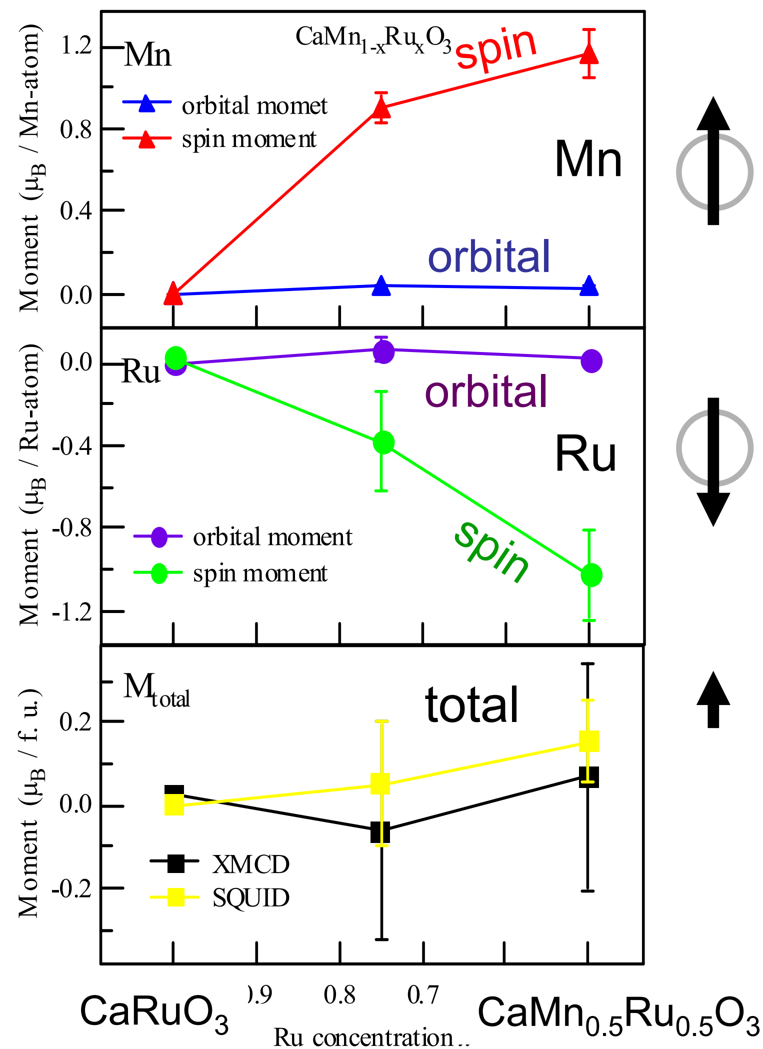

Mechanism for ferromagnetism in $CaMn_{1-x}Ru_xO_3$ – $CaMnO_3/CaRuO_3$, too ?

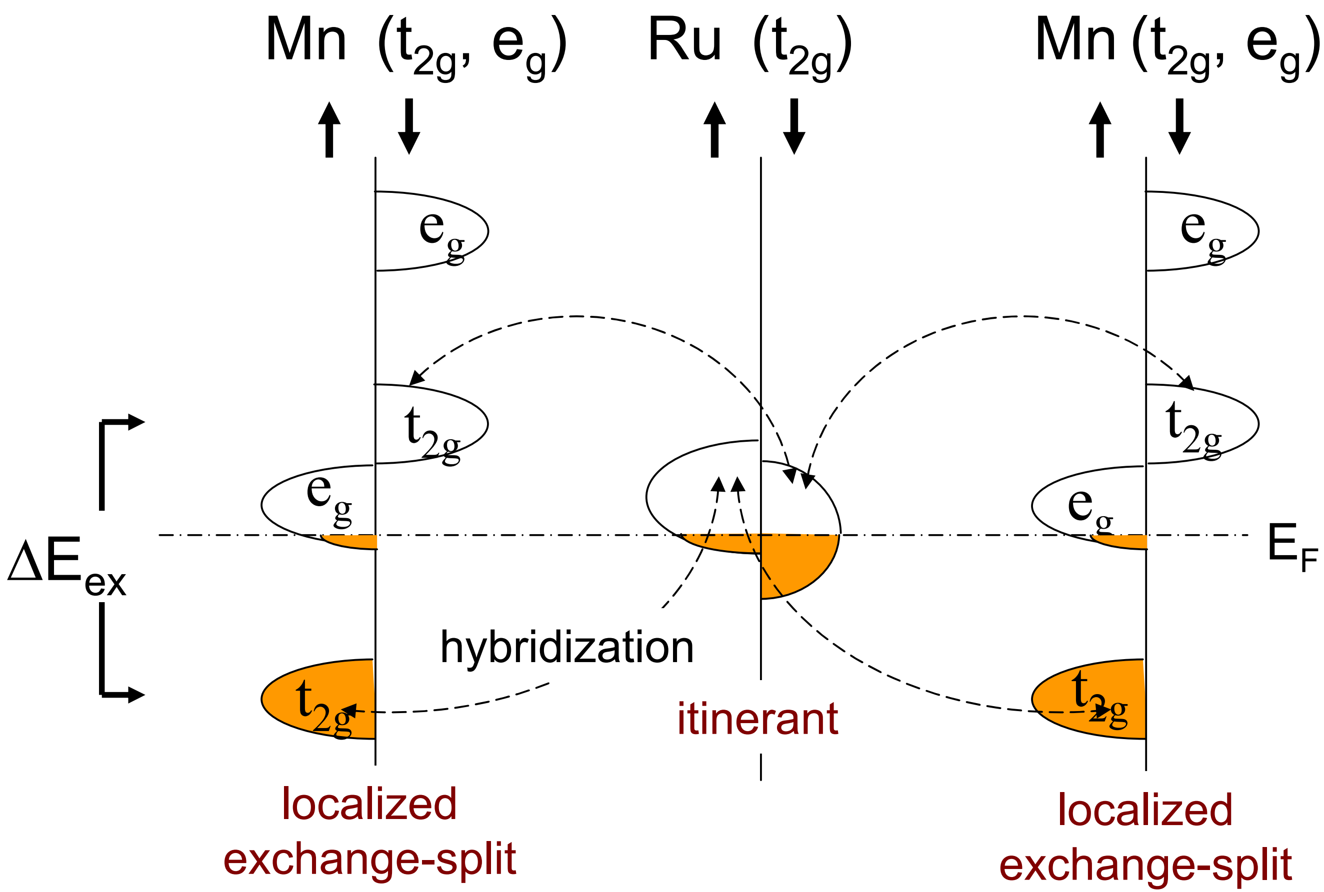

cf.) Double peroskite Sr_2FeMoO_6 D.D. Sarma et al., PRL '00, Z. Fang et al., PRB '01

Interfacial electronic structure

Interface between different ground states

Interfaces

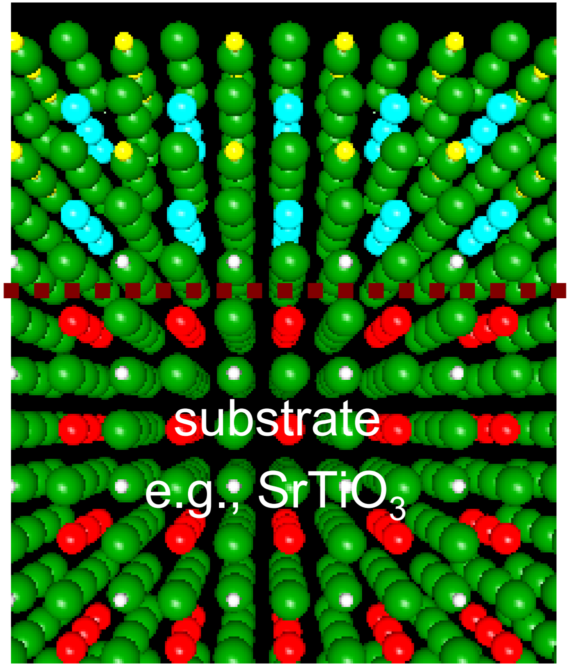

Interface between superconductor $YBa_2Cu_3O_7$ and ferromagnet (La,Ca)MnO_3

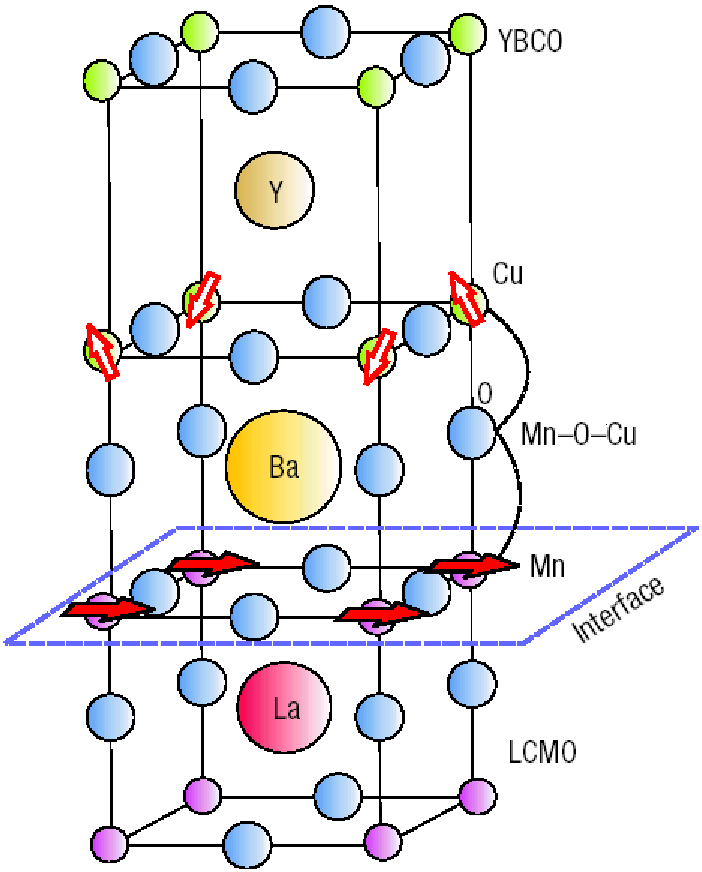

J. Chakhalian et al., Nat. Phys. '06

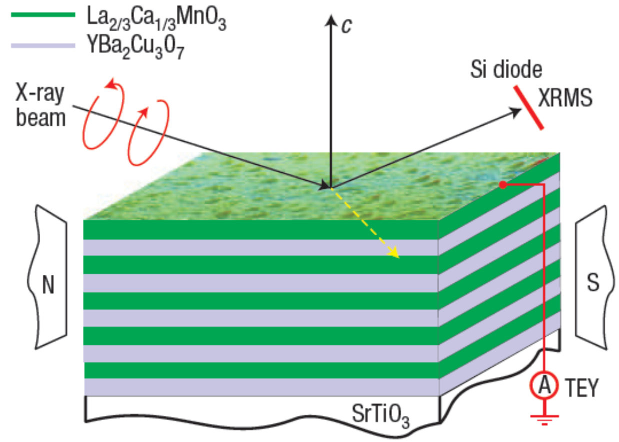

XMCD of Cu and Mn

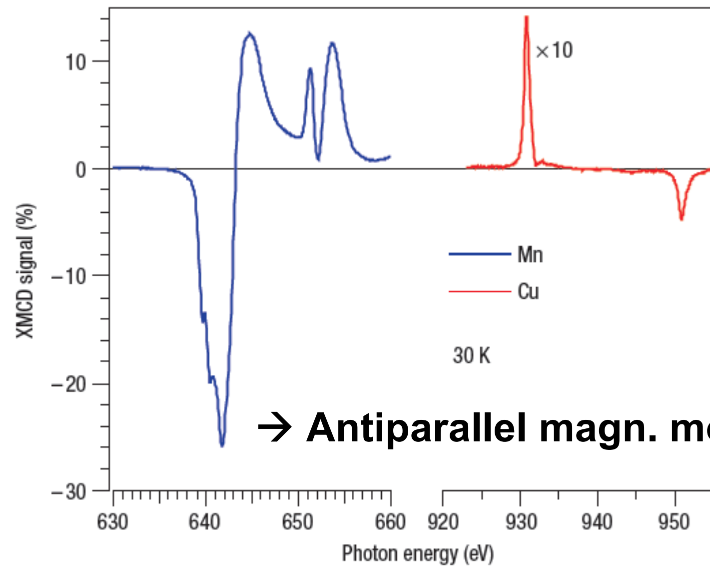

→ **Antiparallel magn. moment**

Interface between superconductor $YBa_2Cu_3O_7$ and ferromagnet (La,Ca)MnO_3

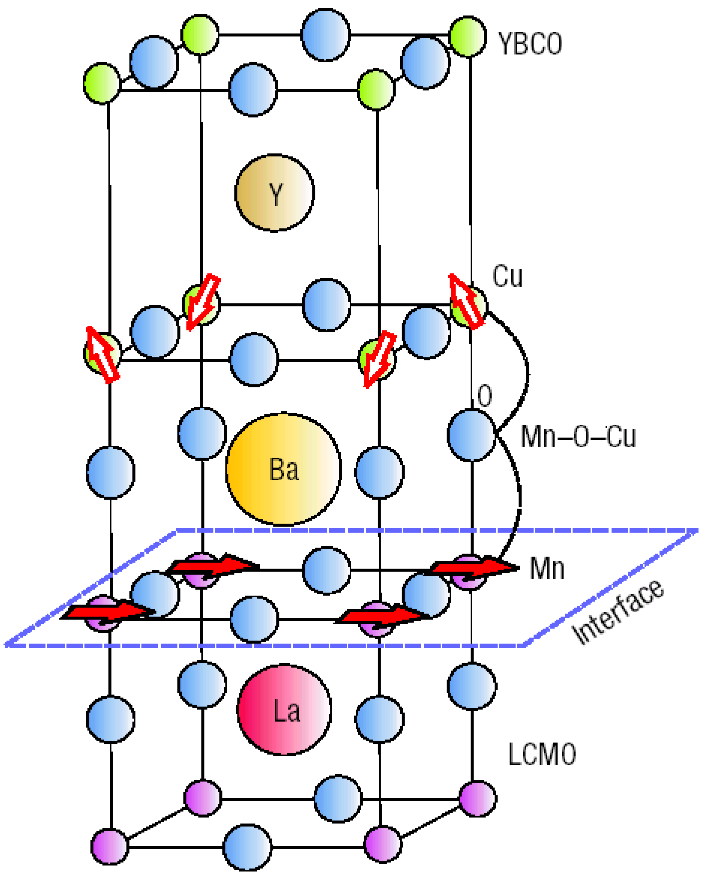

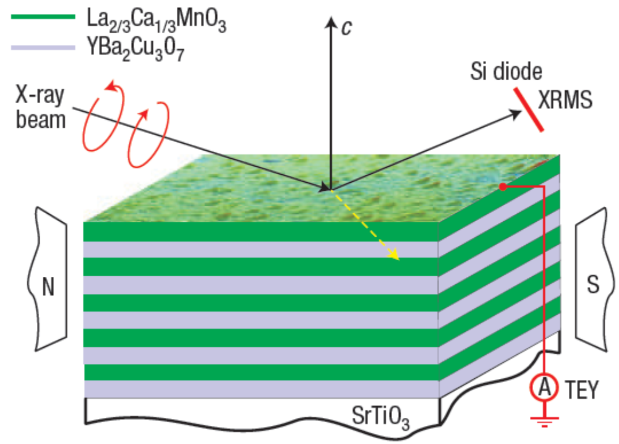

XMCD of Cu and Mn

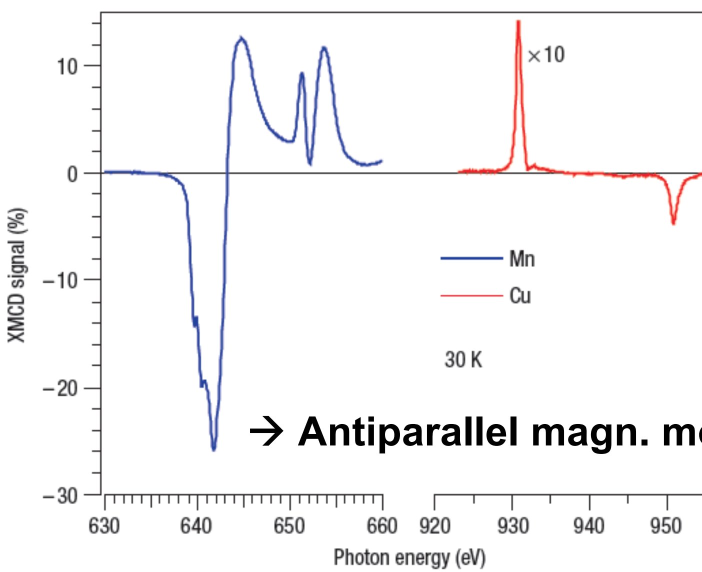

→ Antiparallel magn. moment

J. Chakhalian et al., Nat. Phys. '06

Interfacial electronic structure

Chemical potential

Interfaces

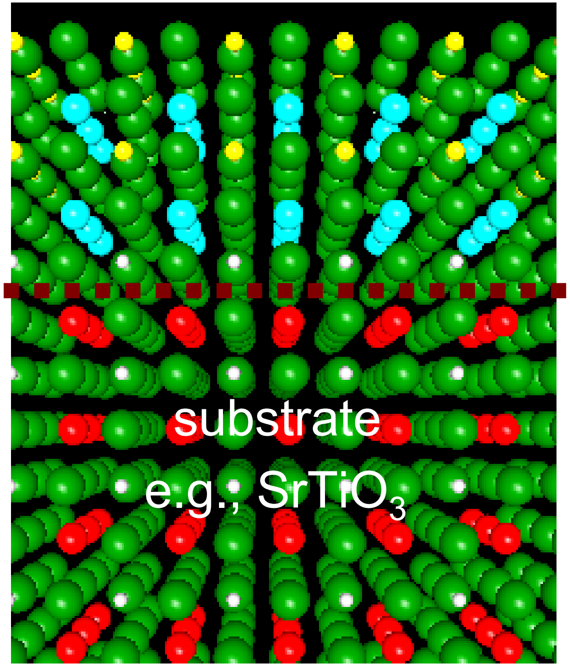

To deduce chemical potential from *I-V* characteristics of junction

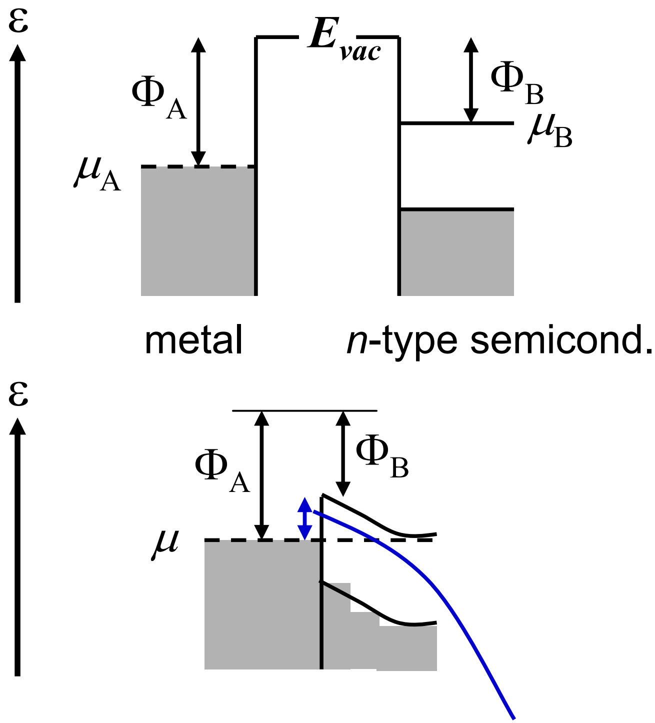

I-V characteristics of $SrRuO_3/SrTiO_3$

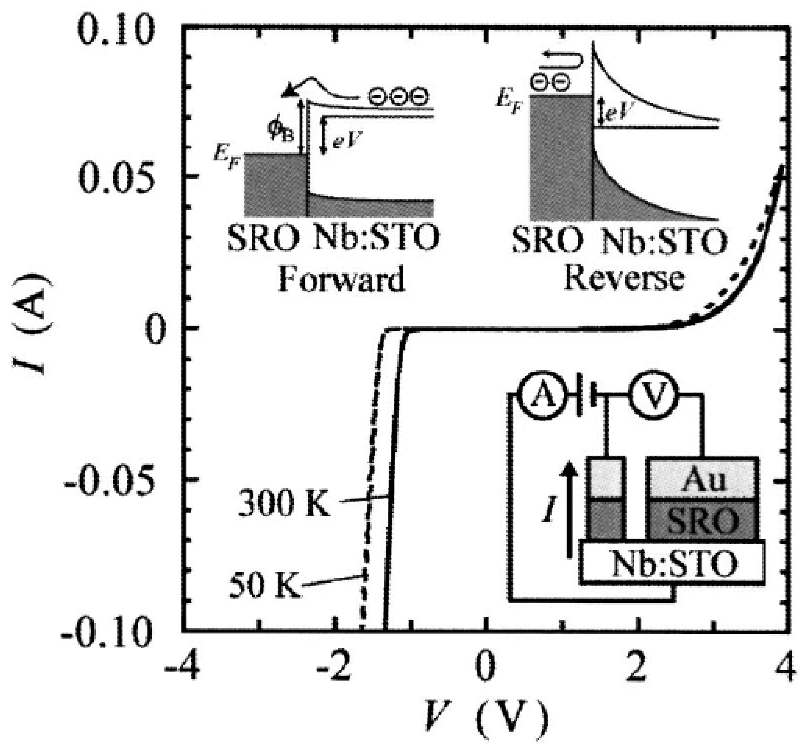

Schottky barrier height = Φ_A - Φ_B = $\mu_B - \mu_A$
(or built-in potential in *p-n* junction)

T. Fujii et al., APL ‘05

To deduce chemical potential shift from *I-V* characteristics of junction

Chemical potential shift from the built-in potential of $La_{1-x}Sr_xMO_3/SrTiO_3$ *p-n* (Schottky) junction

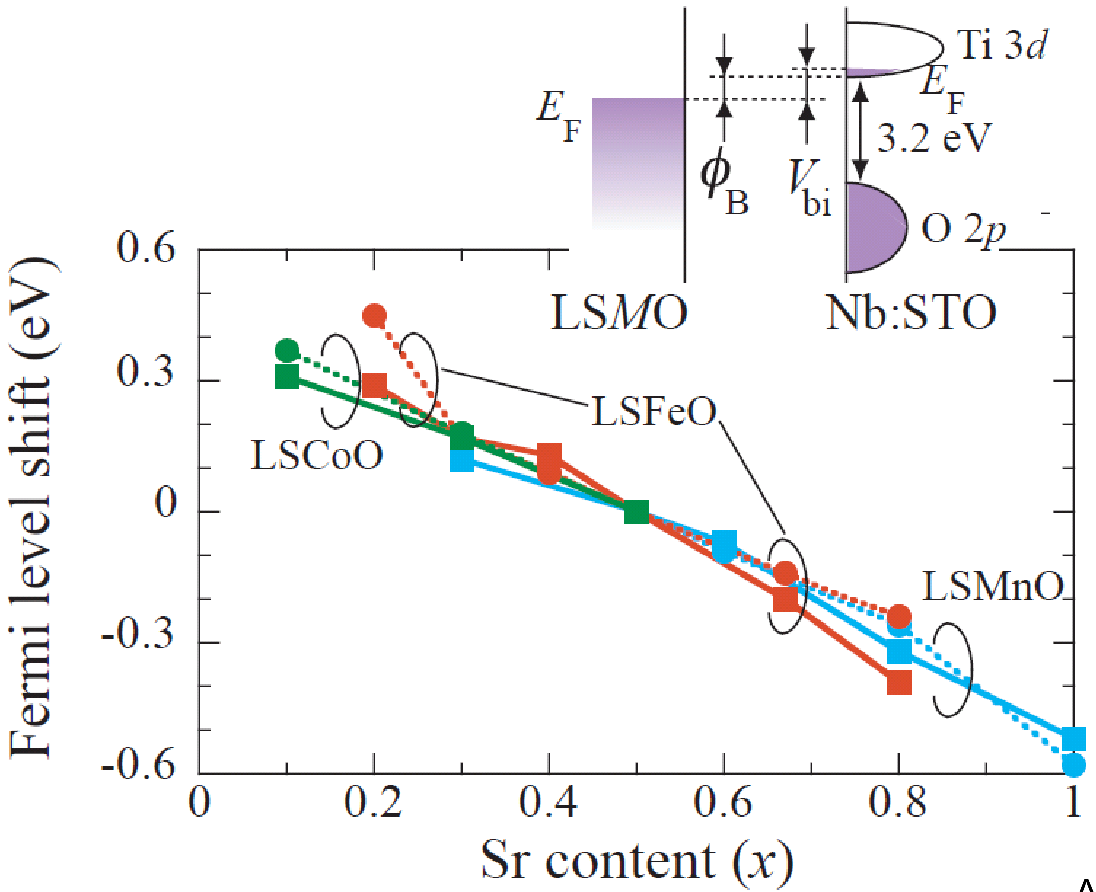

A. Sawa et al., APL '07

To deduce chemical potential shift from *I-V* characteristics of junction

Chemical potential shift from core-level XPS

Chemical potential shift from the built-in potential

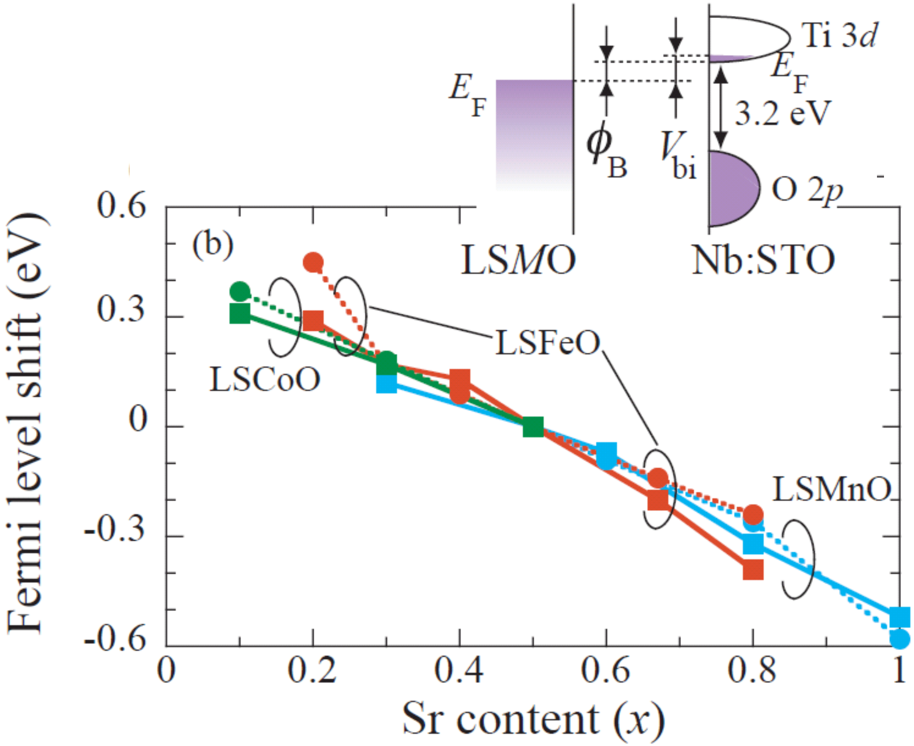

A. Sawa et al., APL '07

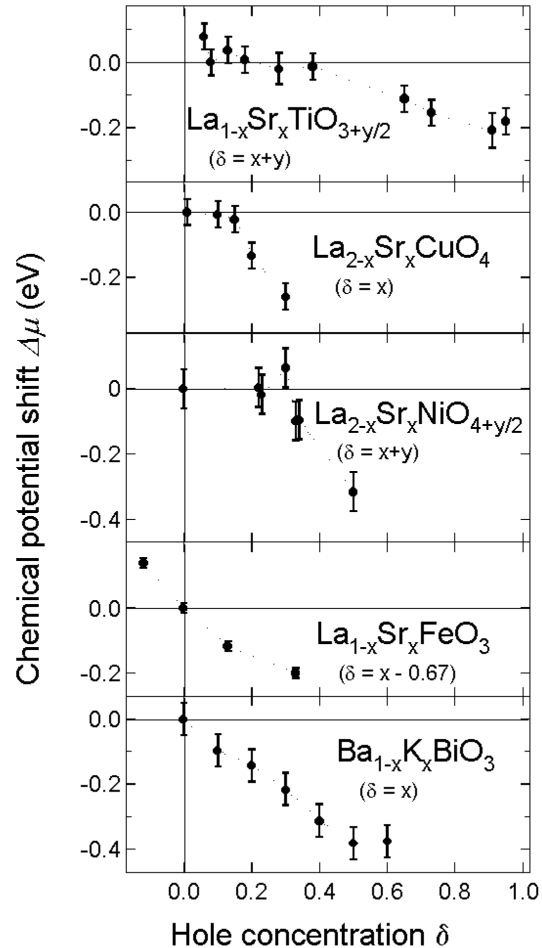

A. Fujimori et al.,
J. Electron Spectrosc. '02

Magnetic field-induced chemical potential shift in $La_{2/3}Sr_{1/3}MnO_3$/organic conductor junction

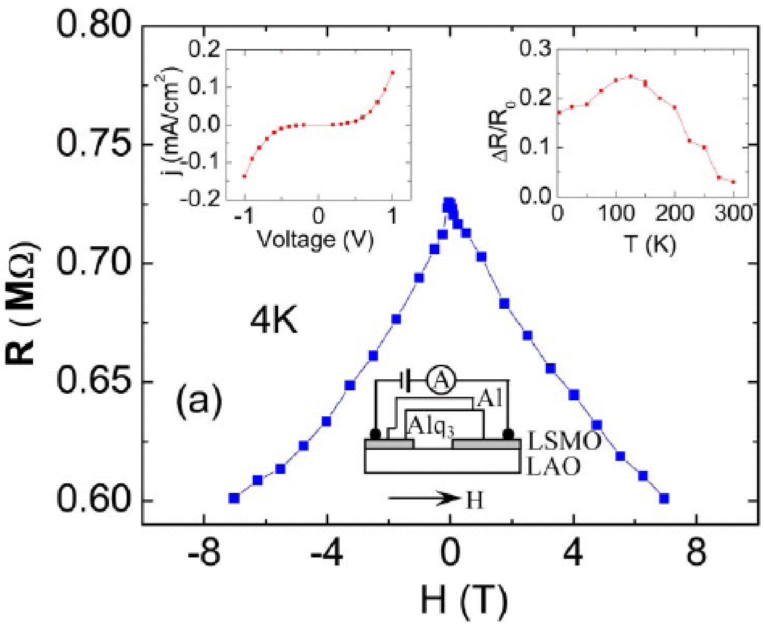

D. Wu et al., PRL ‘05

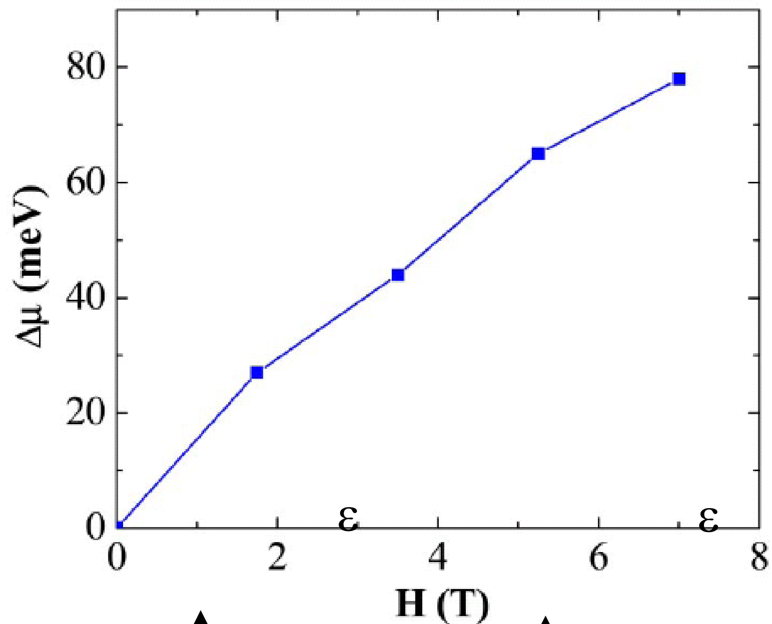

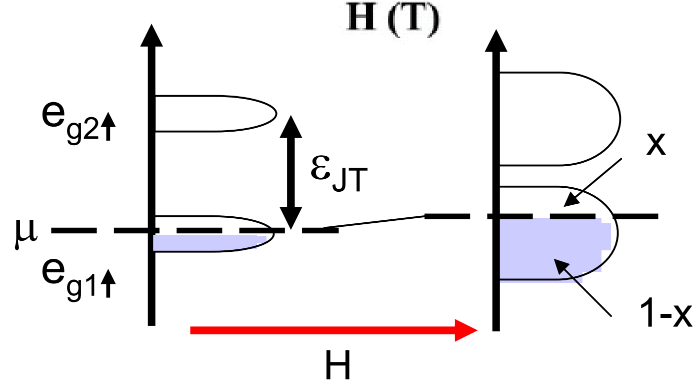

Double exchange in *Jahn-Teller-split* e_g band

To deduce chemical potential shift from core-level photoemission

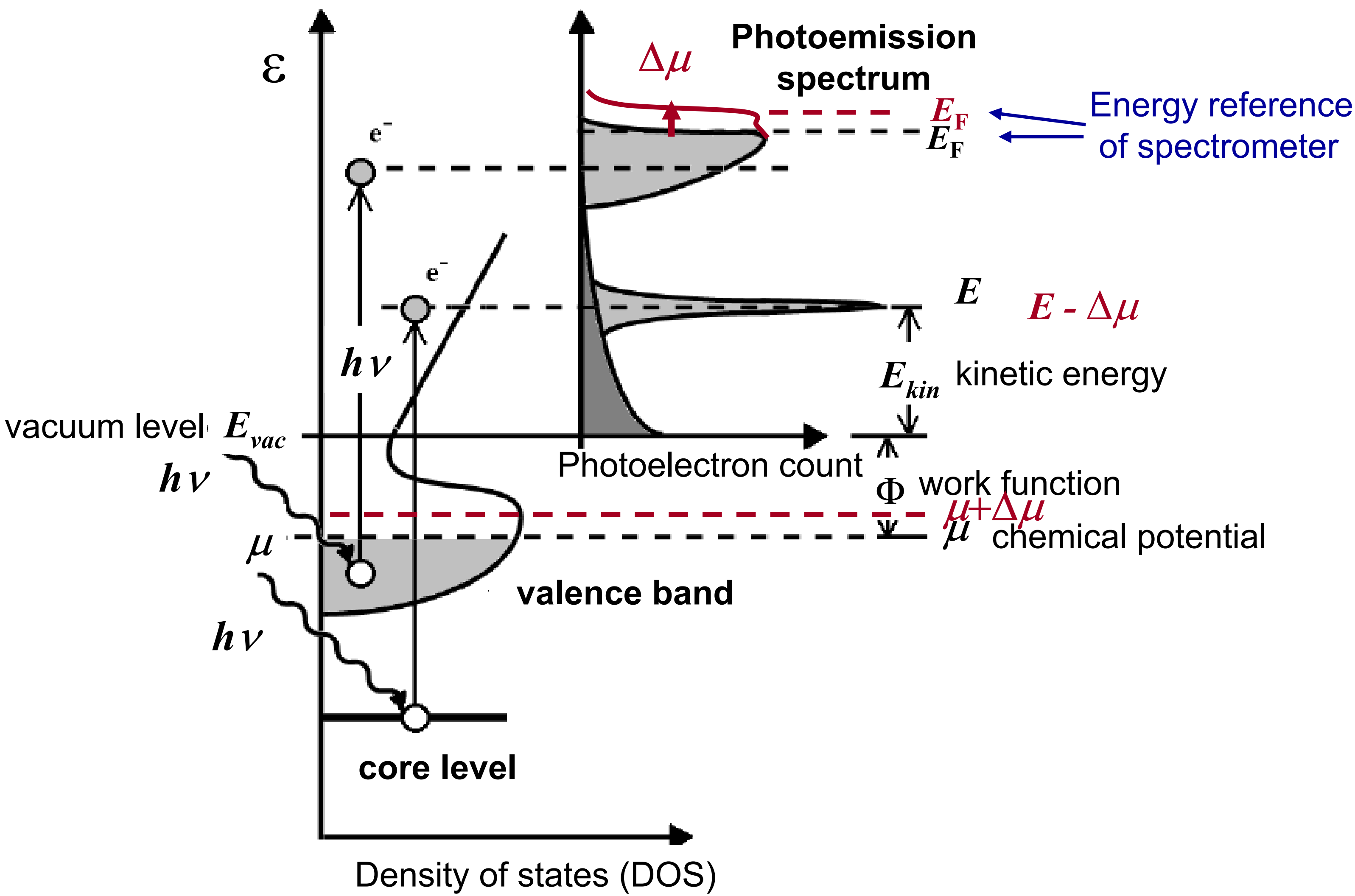

Carrier doping utilizing chemical potential differences

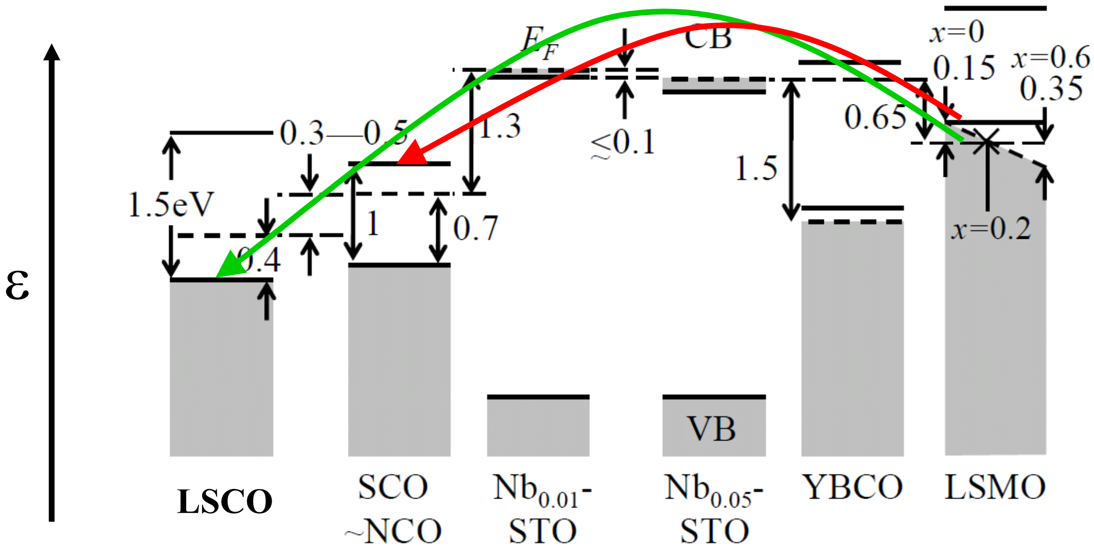

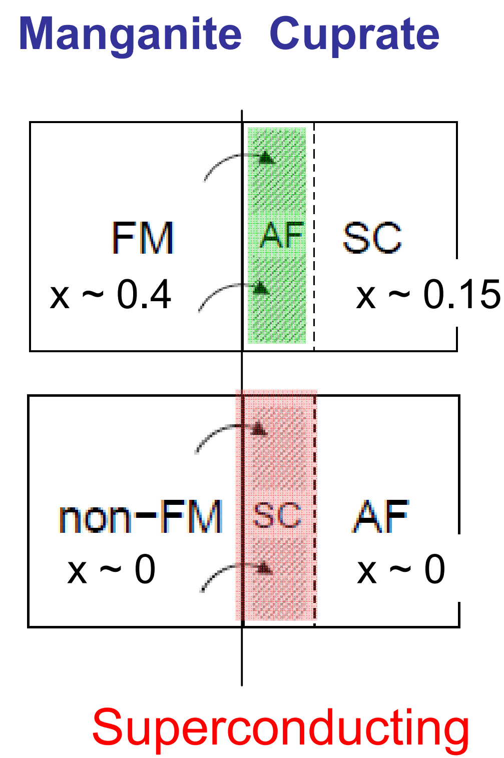

S. Yunoki et al., PRB, 2007

Effects of finite thickness

Metal-insulator transitions

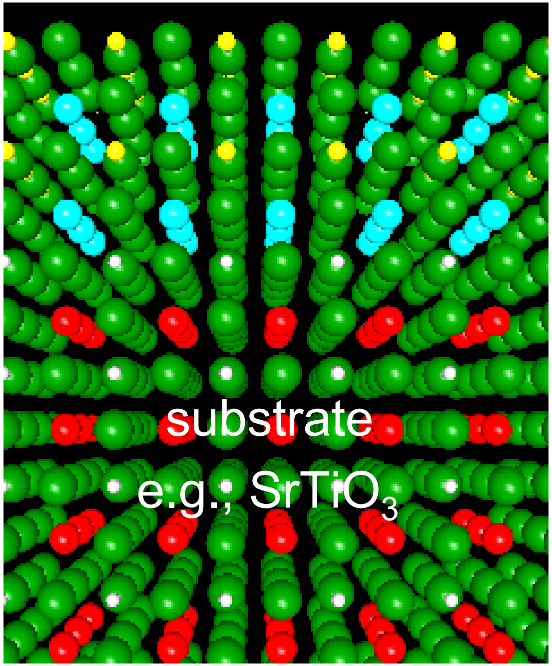

Finite thickness

Metal-to-insulator transition in $SrVO_3$ with decreasing film thickness of

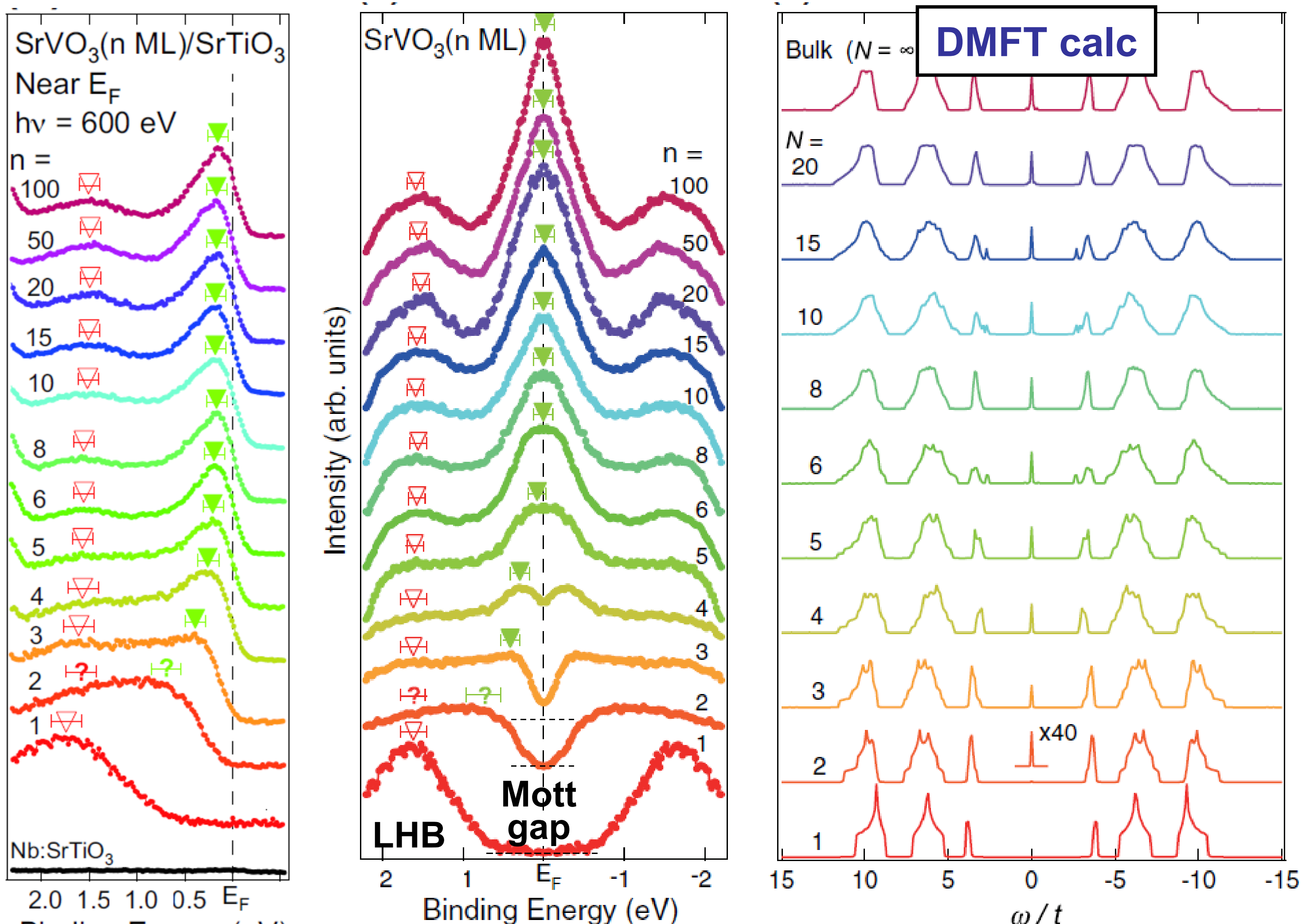

K. Yoshimatsu et al., PRL '10,
Orbital ordering? (P. Mahadevan)

Metal-to-insulator transition in $SrRuO_3$ with decreasing film thickness of

- Small W → large U/W ?
- Orbital-ordering → AFMI ?

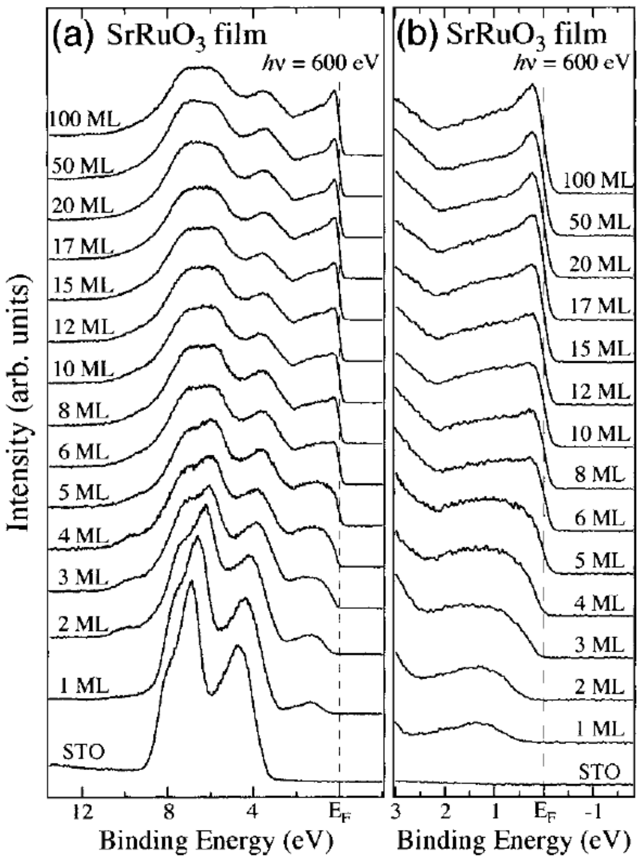

D. Toyota et al., APL '05

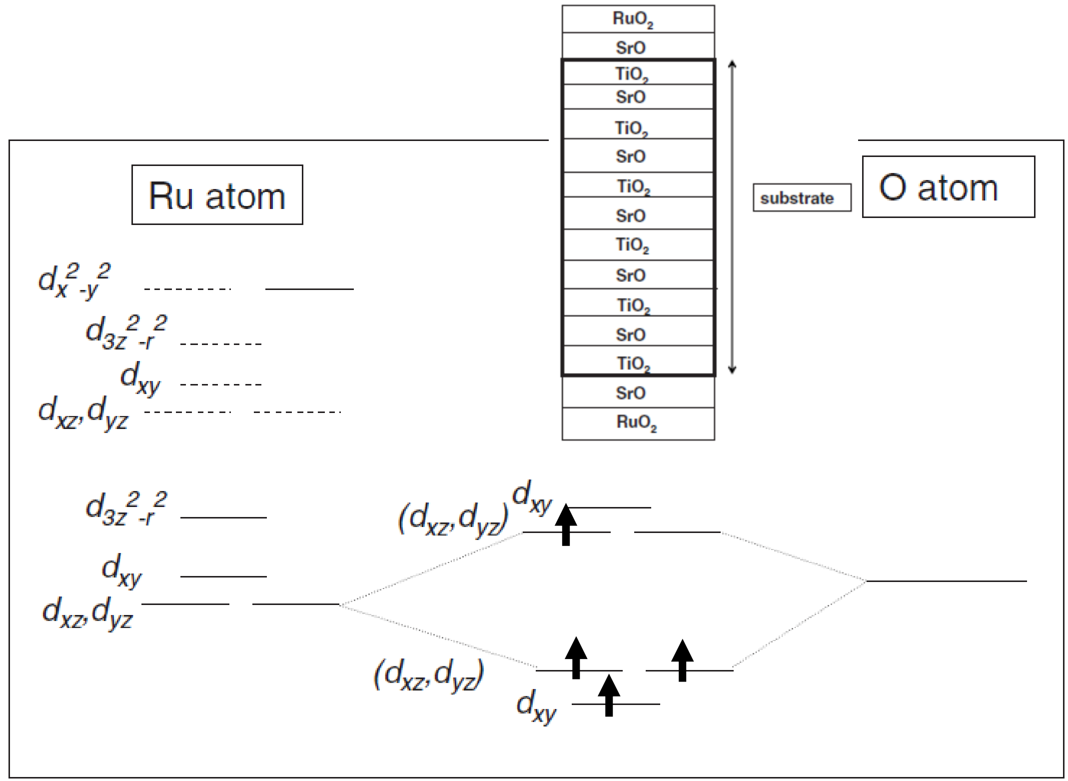

P. Mahadevan et al., PRB '09

Outline

- Electronic structure of transition-metal oxides
- Fabrication and characterization

- Interfacial electronic structure
- Effects of finite thickness
- Effects of epitaxial strain

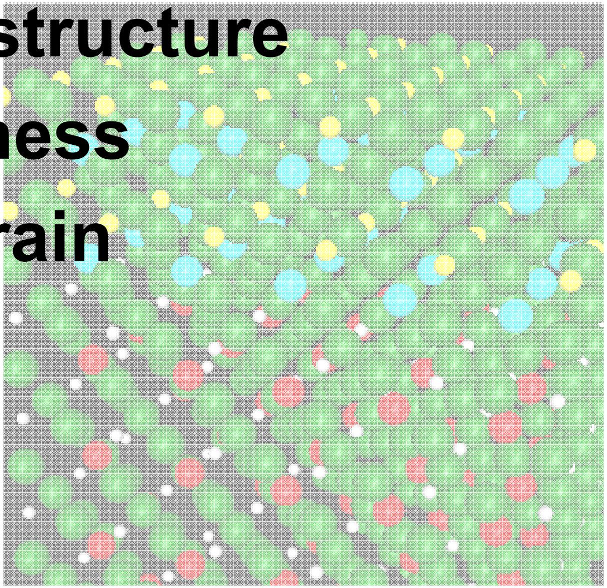

Effects of epitaxial strain

Superconductivity

Epitaxial strain

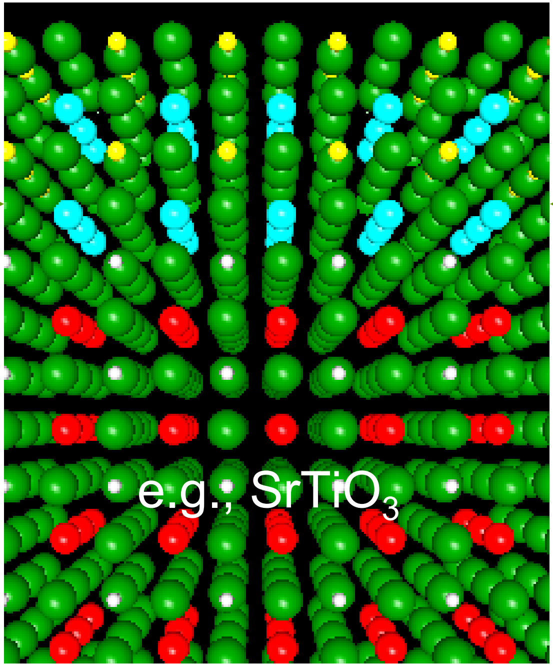

Band structure of $La_{2-x}Sr_xCuO_4$ (x=0.15) under compressive strain studied by ARPES

$La_{2-x}Sr_xCuO_4/SrLaAlO_4(001)$

Bulk

a = 3.784 Å
c =13.23 Å , d_{AP} = 2.43 Å

Thin film

a = 3.754 Å (= $SrLaAlO_4$)
c = 13.29 Å , d_{AP} = 2.50 Å

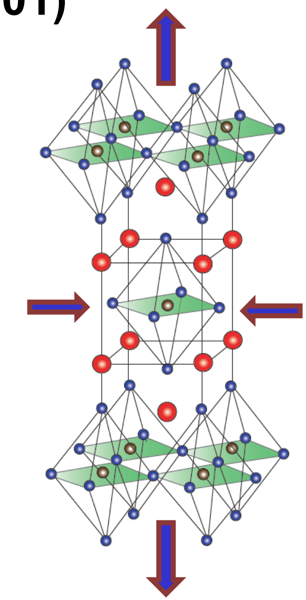

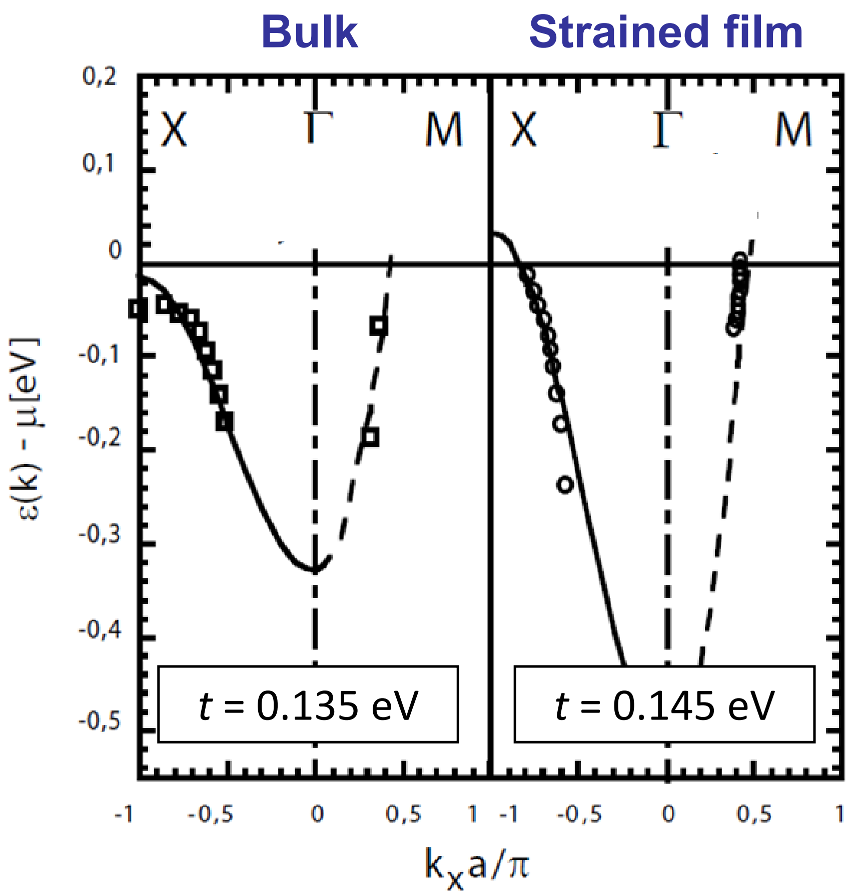

Tight-binding model

$$\xi_k = -2t[\cos(k_x a) + \cos(k_y a)] + 4t' \cos(k_x a)\cos(k_y a) - \mu$$

M. Abrecht et al., PRL '91

Fermi surface of $La_{2-x}Sr_xCuO_4$ (x=0.15) under compressive strain studied by ARPES

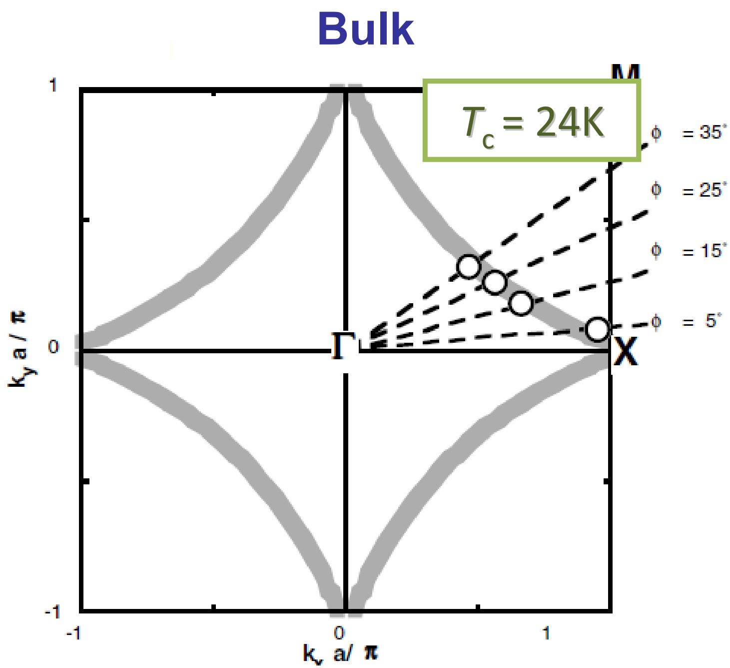

t = 0.135 eV, t' = 0.036 eV

Large t'

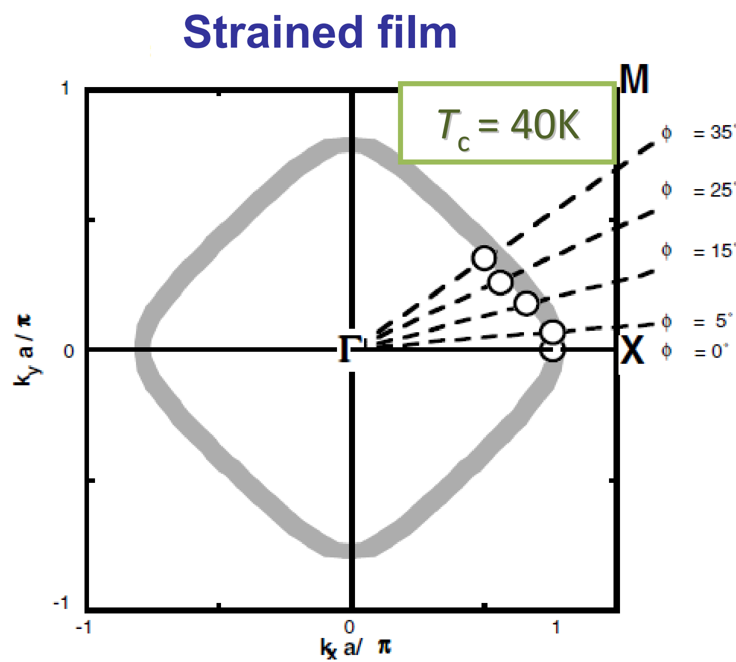

t = 0.145 eV, t' = 0.0052 eV

Small t'

M. Abrecht et al., PRL '91

Tight-binding model

$$\xi_k = -2t[\cos(k_x a) + \cos(k_y a)] + 4t' \cos(k_x a)\cos(k_y a) - \mu$$

cf: Tensile strain: $La_{2-x}Sr_xCuO_4/SrTiO_3(001)$

D. Coleta et al., PRB '06

Empirical correlation between $T_{c,\max}$ and next-nearest-neighbor hopping t'

$T_{c,\max}$ vs $|t'/t|$

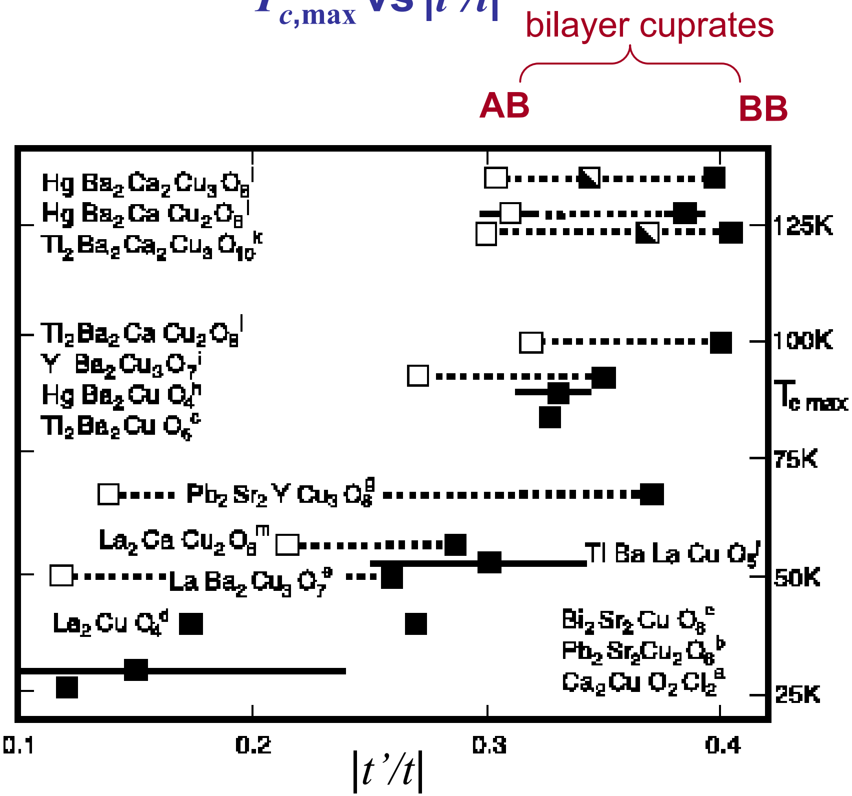

E. Pavarini et al., PRL '01

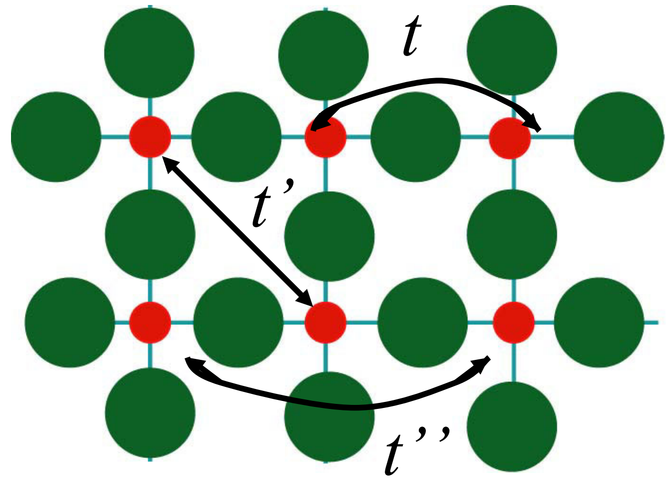

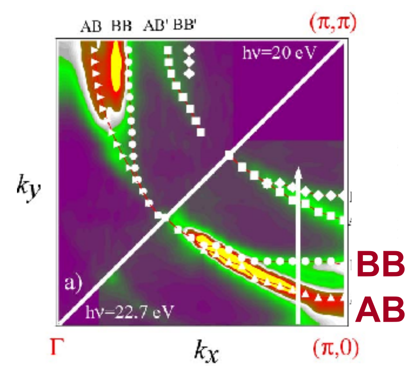

D. Feng et al., PRL '01

Effects of epitaxial strain

Metal-insulator transitions

Epitaxial strain

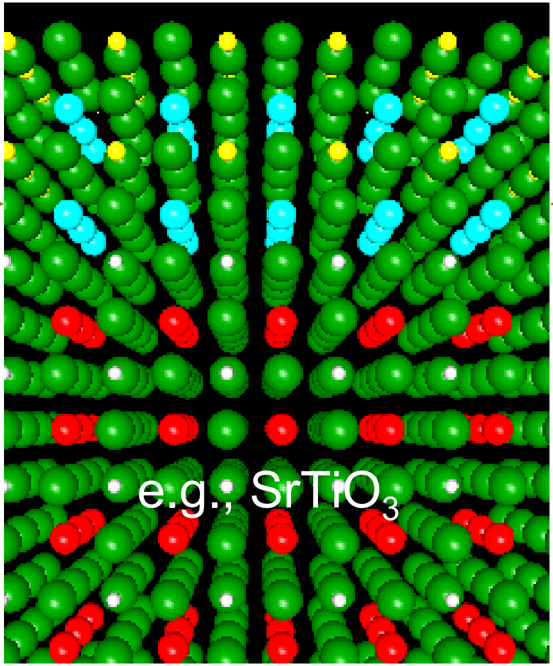

Electronic phase diagram of $R_{1-x}A_x\mathrm{MnO}_3$

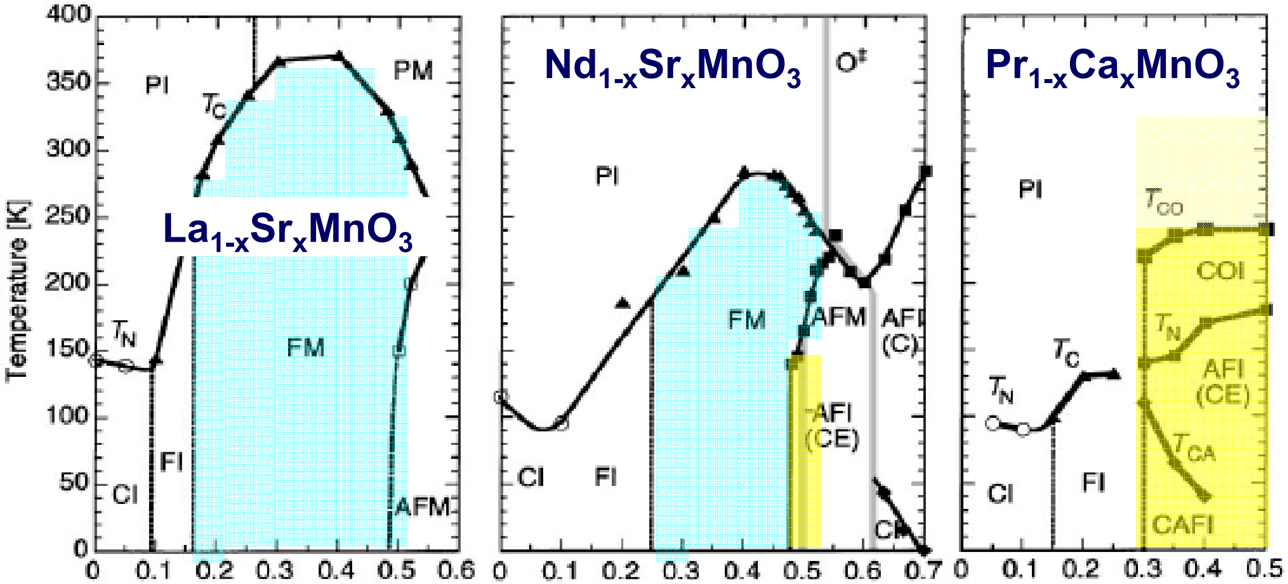

Hole doping x Hole doping x Hole doping x

large ← bandwidth (W) → small

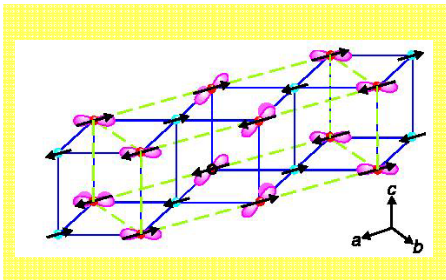

x = 0.5

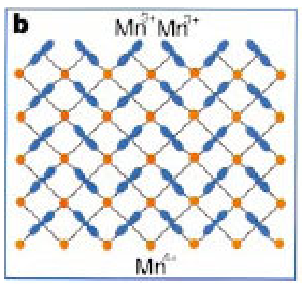

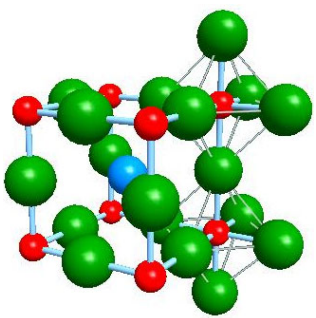

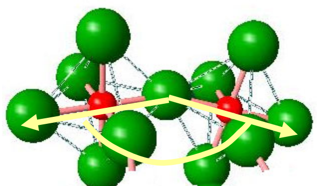

θ

$W \propto \cos^2\theta$

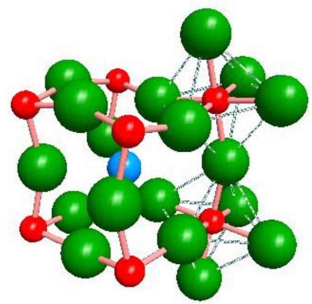

Y. Tokura and Y. Tomioka, JMMM '99

Electronic phase diagram of $La_{1-x}Sr_xMnO_3$ under epitaxial strain

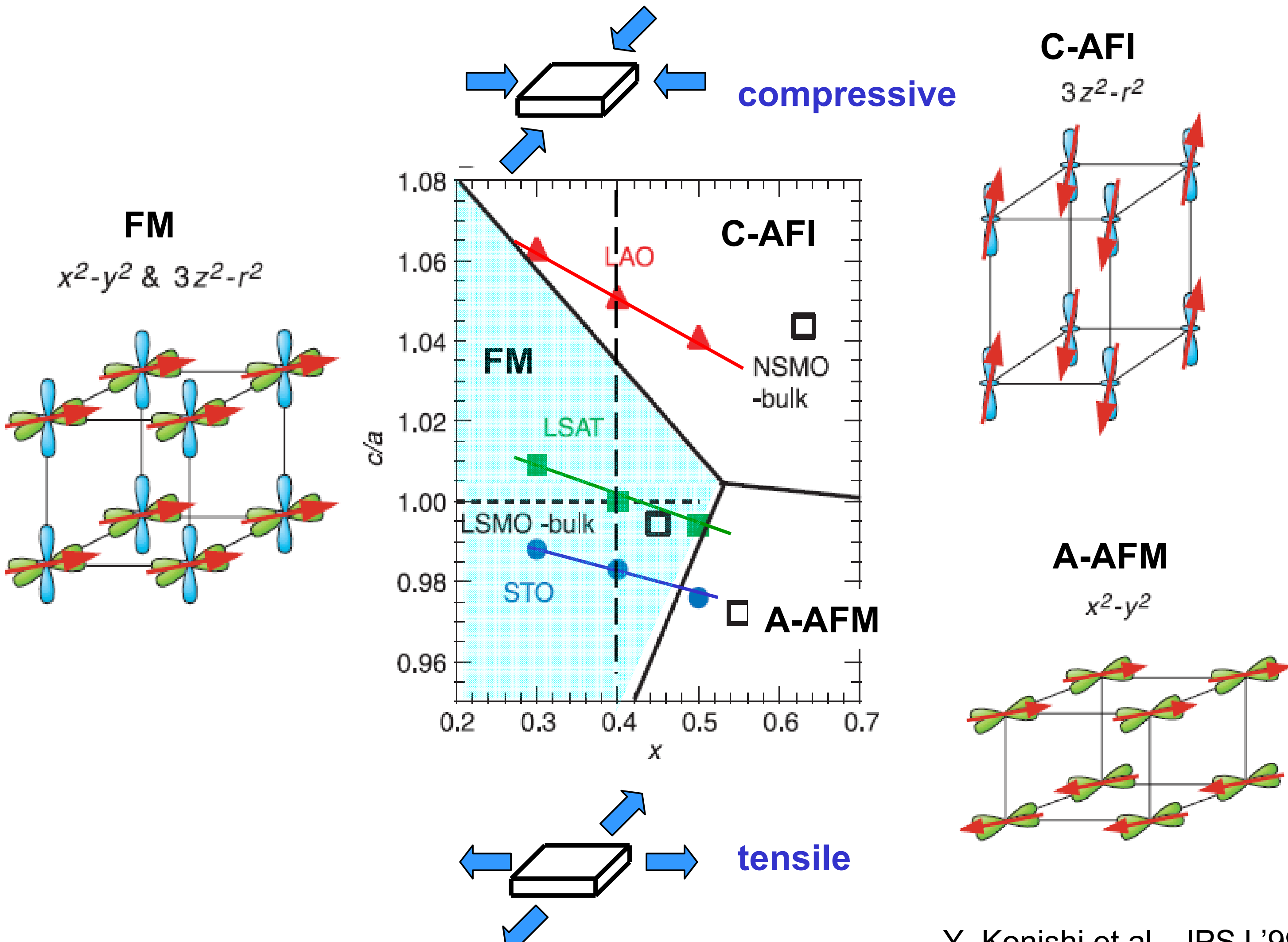

Y. Konishi et al., JPSJ ’99

HX-PES spectra of $La_{1-x}Sr_xMnO_3$ (x=0.4) under epitaxial strain

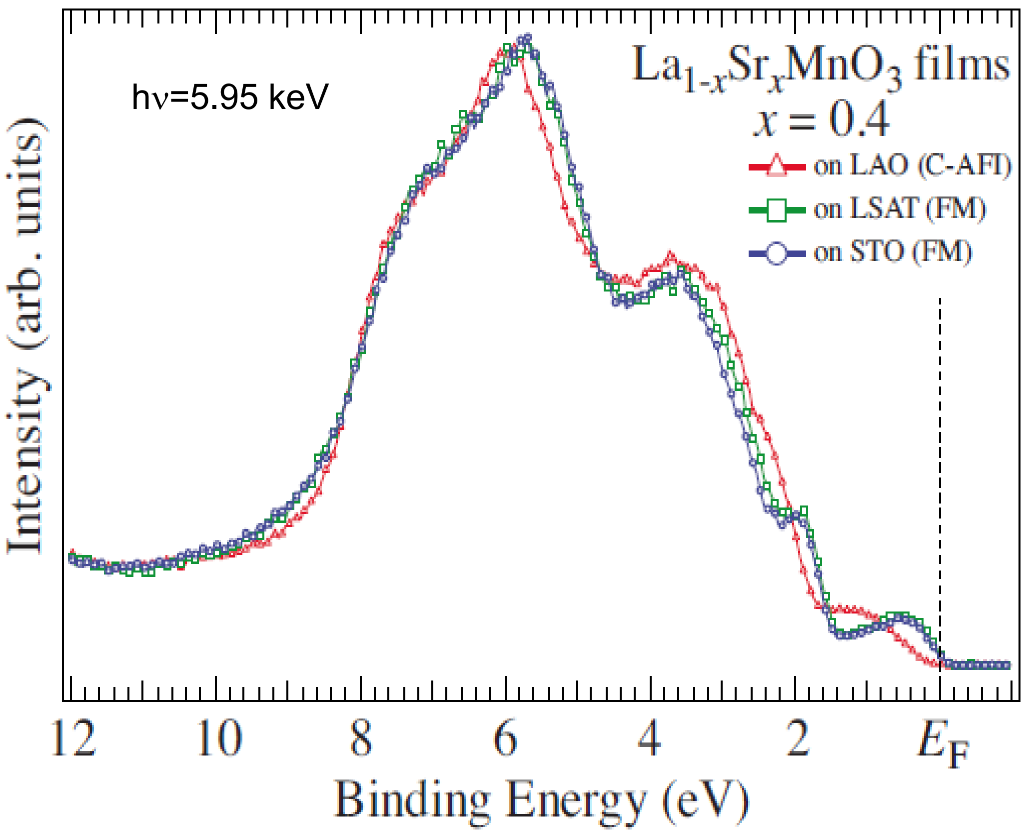

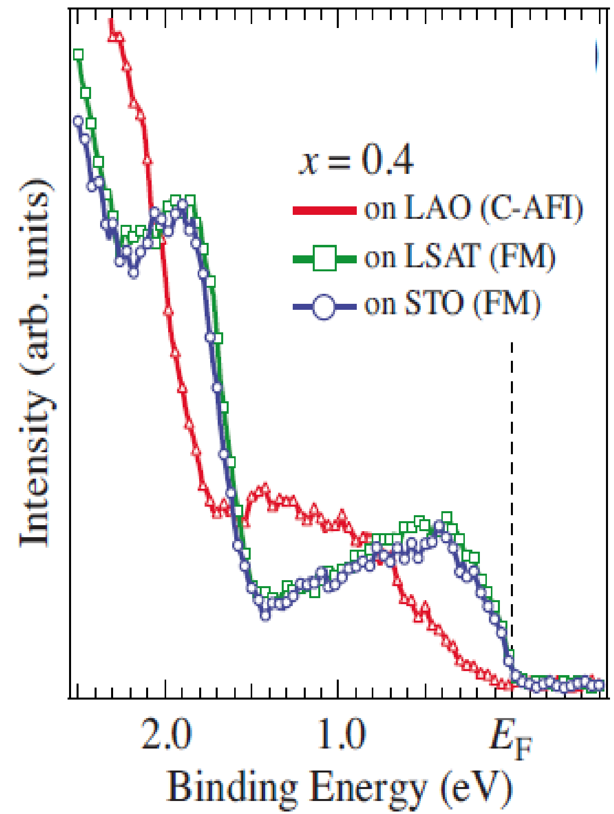

K. Horiba et al., PRB ’09

Electronic phase diagram of $La_{1-x}Sr_xMnO_3$ under epitaxial strain

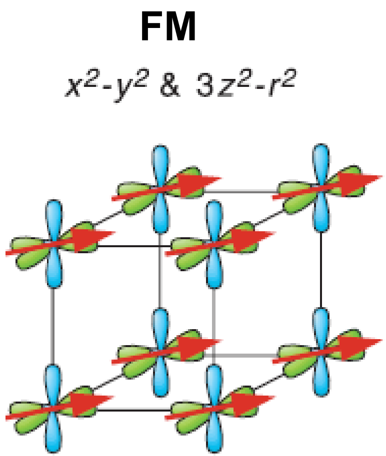

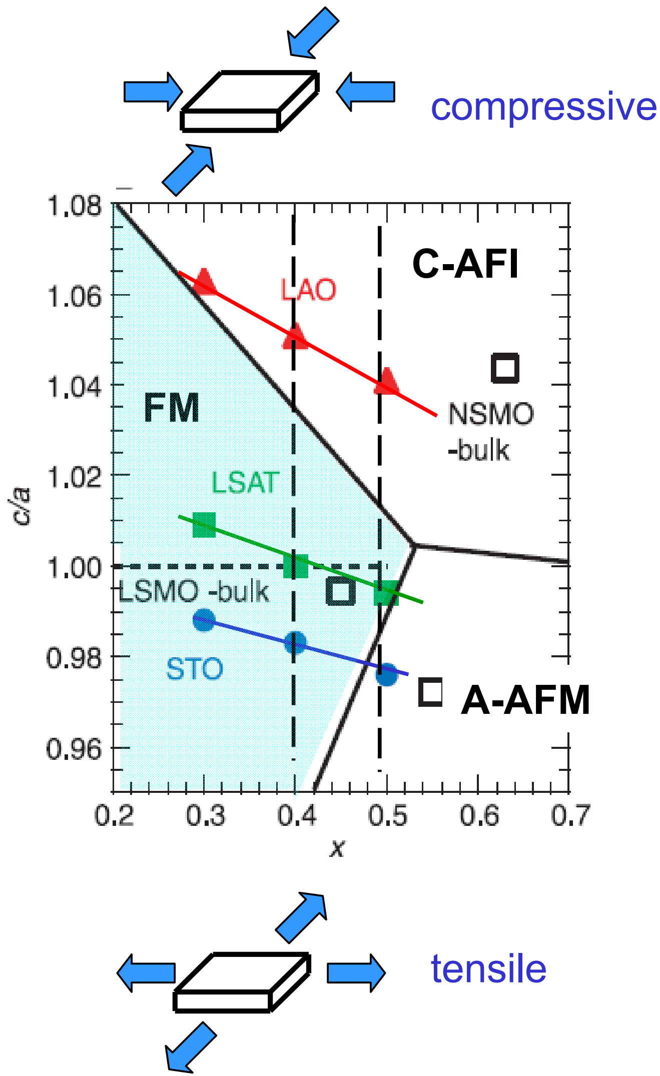

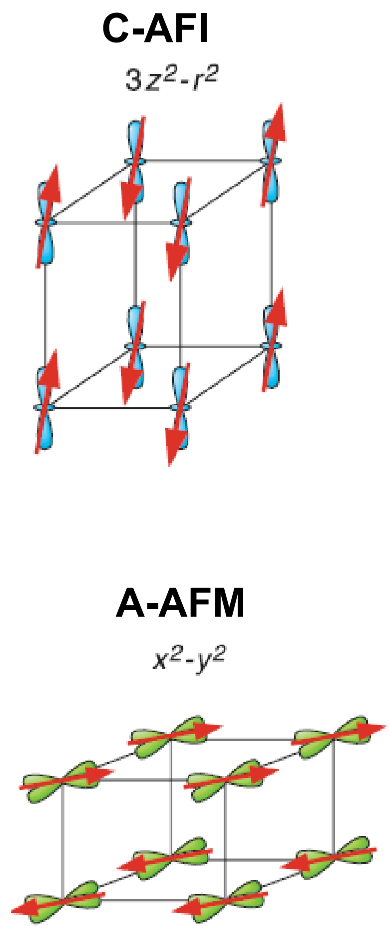

Y. Konishi et al., JPSJ ’99

HX-PES spectra of $La_{1-x}Sr_xMnO_3$ (x=0.5) under epitaxial strain

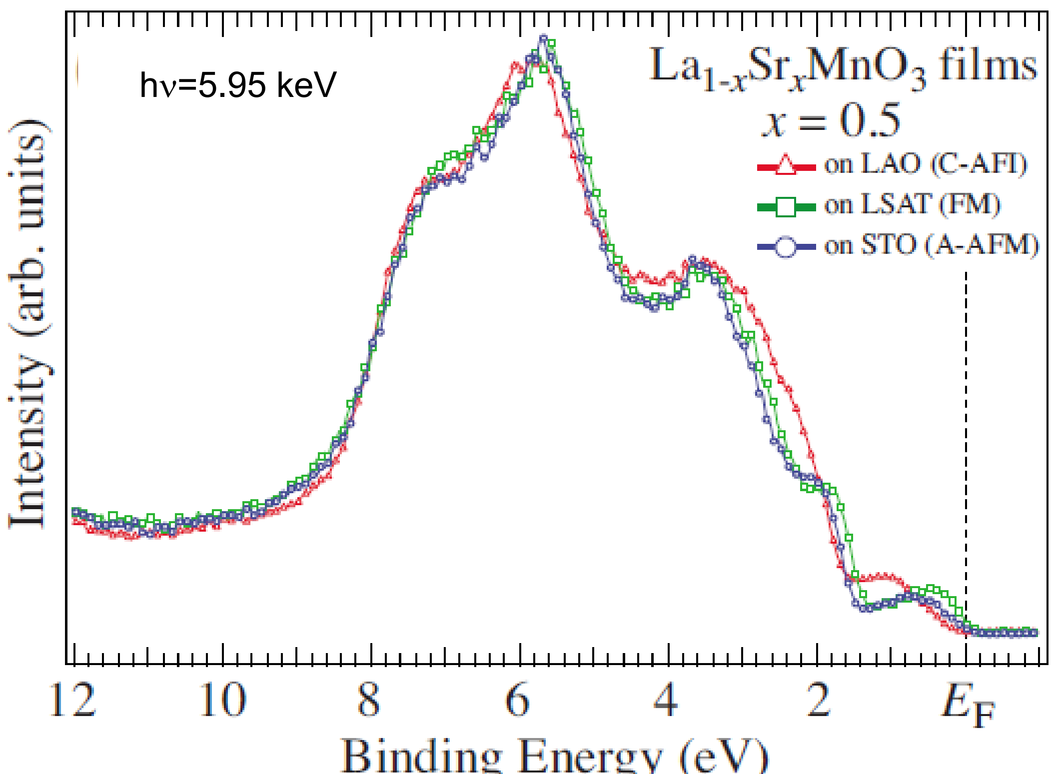

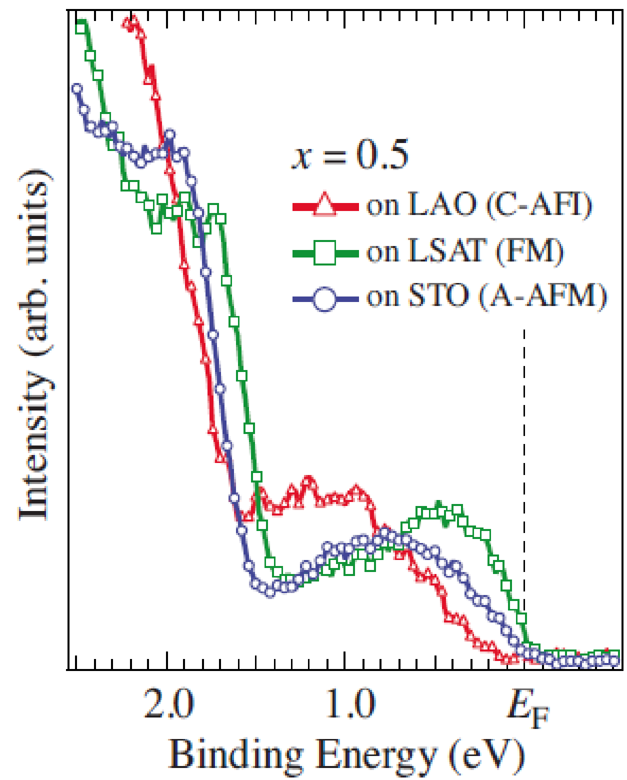

K. Horiba et al., PRB ’09

Summary

- Electronic structure of transition-metal oxides
- Fabrication and characterization
- Interfacial electronic structure
  - Metallic states between two insulators
    - States near the Fermi level
    - Charge transfer in electronic reconstruction
    - Potential change in electronic reconstruction
  - Ferromagnetism between non-magnetic materials
  - Interface between different ground states
  - Chemical potential
- Effects of finite thickness
  - Metal-insulator transitions
- Effects of epitaxial strain
  - Metal-insulator transitions
  - Madelung potential shifts
  - Changes in chemical potential shift

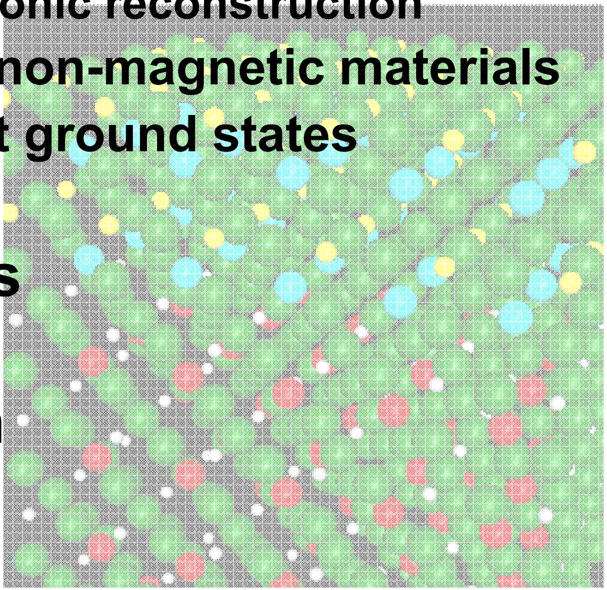

Acknowledgement

VUV, soft x-ray photoemission

M. Takizawa, H. Wadati, M. Takizawa, T. Yoshida, K. Maekawa (U of Tokyo)
H. Kumigashira, K. Horiba, K. Yoshimatsu, T. Okabe, M. Oshima,
A. Maniwa, M. Minohara (U of Tokyo)

Hard x-ray photoemission

S. Shin, Y. Takata, K. Horiba, M. Matsunami, M. Yabashi,
K. Tamasaku, Y. Nishino, D. Miwa, T. Isikawa (SPring-8, RIKEN)
E. Ikenaga, K. Kobayashi (JASRI)

Materials synthesis

H.Y. Hwang, Y. Hotta, S. Tsuda, T. Higuchi, T. Susaki (U of Tokyo)
M. Lippmaa, K. Shibuya, N. Mihara (ISSP)
M. Kawasaki (Tohoku U), H. Koinuma (U Tokyo, JST)
Y. Muraoka (Okayama U), Z. Hiroi (ISSP)

Supported by: a Grant-in-Aid for Scientific Research, JSPS
& Quantum Beam Technology Development Program, JST